1-2-2013

Overcoming Tumor Drug Resistance By Activating Amp-Activated Protein Kinase And Destabilizing Oncoproteins

Min Shen
Wayne State University,

OVERCOMING TUMOR DRUG RESISTANCE BY ACTIVATING AMP-ACTIVATED PROTEIN KINASE AND DESTABILIZING ONCOPROTEINS

by

MIN SHEN

DISSERTATION

Submitted to the Graduate School

of Wayne State University,

Detroit, Michigan

in partial fulfillment of the requirements

for the degree of

DOCTOR OF PHILOSOPHY

2013

MAJOR: PHARMACOLOGY

Approved by:

_____

Advisor Date

_____

_____

_____

_____

DEDICATION

This dissertation is dedicated to my parents, grandparents and close circle of friends for their love and support throughout my life. To these important people in my life, I am most grateful and indebted to.

ACKNOWLEDGMENTS

I would like to express my heartfelt thanks to my mentor Dr. Q. Ping Dou for his guidance and support throughout my graduate study. I gratefully acknowledge my committee members, Dr. Ahmad R. Heydari, Dr. Karin List, Dr. Roy B. (Mac) McCauley and Dr. Izabela Podgorski, for their insightful advices to my research projects.

I am grateful to my laboratory colleagues, Dr. Michael Frezza, Dr. Fathima Kona, Deniela Buac, Rahul Deshmukh, and all other past members. I would like to particularly thank Zhen Zhang and Nan Zhang, who are visiting students from Ocean University of China, for their assistance in the work presented in chapter two and three, respectively. A special thank you goes to Sara Schmitt for our friendship and everything.

I also want to thank Dr. Manohar Ratnam at Wayne State University for providing various truncated AR constructs, Dr. Jeffrey A. Zonder at Karmanos Cancer Institute for helping with multiple myeloma project, as well as Dr. Robert Z. Orlowski and Dr. Deborah Kuhn at University of Texas MD Anderson Cancer Center for providing multiple myeloma cell lines.

My final thanks goes to our graduate officers, Dr. Stanley Terlecky and Dr. Roy B. (Mac) McCauley (again) for their help and advices throughout my Ph.D. training.

TABLE OF CONTENTS

LIST OF FIGURES

CHAPTER 1

Introduction

In the past decades, cancer research has led to a deep understanding in the intricate mechanisms of cancer development and progression as well as a great success in cancer diagnosis and treatment. However, resistance of tumors to drug treatment remains a fundamental challenge to improving patient outcome. In my dissertation study, I explored two different strategies to overcome tumor drug resistance.

The first strategy is to target tumor metabolism. Deregulated cellular energetics has been recognized as an emerging hallmark of cancer (Hanahan and Weinberg, 2011). Not only so, altered tumor metabolism also contributes to drug resistance by producing elevated ATP and NADPH levels. This is because common mechanisms for generating drug resistance are highly ATP-demanding processes, which requires tumor cell to produce enough ATP in order to defeat anti-tumor drugs. Tumor cells also need a large amount of NADPH to combat chemotherapy-induced oxidative stress. Increased glucose consumption gives rise to abundant NAPDH and contributes to tumor drug resistance (Butler et al., 2013). This raises the possibility of overcoming tumor drug resistance by targeting tumor metabolism.

The second strategy that I explored to overcome tumor drug resistance is to target tumor-driving oncoproteins. This is because certain types of cancer cells are heavily dependent on one or a few genes for the maintenance of the malignant phenotype. This phenomenon was termed as “oncogene addiction”. These oncogene(s) are believed to be the “Achilles’ heel” of that particular type of tumor because, once the driving oncoprotein

is destroyed, the tumor cell will lose self-renewal ability. Therefore, regardless of the existence of other survival or drug-resistance mechanisms, the tumor will eventually regress (Ablain et al., 2011). The most successful example for this concept is the cooperative degradation of PML/RARA oncoprotein by arsenic and retinoic acid in acute promyelocytic leukemia which achieved cure in most patients (Ablain et al., 2011). These evidences led me to explore the possibility of overcoming tumor drug resistance by destabilizing key oncoproteins.

In this chapter, I will discuss the mechanisms of tumor drug resistance, the three tumor cell models that I utilized to study my strategies, the key oncoproteins expressed in these tumor cell models, the AMPK signaling pathway that regulates cellular energy balance, the ubiquitin-proteasome pathway that controls intracellular protein turnover, as well as the drugs that are utilized as the pharmacological activators or inhibitors of the proteins of interest.

Mechanisms of tumor drug resistance

Drug resistance can occur through different mechanisms, some of which are inherent while others are acquired after anti-tumor therapy. Acquired resistance is particularly critical, as tumors not only become resistant to the drugs originally used to treat them, but may also become cross-resistant to other drugs with different mechanisms of action (Longley and Johnston, 2005). Studies of tumor drug resistance used to be focused on chemoresistance. With the development of targeted therapies, more and more attention has been paid to resistance to targeted therapies. The molecular mechanisms involved in drug resistance can be divided into three categories. The first category is drug

concentration related, including (1) increased drug efflux by overexpression of drug efflux pumps on the cell surface such as P-gp (P-glycoprotein, a.k.a. multidrug resistance protein 1 or MDR1), MRPs (multidrug resistance-associated proteins) and BCRP (breast cancer resistance protein); (2) increased drug metabolism by induction of drug detoxification enzymes; and (3) increased drug compartmentalization. The second category is drug target related, including (4) increased or altered drug targets by target gene amplification or mutation; and (5) constitutive activation of drug targets. The last category is damage control related, including (6) enhanced processing of drug-induced damage such as enhanced DNA damage repair; (7) resistance to apoptosis due to enhanced anti-apoptotic signaling, suppressed pro-apoptotic signaling or defects in apoptotic machinery; and (8) cell surface receptor-mediated enhanced growth signaling (Gottesman, 2002; Longley and Johnston, 2005; Masui et al., 2013) (Figure 1).

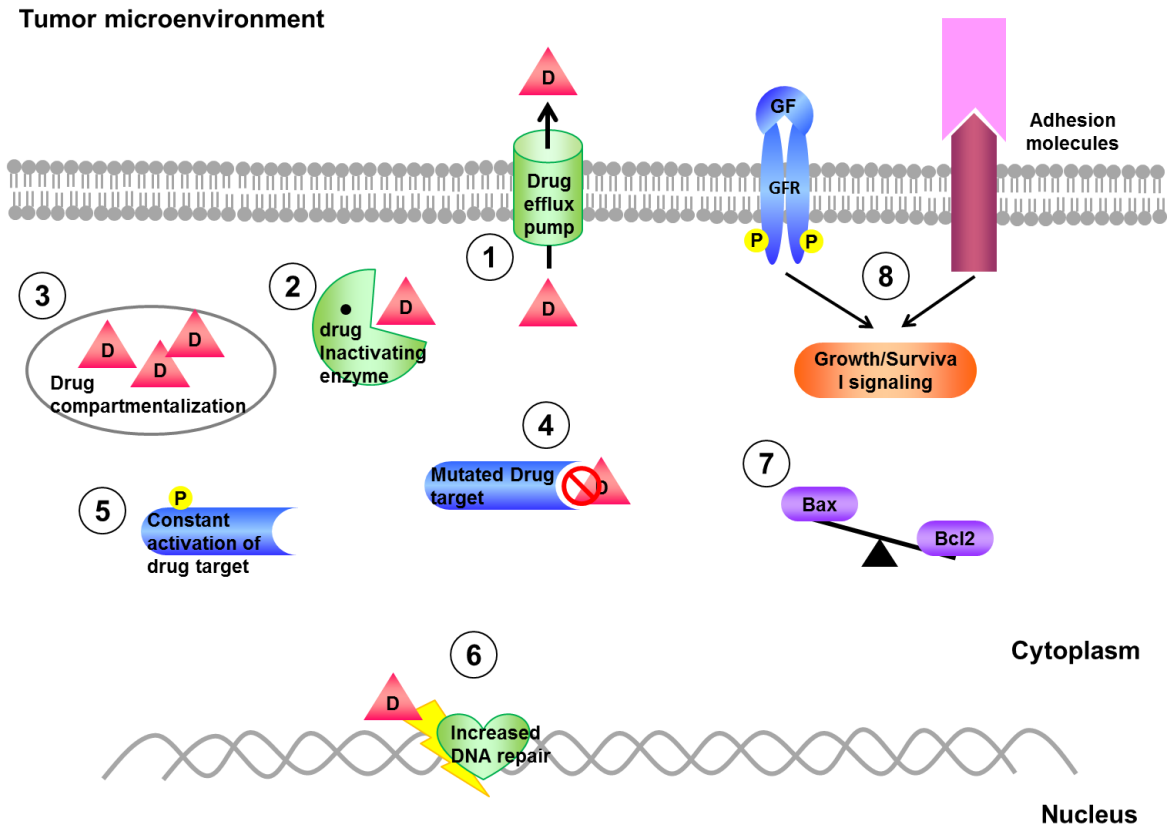

Figure 1. Mechanisms of tumor drug resistance.

The molecular mechanisms involved in drug resistance can be divided into three categories. The first category is drug concentration related, including (1) increased drug efflux by overexpression of drug efflux pumps on the cell surface; (2) increased drug metabolism by induction of drug detoxification enzymes; and (3) increased drug compartmentalization. The second category is drug target related, including (4) increased or altered drug targets by target gene amplification or mutation; and (5) constitutive activation of drug targets. The last category is damage control related, including (6) enhanced processing of drug-induced damage such as enhanced DNA damage repair; (7) resistance to apoptosis due to enhanced anti-apoptotic signaling, suppressed pro-apoptotic signaling or defects in apoptotic machinery; and (8) cell surface receptors-mediated enhanced growth signaling.

Androgen receptor, prostate cancer and resistance to androgen deprivation therapy

Prostate cancer is the most commonly diagnosed cancer and the second leading cause of cancer-related death in men in the United States (Siegel et al., 2013). It is well-known that androgen receptor (AR) signaling plays a critical role in the development and progression of prostate cancer (Richter et al., 2007).

AR is a ligand-dependent transcription factor which belongs to the family of nuclear receptor. It is composed of four distinct domains: the N-terminal domain which comprises the transactivation domain; the DNA-binding domain (DBD); the hinge region which contains the NLS; and the ligand-binding domain (LBD) (Richter et al., 2007; Lonergan and Tindall, 2011). In the cytoplasm, the inactive AR protein forms a complex with heat shock proteins (HSPs) that regulate receptor folding and confer ligand-binding capacity. Binding of ligand to AR induces dissociation from HSPs, receptor dimerization and auto-phosphorylation, as well as nuclear translocation. In the nucleus, the AR dimer binds to androgen responsive elements (ARE) in the promoter and/or enhancer of the target genes and cooperates with coactivators or corepressors which determines either up-regulate or down-regulate gene expression (Feldman and Feldman, 2001; Lonergan and Tindall, 2011) (Figure 2). AR regulates the expression of almost 100 genes including AR itself.

Androgen deprivation therapy (ADT) has been the mainstay of treatment for advanced/metastatic prostate cancer for a long time. Virtually all prostate cancers are androgen-dependent and sensitive to hormone therapy at the beginning. Despite the initial response to ADT, almost all patients eventually progress to a stage of castration-resistant prostate cancer associated with increased drug resistance, metastatic potential and

aggressiveness (Feldman and Feldman, 2001). The mechanisms of development of androgen-independent prostate cancer can be categorized into five major pathways: 1) increased AR production by gene amplification, or enhanced AR sensitivity to ligand, or more potent form of androgen; 2) activation of AR by non-androgenic molecules normally present in the circulation; 3) phosphorylation of AR by either the AKT or the mitogen-activated protein kinase (MAPK) pathway, producing a ligand-independent AR (Figure 2); 4) obviating the need for AR or its ligand by parallel survival pathways such as Bcl-2 pathway; and 5) selection of androgen-independent cancer cells that are present all the time in the prostate by therapy (Feldman and Feldman, 2001; Devlin and Mudryj, 2009).

It is worth noting that, in most cases, the disease progression at castration-resistant stage is still dependent on AR signaling pathway (Chen et al., 2004). Therefore, AR is a druggable target for all stages of the disease. AR degradation is mainly controlled by two proteolytic pathways. The first pathway relies on the 26S proteasome. Growth factor or cytokine stimulation activates Akt kinase, which phosphorylates AR at two Ser sites. Active Akt kinase also phosphorylates the E3 ligase, Mdm2, which ubiquitinates AR and targets it for proteasomal degradation. The second pathway engages phosphatase and tensin homolog (PTEN) and caspase-3. Binding of PTEN to AR detains AR in the cytoplasm and facilitate the recruitment of caspase-3, which processes AR at an Asp site (Lee and Chang, 2003; Jaworski, 2006). Besides these two pathways, we and our collaborates recently reported that calpain, but not caspase-3, execute AR degradation under some conditions such as proteasome inhibitor-induced apoptosis (Pelley et al., 2006; Yang et al., 2008).

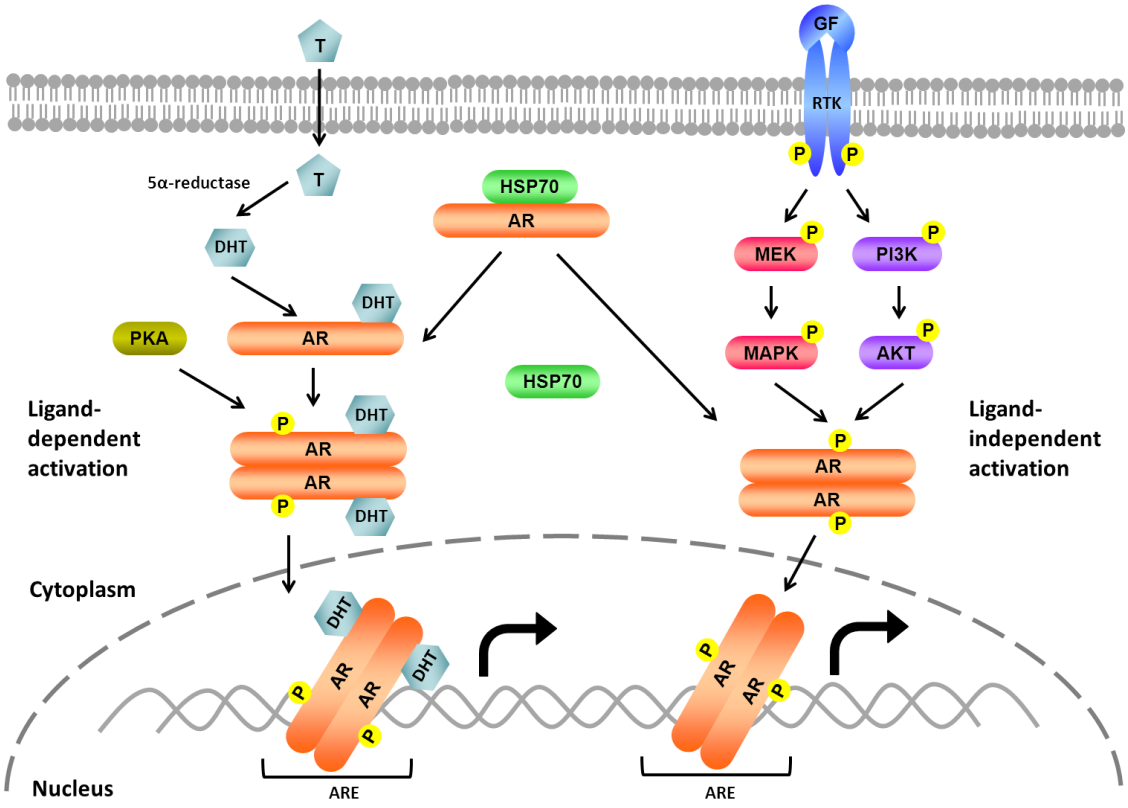

Figure 2. Schematic diagram of androgen receptor signaling.

In the cytoplasm, the inactive AR protein forms a complex with heat shock proteins (HSPs) that regulate receptor folding and confer ligand-binding capacity. Classical AR activation requires ligand binding which induces AR dissociation from HSPs, dimerization, phosphorylation by PKA, and nuclear translocation. Alternatively, AR can be activated in a ligand-independent manner. In this case, the receptor tyrosine kinases (RTKs) on the cell surface are activated by growth factor (GF) binding and subsequent auto-phosphorylation, leading to the activation of downstream MEK/MAPK pathway or PI3K/AKT pathway. Both MAPK and AKT can phosphorylate AR for its ligand-independent activation (dimerization and nuclear translocation). In the nucleus, the AR dimer binds to androgen responsive elements (ARE) in the promoter and/or enhancer of the target genes to regulate gene expression.

Multiple myeloma

Multiple myeloma is characterized by abnormal clonal plasma cell infiltration in the bone marrow. It is generally thought to be a highly treatable but incurable disease. The two factors that have crucial roles in multiple myeloma progression are the adhesion molecules and the cytokines (Mahindra et al., 2010). After class switching in the lymph node, the adhesion molecules expressed on the surface of multiple myeloma cells mediate the homing of multiple myeloma cells to bone marrow and their subsequent binding to the bone marrow stem cells or the extracellular matrix proteins. This binding not only localizes the multiple myeloma cells in the bone marrow microenvironment but also stimulates TGF-β-triggered, NF-κB-mediated transcription and paracrine secretion of interleukin-6 (IL-6) from the bone marrow stem cells. IL-6 is the major cytokine mediating multiple myeloma growth and survival via MAPK, PI3K/Akt and Jak/STAT signaling pathways. Besides IL-6, the bone marrow stem cells also secrete cytokines such as IGF-1 (insulin-like growth factor-1), VEGF (vascular endothelial growth factor) and BAFF (B-cell activating factor) that support multiple myeloma growth, survival and migration in the bone marrow milieu (Figure 3). Additionally, cytokines secreted by multiple myeloma cell itself such as VEGF, IL-15 and IL-21 can augment multiple myeloma cell growth through an autocrine manner (Mahindra et al., 2010). The adhesion of multiple myeloma cells to the bone marrow also generates cell adhesion-mediated resistance to conventional chemotherapies such as melphalan, cyclophosphamide and doxorubicin. Interestingly, novel agents including immunomodulators (e.g., thalidomide, lenalidomide and pomalidomide) and proteasome inhibitors (e.g., bortezomib and carfilzomib) were found to be capable of targeting both the multiple myeloma cells and

the bone marrow microenvironment thereby overcoming conventional cell adhesion-mediated drug resistance (Mahindra et al., 2010; Mahindra et al., 2012).

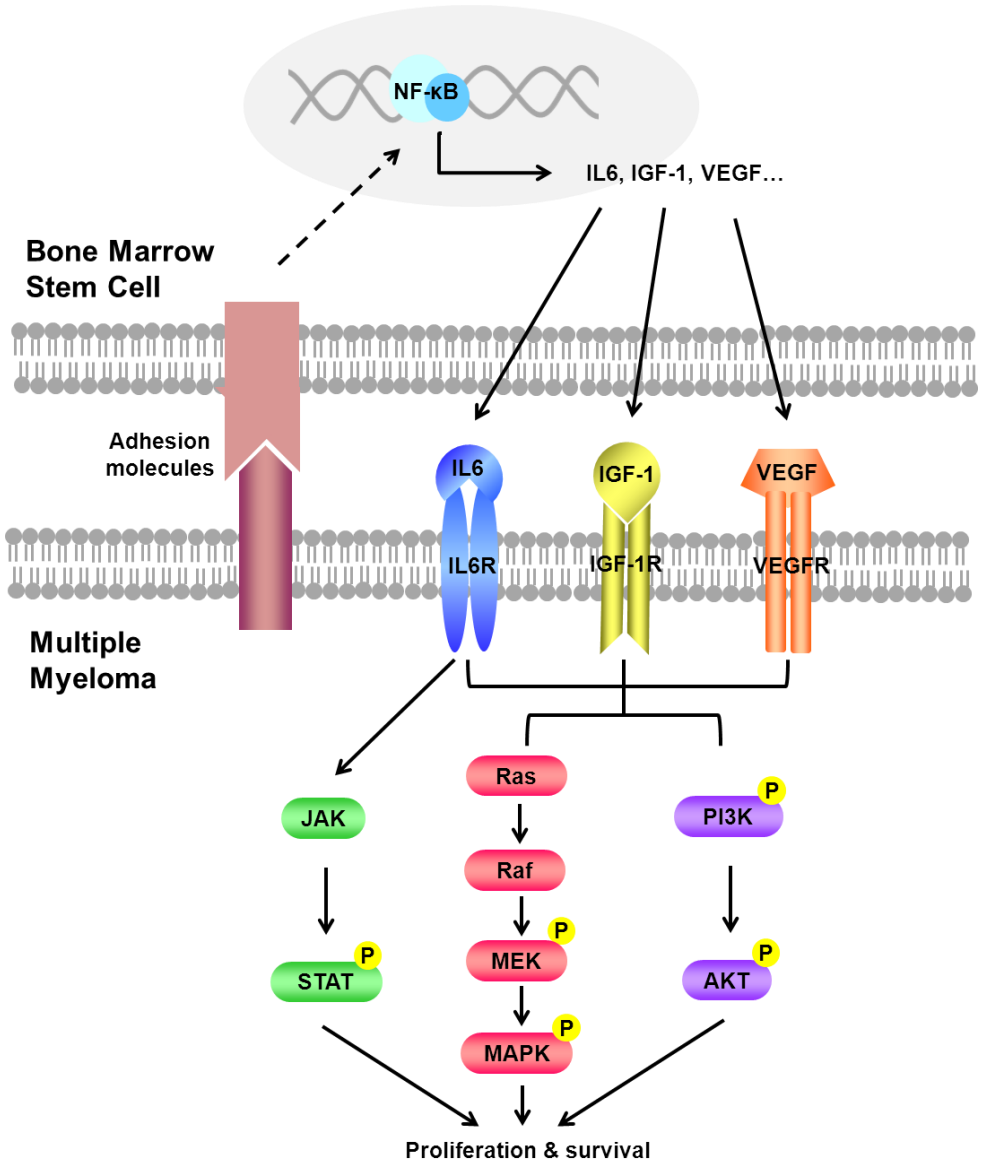

Figure 3. A cross-talk between multiple myeloma and bone marrow stem cell.

The adhesion molecules expressed on the surface of multiple myeloma cells bind to their corresponding receptors expressed on the surface of bone marrow stem cells. This binding not only localizes the multiple myeloma cells in the bone marrow microenvironment but also stimulates NF-κB-mediated transcription and paracrine secretion of IL-6, IGF-1 and VEGF from bone marrow stem cells. Secreted IL-6, IGF-1 and VEGF bind to their corresponding receptors on multiple myeloma cells, mediating cell growth and survival via MAPK, PI3K/Akt and Jak/STAT signaling pathways.

BCR-Abl and chronic myelogenous leukemia

Chronic myeloid leukemia (CML) is characterized by a massive expansion of predominantly granulocytic cell lineage in the bone marrow and the accumulation of these cells in the blood. More than 90% of CML is associated with a chromosomal translocation t(9;22)(q34;q11) known as the Philadelphia chromosome, which was also found in some acute leukemias (Kurzrock et al., 2003). During this process, part of the *bcr* gene from chromosome 22 is fused with the c-*abl* gene on chromosome 9, resulting in a chimeric oncogene, *bcr-abl* (Kurzrock et al., 2003; Ren, 2005) (Figure 4). The fused Bcr-Abl protein has constitutively elevated tyrosine kinase activity and acts as a proliferative activator and an apoptotic suppressor (Kurzrock et al., 2003; Ren, 2005). Bcr-Abl is linked to Ras/MAPK, PI3K-Akt and Jak-STAT signaling pathways (Kurzrock et al., 2003; Ren, 2005) (Figure 4). In addition, Bcr-Abl can abrogate growth factor dependence by inducing expression of cytokines such as IL-3 and GM-CSF. Bcr-Abl also enhances DNA damage repair, causes adhesion defects of the cell, and indirectly modulates Bcl-2 family proteins (Kurzrock et al., 2003; Ren, 2005). All of these modulations contribute to leukocyte growth and survival.

Inhibition of Bcr-Abl tyrosine kinase activity by kinase inhibitors such as imatinib has achieved great success in the treatment of Bcr-Abl-driven leukemia in the past decade (Ren, 2005; An et al., 2010). However, single point mutation in the Abl kinase domain may make Bcr-Abl escape from kinase inhibition (Ren, 2005; An et al., 2010). Therefore another strategy to inhibit Bcr-Abl function is to reduce the amount of Bcr-Abl protein by either decreasing its synthesis or promoting its degradation. Knocking down Bcr-Abl by RNA interference effectively induced apoptosis and reduced viability in

human K562 cell line and primary CML cells (Wilda et al., 2002; Withey et al., 2005). Studies from our group found that treatment with proteasome inhibitors caused significant reduction of Bcr-Abl protein, associated with subsequent induction of apoptosis in K562 cells (Dou et al., 1999).

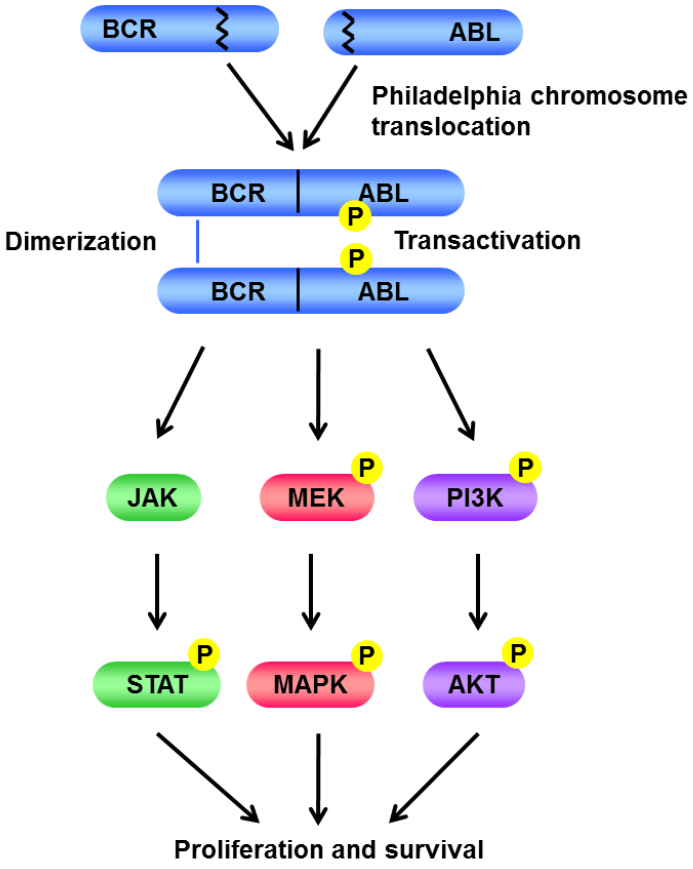

Figure 4. Schematic diagram of Philadelphia chromosome translocation and BCR-Abl signaling.

Philadelphia chromosome translocation refers to a process during which part of the *bcr* gene from chromosome 22 is fused with the c-*abl* gene on chromosome 9, resulting in the generation of a chimeric oncogene, *bcr-abl*. The fused Bcr-Abl protein has constitutively elevated tyrosine kinase activity, leading to the activation of Ras/MAPK, PI3K-Akt and Jak-STAT signaling pathways that support leukemia cell growth and survival.

The ubiquitin proteasome pathway

The UPS was discovered in the late 1970s and early 1980s. The importance of this discovery was acknowledged through the award of the 2004 Nobel Prize in Chemistry to its discoverers, Aaron Ciechanover, Avram Hershko and Irwin Rose**.**

Protein degradation by the UPP usually includes two steps, ubiquitin conjugation and proteasomal degradation. Ubiquitin (8.5 kDa) is a highly conserved small regulatory protein. Ubiquitin conjugation occurs through an enzymatic cascade that involves three distinct enzymes, Ub-activating (E1), Ub-conjugating (E2) and Ub-ligating (E3) enzymes (Glickman and Ciechanover, 2002). Only proteins conjugated with four or more Lys48-linked ubiquitin can be recognized and processed by the proteasome for degradation. When the poly-ubiquitinated proteins are directed to the 26S proteasome complex, the poly-ubiquitin chain will be removed and recycled while the protein substrates will be progressively degraded into oligopeptides that are 3- to 25- amino acids long (Adams, 2004; Sorokin et al., 2009) (Figure 5). The eukaryotic 26S proteasome is a 2.4MDa large complex consisting of the 20S core proteasome and two 19S regulatory caps. The 20S core proteasome harbors seven different α-subunits and seven different β-subunits in their twofold symmetrical $\alpha_7\beta_7\beta_7\alpha_7$ stacked complex, among which only three β-subunits per β-ring [β1 (caspase-like, or peptidyl-glutamyl peptide-hydrolyzing-like, PGPH-like), β2 (trypsin-like), β5 (chymotrypsin-like)] are proteolytically active. The 19S regulatory caps consist of the lid, which is responsible for recognition and docking of polyubiquitinylated proteins into the proteasome, and the base, which also contains ATPase activity required for unfolding and linearization of large proteins (Glickman and Ciechanover, 2002) (Figure 5).

Unlike common proteolytic enzymes which contain a catalytic triad, proteasome subunits belong to a special group termed N-terminal nucleophile hydrolases which all utilize the side chain of the N-terminal residue as the catalytic nucleophile. A variety of observations indicate that all three catalytic β-subunits, namely β1, β2, β5, indeed react with peptide bonds of substrates as well as with electrophilic functional groups of inhibitors through their hydroxyl group of the N-terminal threonine. Selectivity is dictated by the composition of the substrate binding pockets which differs in the three catalytic β-subunits (Kisselev *et al*., 2000; Moore *et al*., 2008).

Differing from the lysosome, which is mainly responsible for degrading extracellular and transmembrane proteins, the proteasome is in charge of degrading intracellular proteins that are aberrantly folded or normally short-lived. More than 90% of intracellular protein degradation is performed by the ubiquitin-proteasomal system (Lee and Goldberg, 1998). A large and growing body of evidence indicates that the proteasome affects cell-cycle progression in part by regulating the turnover of cyclins; inhibition of proteasome function causes cell-cycle arrest (Benanti, 2012). In addition, the proteasome can regulate apoptotic activity through effects on Bcl-2 family, NF-κB family, CIP/KIP family and p53-MDM2 complex (Shen et al., 2013). Therefore, the proteasome is crucial for cell survival and proliferation.

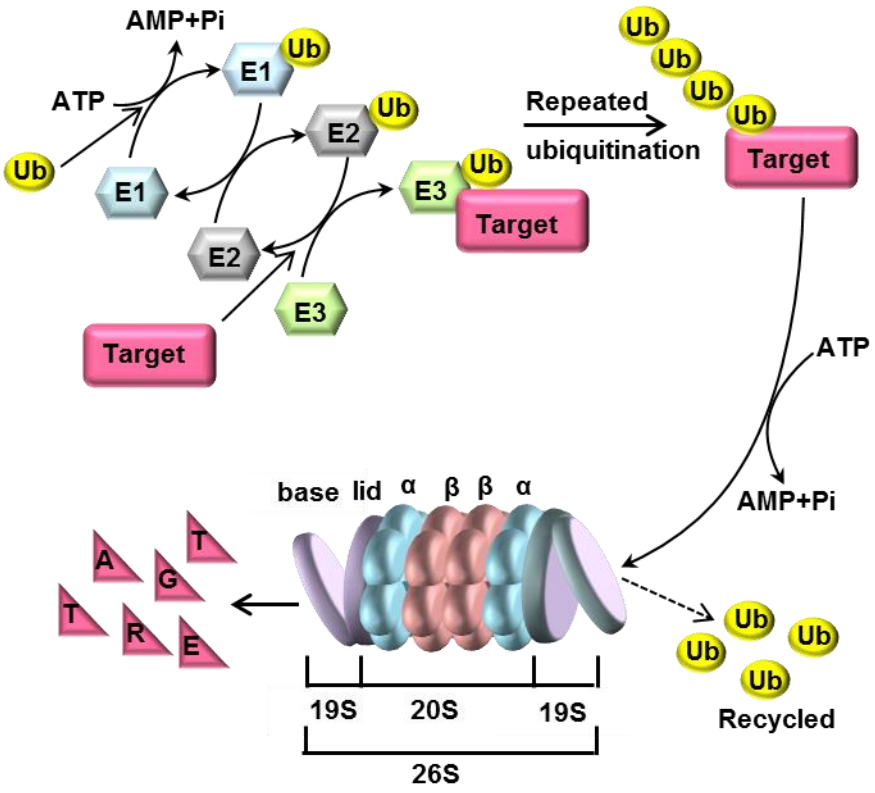

Figure 5. Schematic diagram of the ubiquitin proteasome pathway and the structure of the 26S proteasome.

Protein degradation by the UPS involves two distinct and successive steps, ubiquitination and proteasomal degradation. Ubiquitin conjugation occurs through an enzymatic cascade that involves three distinct enzymes, Ub-activating (E1), Ub-conjugating (E2) and Ub-ligating (E3). Ubiquitin is first activated by E1, then transferred to an E2, and finally transferred from the E2- to the E3-bound substrate. The poly-ubiquitinated proteins with a ubiquitin chain containing four or more K48-linkages are then directed to the 26S proteasome complex where the poly-ubiquitin chain will be removed and recycled and the protein substrates degraded into oligopeptides. The 26S proteasome complex is composed of the 20S catalytic core and two 19S regulatory particles. The 20S core is formed by two identical α rings and two identical β rings stacked in a symmetrical manner with the outside α rings surrounding the inner β rings. Each α or β ring contains seven different subunits, named α1-α7 or β1-β7, respectively. The 19S regulatory particle binds to both ends of the 20S core proteasome.

Proteasome inhibitors and resistance to proteasome inhibitors

A wide range of proteasome inhibitors has been developed during the past decade, most of which fall into six classes: peptide aldehydes (calpain inhibitor I and leupeptin), peptide boronates, peptide vinyl sulfones, peptide epoxyketones (epoxomycin and eponomycin), TMC-95 family of cyclic peptides (TMC-95A), and non-peptidic β-lactones (lactacystin and its derivatives such as salinosporamide A (NPI-0052)) (Adams, 2004; Borissenko and Groll, 2007). The last three classes are mainly composed of natural products. Most proteasome inhibitors bind covalently to the catalytic Thr1 residue in β1, β2 and β5 subunits with the exception of the cyclic peptide TMC-95 which shows non-covalent binding. As opposed to the reversible binding mode of peptide aldehydes and peptide boronates, binding of peptide vinyl sulfones, peptide epoxyketones and β-lactones to the proteasome has been shown to be irreversible (Moore *et al*., 2008).

Bortezomib (Velcade, PS-341), a dipeptide boronic acid (Figure 6), is the first proteasome inhibitor approved by the FDA for the treatment of relapsed multiple myeloma and mantle cell lymphoma. Despite the appreciable therapeutic outcome of bortezomib in the clinic, like almost all anti-cancer drugs, resistance to their use becomes an issue after some period of time (Richardson et al., 2003; Ruschak et al., 2011). Bortezomib resistance has also been observed in newly diagnosed patients receiving bortezomib monotherapy treatment for the first time (Dispenzieri et al., 2010; Ruschak et al., 2011). These clinical observations indicate that bortezomib resistance could be either acquired or inherent. The results from cell-based studies suggest that the mechanisms mediating bortezomib resistance include increased mRNA and protein expression of the proteasomal β5 subunit (Lu et al., 2008; Oerlemans et al., 2008; Shuqing et al., 2011),

mutations in the β5 subunits that impair bortezomib binding (Oerlemans et al., 2008; Franke et al., 2011), upregulation of the endoplasmic reticulum chaperone protein GRP78 (Kern et al., 2009), upregulation of multidrug transporter P-glycoprotein (Gutman et al., 2009), constitutive activation of NF-κB pathway (Markovina et al., 2008), as well as upregulation of insulin-like growth factor 1 (IGF-1) signaling (Kuhn et al., 2012). Indeed, it is unlikely that one specific mechanism confers bortezomib resistance and likely that the contribution of diverse factors may lead to the development of bortezomib resistance (Chauhan et al., 2005).

Therefore, second generation proteasome inhibitors have been developed in an attempt to increase the efficacy and overcome bortezomib resistance. Among them, carfilzomib (Kyprolis®, PR-171) became the runner-up approved by the FDA for the treatment of multiple myeloma in 2012. Carfilzomib belongs to the peptide epoxyketone class of proteasome inhibitors (Figure 6). This class represents the most specific and potent proteasome inhibitors discovered thus far. Carfilzomib has been shown to be more specific than borzetomib, with little or no off-target activity outside of the proteasome (Ruschak et al., 2011).

Besides the above-mentioned proteasome inhibitors, a growing group of natural dietary or medicinal products have been found to possess proteasome-inhibitory activity. These include epigallocatechin gallate (EGCG), genistein, apigenin, quercetin, resveratrol, curcumin, shikonin, celastrol, and withaferin A (Landis-Piwowar *et al*., 2006; Yang *et al*., 2009).

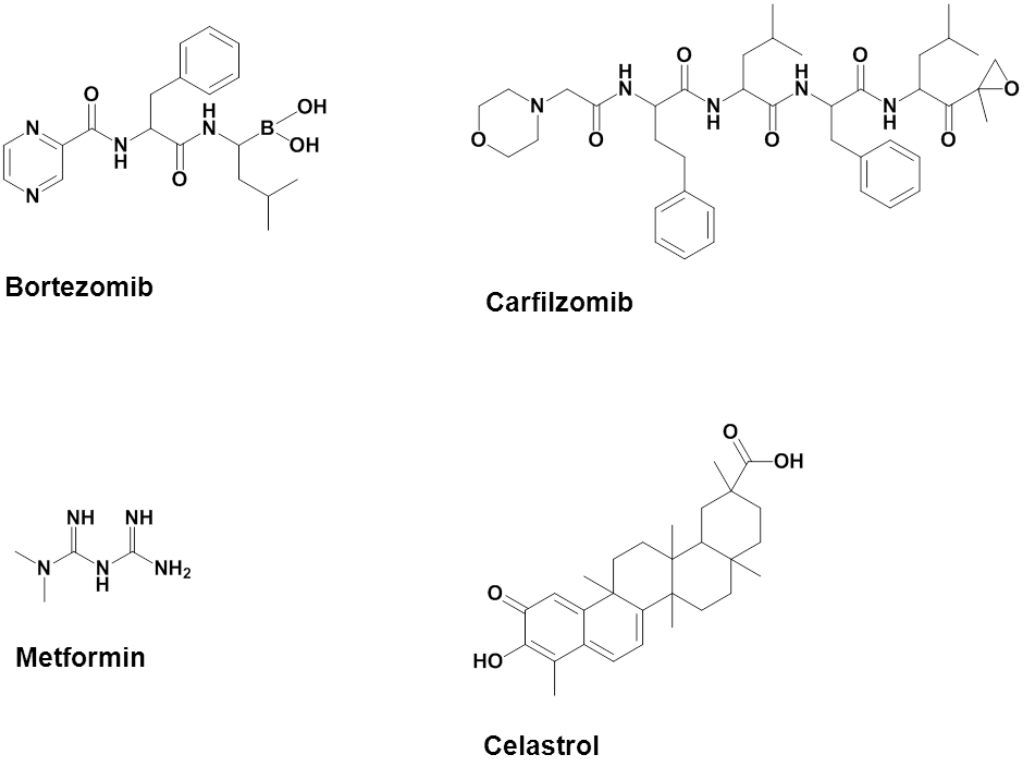

Figure 6. Chemical structures of bortezomib, carfilzomib, metformin and celastrol.

Metformin and AMP-activated protein kinase signaling

AMP-activated protein kinase (AMPK) has recently drawn more and more attention for being a potential target in cancer therapy. The idea was initially derived from the fact that AMPK is a major mediator of the function of metformin, a widely prescribed anti-diabetic drug, and that consumption of metformin is associated with reduced cancer risk (Zhou et al., 2001; Evans et al., 2005). AMPK is a highly conserved serine/threonine kinase that serves as a metabolic sensor for the maintenance of cellular energy homeostasis. It is activated under conditions that increase AMP:ATP ratio such as nutrition deprivation, hypoxia, ischemia and heat shock. AMPK is a heterotrimer consisting of one catalytic subunit (α) and two regulatory subunits (β and γ) (Woods et al., 1996). Phosphorylation of AMPKα at Thr172 is required for its catalytic activity (Hawley et al., 1996; Stein et al., 2000). AMPKβ is the scaffold that connects AMPKα and AMPKγ (Woods et al., 1996). AMPKγ senses intracellular AMP:ATP ratio and facilitates AMPKα activation upon AMP binding (Cheung et al., 2000). Several upstream serine/threonine kinases have been identified as capable of phosphorylating AMPKα, including liver kinase B1 (LKB1, also known as STK11) (Hawley et al., 2003), calcium/calmodulin-dependent protein kinase kinase β (CaMKKβ) (Hawley et al., 2005), and transforming growth factor β-activated kinase 1 (TAK1, also known as MAP3K7) (Momcilovic et al., 2006). Activated AMPK in turn phosphorylates its substrates such as acetyl-Coenzyme A carboxylase (ACC) at Ser79 (Davies et al., 1990), regulatory-associated protein of mTOR (Raptor) at Ser792 (Gwinn et al., 2008), and tuberous sclerosis protein 2 (TSC2) at Ser1345 (Inoki et al., 2003) (Figure 7).

Metformin is a biguanide compound (Figure 6), originates from the French lilac. It is transported into cells by organic cation transporter 1 (OCT1). Once entered the cell, it inhibits complex 1 of the mitochondrial respiratory chain, thereby increases intracellular AMP level. Accumulated AMP binds to AMPK and promotes its activation (Fogarty and Hardie, 2010). Besides metformin, AMPK can be activated by several other pharmacological activators such as 5-aminoimidazole-4-carboxamide riboside (AICAR) (Corton et al., 1995), resveratrol (Hwang et al., 2007), berberine (Turner et al., 2008), A-769662 (Cool et al., 2006), PT1 (Pang et al., 2008) and salicylate (Hawley et al., 2012) through different mechanisms of action. We have also reported that green tea polyphenol epigallocatechin gallate (EGCG) analogs and a formulated 3,3'-Diindolylmethane (B-DIM) can act as AMPK activators (Chen et al., 2012a; Chen et al., 2012b). The overall goal of AMPK activation is to restore cellular energy balance by promoting ATP generating processes meanwhile suppressing ATP consuming processes. In actively proliferating cells, it has been reported that AMPK activation caused cell cycle arrest *via* up-regulation of the p53-p21 axis (Motoshima et al., 2006).

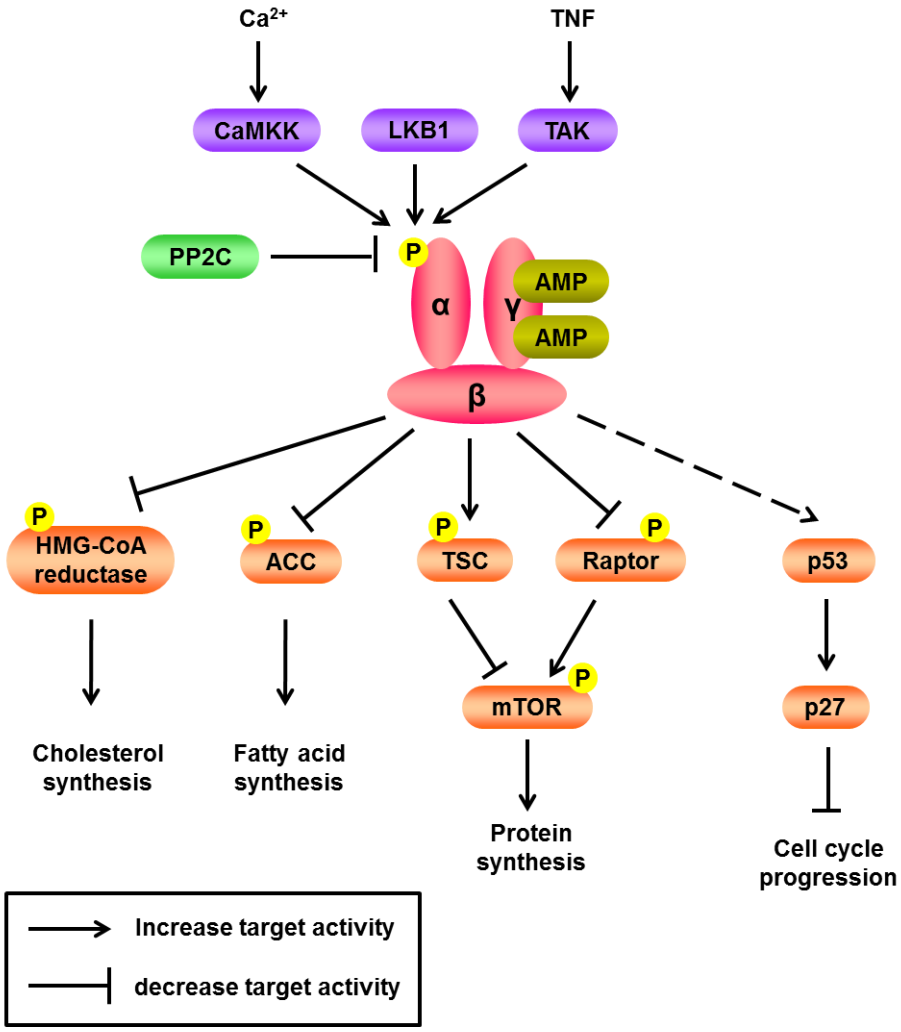

Figure 7. Schematic diagram of AMPK complex and signaling pathway.

AMPK is a heterotrimer consisting of one catalytic subunit (α) and two regulatory subunits (β and γ). Phosphorylation of AMPKα at Thr172 is required for its catalytic activation. AMPKβ is the scaffold that connects AMPKα and AMPKγ. AMPKγ senses intracellular AMP:ATP ratio and facilitates AMPKα phosphorylation upon AMP binding. Several upstream serine/threonine kinases have been identified as capable of phosphorylating AMPKα, including liver kinase B1 (LKB1, also known as STK11), calcium/calmodulin-dependent protein kinase kinase β (CaMKKβ), and transforming growth factor β-activated kinase 1 (TAK1, also known as MAP3K7). Activated AMPK in turn phosphorylates its substrates such as acetyl-Coenzyme A carboxylase (ACC), regulatory-associated protein of mTOR (Raptor), tuberous sclerosis protein 2 (TSC2), and HMG-CoA reductase.

Celastrol

Celastrol, a quinone methide triterpene (Figure 6), is isolated from the root bark of Thunder God Vine (*Tripterygium wilfordii* Hook F., TWHF), a perennial vine of Celastraceae family (bittersweet) (Salminen et al., 2010; Yang and Dou, 2010). Celastrol has exhibited promising anticancer activity in different cancer cells including leukemia and solid tumors both *in vitro* and *in vivo* (Salminen et al., 2010; Yang and Dou, 2010). It can inhibit cancer cell proliferation, induce apoptosis, prevent their malignant tissue invasion and suppress tumor angiogenesis (Salminen et al., 2010; Yang and Dou, 2010). It has also been reported that celastrol is able to eradicate acute myeloid leukemia at the progenitor and stem cell level (Hassane et al., 2008). Several molecular targets of celastrol have been identified, including HSP90 (Hieronymus et al., 2006), NF-κB (Lee et al., 2006) as well as proteasome (Yang et al., 2006). Besides, celastrol has been reported as a chemosensitizer and a radiosensitizer. It can sensitize resistant melanoma cells to the effect of temozolomide, an alkylating agent, in a synergistic manner (Chen et al., 2009). It also potentiates radiotherapy in hormone-refractory prostate cancer cells by impeding DNA damage repair and augmenting apoptosis (Dai et al., 2009). Additionally, we found that celastrol exhibited potent chemosensitizing activity in K562 leukemia cells, associated with decreased level of Bcr-Abl oncoprotein (Davenport et al., 2010).

A few studies have been done to identify the molecular targets of celastrol. In 2006, our group, for the first time, reported that inhibition of the proteasome by celastrol is one of the mechanisms responsible for its anticancer activity. Celastrol potently and preferentially inhibits the chymotrypsin-like activity of a purified 20S proteasome (IC_{50} = 2.5 μmol/L) and human prostate cancer cellular 26S proteasome (at 1-5 μmol/L).

Inhibition of the proteasome activity by celastrol in prostate cancer cells results in the accumulation of ubiquitinated proteins and cellular proteasome substrates (I-κBα, Bax, and p27) as well as induction of apoptosis. Treatment of tumor-bearing nude mice with celastrol (1-3 mg/kg/d, i.p., 1-31 days) resulted in significant inhibition of the tumor growth, as well as inhibition of the proteasomal activity and induction of apoptosis in tumor tissue (Yang *et al*., 2006). In the same year, the HSP90 inhibitory activity of celastrol was reported by the Golub group through a chemical genomic approach (Hieronymus *et al.*, 2006). Also in the same year, the Lee group reported that celastrol is a NF-κB inhibitor through inhibiting IKK (inhibitor of NF-κB kinase) activity (Lee *et al.*, 2006). Ensuing studies further demonstrated that celastrol activates HSF1 (heat shock transcription factor-1) and induces HSP70 response. Besides, celastrol was reported to inactivate Cdc37 and p23, both of which are co-chaperones of HSP90 (Salminen *et al.*, 2010).

CHAPTER 2

Sensitizing Hormone-Refractory Prostate Cancer Cells by Targeting an AMP-activated Protein Kinase-Androgen Receptor Regulatory Loop

Metformin is a widely prescribed anti-diabetic drug. One of the major mechanisms responsible for the biological activity of metformin is activation of AMPK, a central metabolic sensor within the cell (Zhou et al., 2001). Epidemiological studies have suggested that metformin consumption is associated with a reduced risk of several types of cancer, including prostate cancer (Evans et al., 2005). It is well-known that androgen receptor is critical to the development and progression of prostate cancer (Richter et al., 2007). So far, the effect of metformin on prostate cancer has been investigated in preclinical studies as well as in clinical trials. However, the potential crosstalk between AMPK and AR signaling pathways remains unknown. In the current study, we investigated the interaction between AMPK and AR in prostate cancer cell models. We found that activation of AMPK by metformin caused decrease of AR protein level through suppression of AR mRNA expression and promotion of AR protein degradation, demonstrating that AMPK activation is upstream of AR downregulation. We also found that inhibition of AR function by an anti-androgen or its siRNA enhanced metformin-induced AMPK activation and cell growth inhibition whereas overexpression of AR delayed AMPK activation and increased prostate cancer cellular resistance to metformin treatment, suggesting that AR suppresses AMPK signaling-mediated growth inhibition in

a feedback mechanism. Our findings thus reveal a novel AMPK-AR regulatory loop in prostate cancer cells and should have a potential clinical significance.

Materials and Methods

Materials. Metformin and bicalutamide (Casodex®) were purchased from Toronto Research Chemicals (North York, Ontario, Canada). 6-[4-(2-Piperidin-1-ylethoxy)phenyl]-3-pyridin-4-ylpyrazolo[1,5-a]pyrimidine (Compound C) and 3-(4,5-dimethylthiazol-2-yl)-2,5-diphenyltetrazolium bromide (MTT) were obtained from Sigma-Aldrich (St. Louis, MO). Dimethyl sulfoxide (DMSO) was obtained from Fisher Scientific (Pittsburgh, PA). Antibodies against poly(ADP-ribose) polymerase (PARP)-1 (F-2), AR (N-20), cyclin A (BF-683), and actin (C-11) were from Santa Cruz Biotechnology (Santa Cruz). Antibodies against AMPKα (23A3), phospho-AMPKα (Thr172) (40H9), phospho-ACC (Ser79), and phospho-Raptor (Ser792) were purchased from Cell Signaling Technology (Danvers, MA). RPMI1640, penicillin and streptomycin were obtained from Invitrogen (Carlsbad, CA) and fetal bovine serum (FBS) was from Aleken Biologicals (Nash, TX).

Cell culture. LNCaP and PC3 cells were obtained from American Type Culture Collection (Manasssa, VA). C4-2B cells were obtained from Prof. Leland Chung (Emory University, Atlanta, GA; and currently at Cedars-Sinai, Los Angeles, CA). PC3-AR cells (PC3 cells stably transfected with wild type AR) were obtained from Dr. Fazlul Sarkar (Wayne State University, Detroit, MI). These cell lines were grown in RPMI1640 medium supplemented with 10% FBS, 100 units/ml of penicillin and 100 µg/ml of streptomycin, and maintained in a humidified incubator at 37^{o}C and 5% CO_2.

MTT assay. Cells were seeded in a 96-well plate at ~70% (for 24 or 48 h treatment) or ~30% confluency (for more than 48 h treatment) 24 h ahead, followed by addition of drugs as indicated. After drug incubation, the media was removed and 100 µl

of MTT (1 mg/ml) was added. After 2 h incubation at 37°C, MTT was removed and 100 µl of DMSO was added to dissolve the purple formazon crystals. Colorimetric analysis was then performed at 560 nm by Wallac Victor 3 Multilabel Counter (PerkinElmer, Boston, MA). For experiments carried out with different duration periods, the longest time point was treated first and each subsequent treatment was carried out counting down to the shortest time point. After the incubation period for the longest time point, MTT assay was performed at the same time. This was to ensure that all the cells had the same environmental exposure for the same amount of time to reduce variability. The relative absorbance values are expressed as percentage of control (100%) and shown as means ± SD of triplicates.

DNA and siRNA transfection. For DNA transfection, PC3 cells were seeded in 60 mm dishes overnight and then transfected with AR DNA constructs (0.5 µg/ml in the medium) using Lipofectamine LTX (Invitrogen, Carlsbad, CA) for 24 hours. Empty vector transfection served as negative control. For siRNA transfection, LNCaP cells were seeded in six-well plates overnight and then transfected with AR siRNA duplexes (2.5 µg/ml in the medium) using RNAiFect (QIAGEN, Valencia, CA) for 72 hours. Both AR-specific siRNA (sense: 5'-GGAACUCGAUCGUAUCAUUTT-3'; antisense: 5'-AAUGAUACGAUCGAGUUCCTT-3') and negative control siRNA were ordered from QIAGEN (Valencia, CA).

Whole cell extract preparation. Cells were harvested, washed with ice-cold PBS twice, and homogenized in a lysis buffer [50 mM Tris-HCl at pH 8.0, 150 mM NaCl, 0.5% NP40 (v/v)]. After rocking at 4 ℃ for 30 min, the mixtures were centrifuged at 12,000 g for 15 minutes, and the supernatants were collected as whole cell extracts. The

protein concentrations in whole cell extracts were determined by Bio-Rad Protein Assay Kit (Bio-Rad Laboratories, Hercules, CA).

Caspase-3 activity assay. Fresh-made whole cell extract (20 μg per sample) was incubated with 20 μM fluorogenic caspase-3 substrate Ac-DEVD-AMC (Calbiochem, La Jolla, CA) in 100 μL of Tris-HCl (20 mM, pH 7.5). After 2 hours incubation at 37^{o}C, the AMC liberated from the fluorogenic substrate was detected spectrofluorometrically (λex = 355 nm and λem = 460 nm) by Wallac Victor 3 Multilabel Counter (PerkinElmer, Boston, MA). The data are expressed as percentage of control (100%) and shown as means ± SD of triplicates.

Western blot analysis. Whole cell extract (40 μg per sample) was denatured by boiling with 2x SDS sample buffer containing 5% β-mercaptoethanol (v/v), separated by 10% or 6% SDS-PAGE (Bio-Rad Laboratories, Hercules, CA) with Tris-glycine-SDS running buffer, transferred to a nitrocellulose membrane (GE Healthcare, Piscataway, NJ) with semi-dry transfer buffer, immunoblotted with indicated antibodies, and detected by HyGLO Chemiluminescent HRP Antibody Detection Reagent (Denville Scientific, Metuchen, NJ).

RNA isolation, reverse transcription, and quantitative real-time PCR. Total RNA from cells was isolated using the RNeasy Mini Kit (QIAGEN, Georgetown, MD) according to the manufacturer's protocol. RNA concentration was determined by NanoDrop 2000 spectrophotometer (Thermo Scientific, Wilmington, DE). Total RNA (170 ng) was reverse transcribed with random hexamer primers using the SuperScript III First-Strand Synthesis System (Invitrogen, Carlsbad, CA) according to the vendor's protocol. Two μL of the cDNA product was subjected to quantitative real-time PCR

using the StepOnePlus Real-Time PCR System (Applied Biosystems, Invitrogen) and TaqMan Fast Universal PCR Master Mix (Applied Biosystems, Invitrogen). All primers and TaqMan probes were purchased from the Applied Biosystems inventory (Invitrogen). All samples were measured in triplicates and normalized to the values for GAPDH. Data are expressed as fold change of 0 hour control (1.00) and shown as mean ± SD of triplicates.

Data analysis. Data are presented as means ± SD of triplicates.

Results

Decreased AR protein levels following AMPK activation in AR-positive prostate cancer cells. Toward the goal of understanding the roles of AR and AMPK in prostate cancer cell growth and death, we first measured the effect of metformin, a pharmacological AMPK activator, in AR-positive prostate cancer LNCaP and C4-2B cells. Both cell lines were treated with different concentrations of metformin for 48 hours followed by measurement of growth inhibition using MTT assay. Both LNCaP and C4-2B cell lines showed a dose-dependent growth inhibition after metformin treatment (Figure 8). To explore the molecular mechanism responsible for metformin-mediated growth inhibition, we performed a kinetic experiment in which LNCaP or C4-2B cells were treated with 30 mM metformin for 2, 4, 8, 12, 16 or 24 hours. We observed that AMPK activation occurred as early as 2 hours after treatment, manifested by increased levels of phospho-AMPKα (Thr172) as well as its downstream target phospho-ACC (Ser79), whereas the total AMPKα level remained the same (Figure 9). Importantly, following AMPK activation, AR protein level decreased significantly in a time-dependent manner (Figure 9). Following AR protein level decrease, a significant induction of apoptosis was observed after 24-hour metformin treatment, as measured by increased levels of caspase-3 activity and PARP cleavage (Figures 9 & 10). PARP is the best characterized cellular proteolytic substrate of caspase-3/7, being cleaved during the execution phase of apoptosis. These results suggest that metformin-induced AMPK activation is associated with AR protein decrease which could further contribute to apoptosis induction in AR-positive prostate cancer cells.

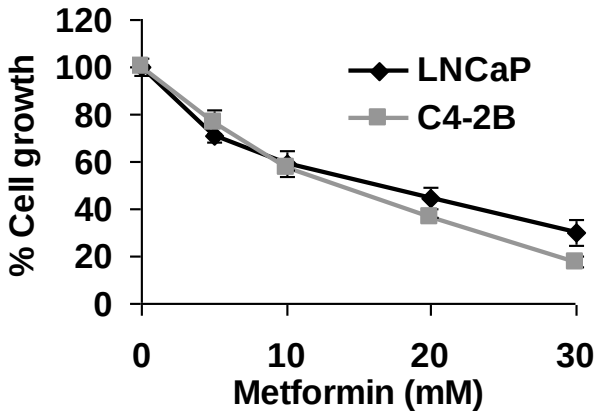

Figure 8. Metformin induced growth inhibition in LNCaP and C4-2B cells.

LNCaP and C4-2B cells were seeded in a 96-well plate at ~70% confluency 24 hours ahead. The cells were treated with metformin at concentrations of 5, 10, 20 or 30 mM for 48 hours, followed by MTT assay. The data are expressed as percentage of vehicle-treated control (100%) and shown as means ± SD of triplicates.

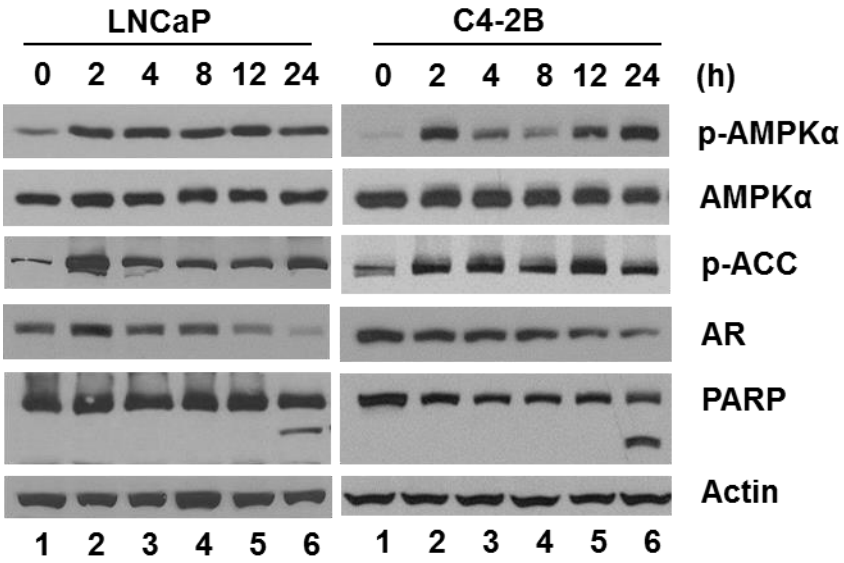

Figure 9. Kinetic analysis of the effect of metformin in LNCaP cells and C4-2B cells.

LNCaP and C4-2B cells were treated with 30 mM metformin for up to 24 hours, followed by Western blot analysis. p-AMPKα, AMPKα phosphorylated at Thr172; p-ACC, ACC phosphorylated at Ser79.

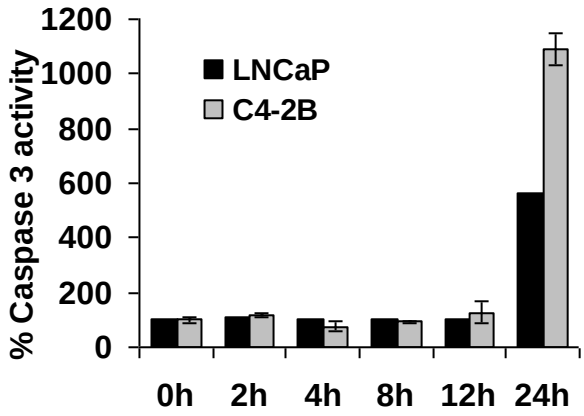

Figure 10. Activation of caspase-3 in LNCaP and C4-2B cells with metformin treatment.

LNCaP and C4-2B cells were treated with 30 mM metformin for up to 24 hours. Whole cell extraction was prepared and subjected to caspase-3 activity assay using a fluorogenic substrate (Ac-DEVD-AMC) specific for caspase-3/7, as described in Materials and Methods. The data are expressed as percentage of control at time 0 (100%) and shown as means ± SD of triplicates.

To elucidate the mechanism(s) through which AMPK activation decreases AR protein level, we performed a quantitative real-time PCR analysis to measure the change of AR mRNA expression over the same time period of metformin treatment. As shown in Figure 11, the expression of AR mRNA decreased in a time-dependent manner (black solid line), which matched the decrease of AR protein level (grey dash line, quantification of AR protein from Figure 9, left panel), suggesting that the decrease of AR protein level is, at least partially, due to the decrease of AR mRNA expression. These data also indicate that AR protein decrease is a direct effect of AMPK activation rather than a consequence of apoptosis.

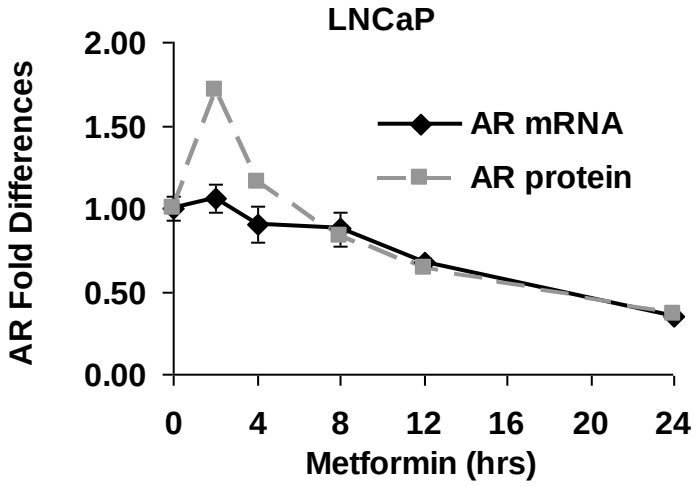

Figure 11. Expression of AR mRNA and protein in LNCaP cells after treatment with metformin.

LNCaP cells were treated with 30 mM metformin for up to 24 hours, followed by quantitative real-time PCR analysis. Black solid line is the quantification of AR mRNA expression after normalizing to GAPDH; data are expressed as fold change of 0 hour control (1.00) and shown as mean ± SD of triplicates. Grey dash line is the quantification of AR protein expression in the left panel of Figure 9 after normalizing to actin.

Even though metformin has been proved as a quite safe drug when used for the treatment of type 2 diabetes, the concentrations used in cultured cancer cells are significantly higher than that used in diabetic patients. To test if chronic exposure to low dose metformin can also induce AR protein decrease and cell death, we treated LNCaP and C4-2B cells with 1.25, 2.5, 5 or 10 mM metformin for up to five days. In this experiment, cells were plated at ~30% confluency 24 hours ahead. The five-day treatment was carried out first and each subsequent treatment was carried out counting down to the one-day treatment. At the end of treatment, MTT assay was performed at the same time. This was to ensure that all the cells had the same environmental exposure for the same amount of time to reduce variability. In both cell lines, we observed a dose- and time-dependent cell growth inhibition by metformin exposure (Figures 12 & 13). We further studied protein expression and phosphorylation profile in LNCaP cells treated with 5 mM metformin for up to 5 days. The phospho-AMPK level increased gradually, along with the increase of phospho-ACC level; whereas the total AMPK level remained the same throughout the experiment (Figure 14). Accompanied with AMPK activation was the gradual decrease of AR protein level and full-length PARP (Figure 14). These results verified that metformin at a clinically relevant setting was capable of inducing AR protein decrease and inhibiting prostate cancer cell growth.

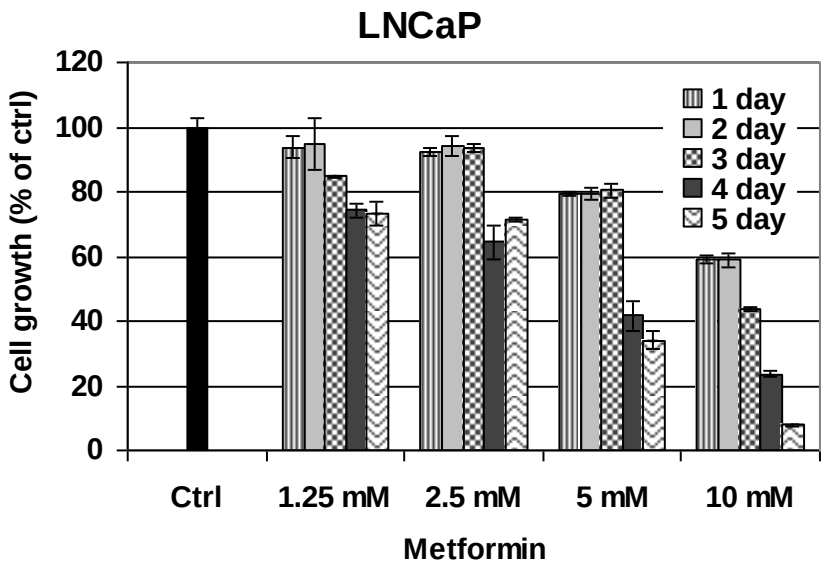

Figure 12. Growth inhibitory effect of metformin in LNCaP cells.

LNCaP cells were seeded in a 96-well plate at ~30% confluency 24 hours ahead. The cells were treated with metformin at concentrations of 1.25, 2.5, 5 or 10 mM for up to 5 days. The five-day treatment was carried out first and each subsequent treatment was carried out counting down to the one-day treatment. At the end of treatment, MTT assay was performed at the same time. The data are expressed as percentage of vehicle-treated control (100%) and shown as means ± SD of triplicates.

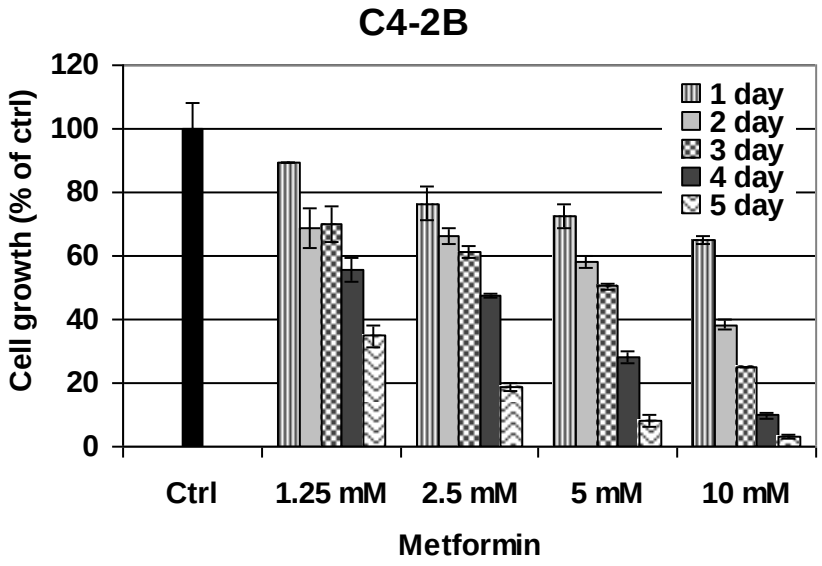

Figure 13. Growth inhibitory effect of metformin in C4-2B cells.

C4-2B cells were seeded in a 96-well plate at ~30% confluency 24 hours ahead. The cells were treated with metformin at concentrations of 1.25, 2.5, 5 or 10 mM for up to 5 days. The five-day treatment was carried out first and each subsequent treatment was carried out counting down to the one-day treatment. At the end of treatment, MTT assay was performed at the same time. The data are expressed as percentage of vehicle-treated control (100%) and shown as means ± SD of triplicates.

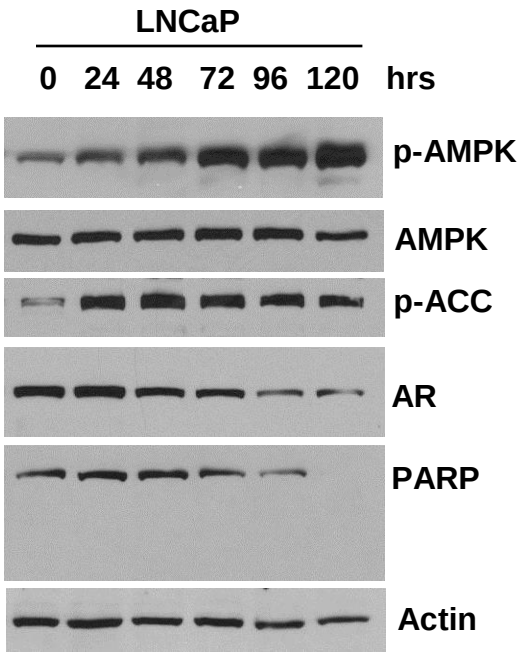

Figure 14. Kinetics of low-dose metformin in LNCaP cells.

LNCaP cells were treated with 5 mM metformin for 24, 48, 72, 96 or 120 hours, followed by Western blot analysis. p-AMPKα, AMPKα phosphorylated at Thr172; p-ACC, ACC phosphorylated at Ser79.

Inhibition of AR function facilitates metformin-induced AMPK activation and growth inhibition in AR-positive prostate cancer cells. That AR is located downstream of AMPK activation suggests that AR might function as an inhibitor of AMPK-mediated prostate cancer cell growth suppression. If so, we would predict that targeting and inhibiting AR could facilitate AMPK signaling. For this purpose, we used bicalutamide, a clinically used non-steroidal anti-androgen for the treatment of prostate cancer (Kolvenbag et al., 1998). We first evaluated the effect of metformin plus bicalutamide or each alone in AR-positive LNCaP and C4-2B cells by MTT assay. Bicalutamide enhanced metformin-induced growth inhibition in both cell lines (Figures 15 & 16). To understand the involved molecular mechanism, we performed a kinetic experiment using LNCaP cells treated with metformin alone or in combination with bicalutamide for up to 24 hours, followed by measuring AMPK signaling and AR status. Compared to metformin treatment alone, the bicalutamide plus metformin combination induced an earlier (2 h *vs*. 4 h) and higher (up to 5.0 fold *vs*. 2.3 fold at 4-8 h) level of AMPK activation, manifested by phosphorylation of AMPKα (Figure 17, lanes 7-12 *vs*. 1-6). In comparison, there was little difference in total AMPKα protein levels between metformin alone and combination treatment (Figure 17). Consistently, we also observed earlier phosphorylation of AMPK downstream targets ACC (at Ser79) and Raptor (at Ser792) (Figure 17). These data support the conclusion that AR is an inhibitor of AMPK signaling in prostate cancer cells. Along with prompt and enhanced AMPK activation induced by the combination treatment, earlier AR protein level decrease (12 h *vs.* 24 h) was also observed (Figure 17). Taken together, these data demonstrate that addition of

bicalutamide promotes AMPK activation and AR protein decrease in AR-positive prostate cancer cells.

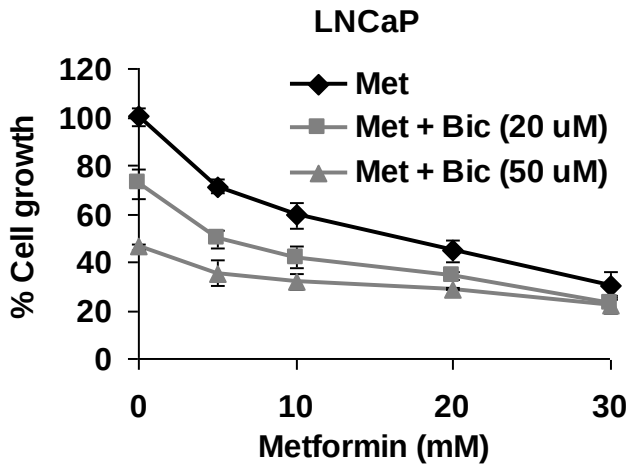

Figure 15. Bicalutamide promoted metformin-induced growth inhibition in LNCaP cells.

LNCaP cells were seeded in a 96-well plate at ~70% confluency 24 hours ahead. The cells were treated with various concentrations of metformin in the presence or absence of bicalutamide (Bic) at indicated concentrations for 24 hours, followed by MTT assay. The data are expressed as percentage of vehicle-treated control (100%) and shown as means ± SD of triplicates.

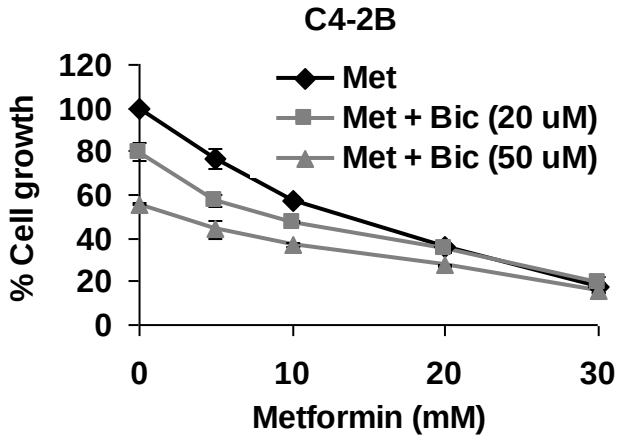

Figure 16. Bicalutamide promoted metformin-induced growth inhibition in C4-2B cells.

C4-2B cells were seeded in a 96-well plate at ~70% confluency 24 hours ahead. The cells were treated with various concentrations of metformin in the presence or absence of bicalutamide (Bic) at indicated concentrations for 24 hours, followed by MTT assay. The data are expressed as percentage of vehicle-treated control (100%) and shown as means ± SD of triplicates.

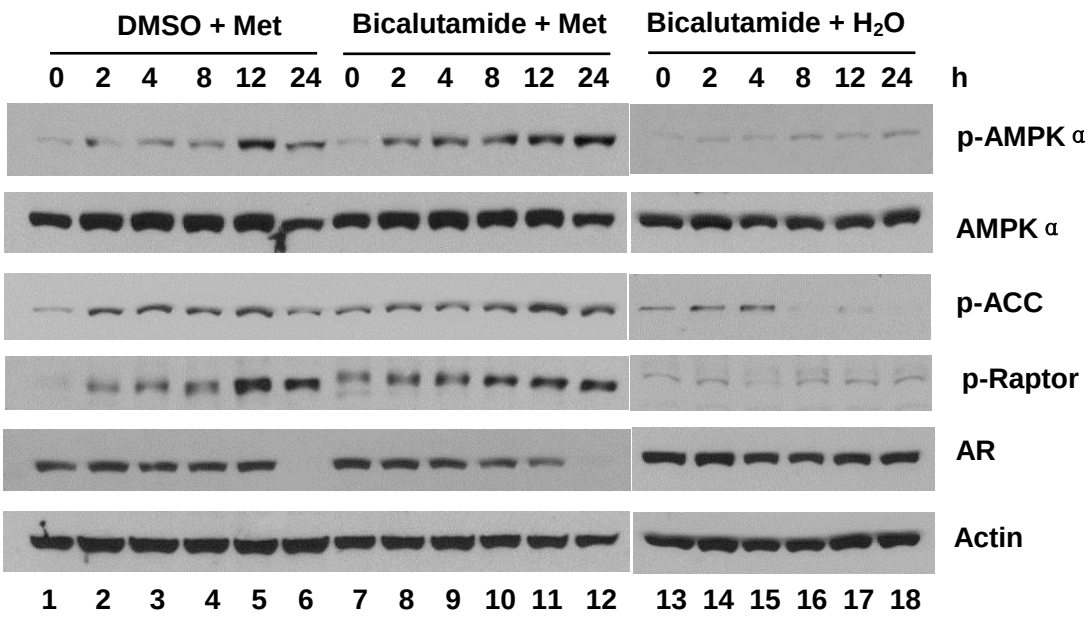

Figure 17. Bicalutamide promoted metformin-induced AMPK activation and AR degradation in LNCaP cells.

LNCaP cells were treated with metformin (30 mM), bicalutamide (20 μM), or metformin (30 mM) plus bicalutamide (20 μM) for up to 24 hours, followed by Western blot analysis. p-AMPKα, AMPKα phosphorylated at Thr172; p-ACC, ACC phosphorylated at Ser79; p-Raptor, Raptor phosphorylated at Ser792.

AR inhibits AMPK activation. To further examine the hypothesis that AR is an inhibitor of AMPK signaling-mediated growth suppression in prostate cancer cells, we determined whether knockdown of AR by its specific siRNAs could facilitate metformin-induced AMPK activation. In this experiment, AR-positive prostate cancer LNCaP cells were transfected with scramble or AR-specific siRNA for 72 hours, followed by treatment of metformin at 10 and 20 mM for 4 hours. Compared to control cells, knockdown of AR resulted in significantly higher level of phospho-AMPKα induction upon metformin treatment, while total AMPKα protein remained unchanged (Figure 18), confirming that AR plays an inhibitory role upstream of AMPK activation, but not on AMPK protein level.

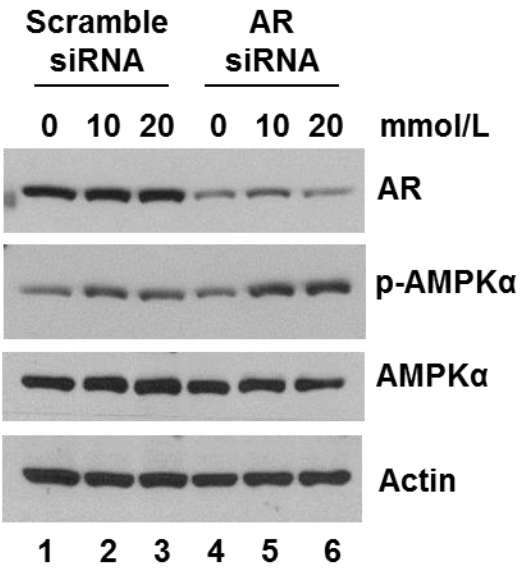

Figure 18. Effect of AR downregulation on metformin-induced AMPK activation in LNCaP cells.

AR-positive LNCaP cells were seeded at ~30% confluency 24 hours ahead and transfected with AR-specific siRNA (lanes 4-6) or scramble control (lanes 1-3) for 72 hours, and then treated with 10 or 20 mM metformin for 4 hours, followed by Western blot analysis. p-AMPKα, AMPKα phosphorylated at Thr172.

If AR is an inhibitor of AMPK signaling-mediated growth inhibition in prostate cancer cells, reintroduction of AR gene into AR-negative cells should be able to increase resistance to metformin. To test this, we compared the efficacy of metformin in parental PC3 cells (AR-negative) and PC3 cells with stable transfection of AR (PC3-AR) by MTT assay. As shown in Figure 19, PC3-AR cells exhibited much higher resistance to metformin than parental PC3 cells.

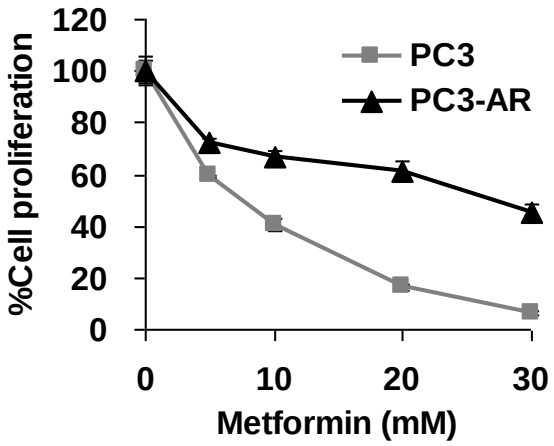

Figure 19. Effect of AR overexpression on metformin-induced growth inhibition in PC3 cells.

AR-negative parental PC3 cells and AR-transfected PC3-AR cells (stable transfection) were seeded in a 96-well plate at ~70% confluency 24 hours ahead. The cells were treated with metformin at 5, 10, 20 or 30 mM for 48 hours, followed by MTT assay. The data are expressed as percentage of vehicle-treated control (100%) and shown as means ± SD of triplicates.

We then studied the effect of AR on metformin-induced AMPK activation in PC-3 cells transiently transfected with AR construct. Compared to empty vector control, AR re-expression in PC3 cells delayed and suppressed metformin-induced AMPK activation (Figure 20, lanes 4-6 *vs*. 1-3). The total AMPKα levels were unchanged (Figure 20). We again observed decreased levels of transfected AR protein during metformin treatment (Figure 20). Taken together, these data suggest that reintroduction of AR into AR-negative prostate cancer cells enhances resistance to metformin by suppressing AMPK activation, further confirming that AR is an inhibitor of AMPK signaling-mediated growth suppression in prostate cancer cells.

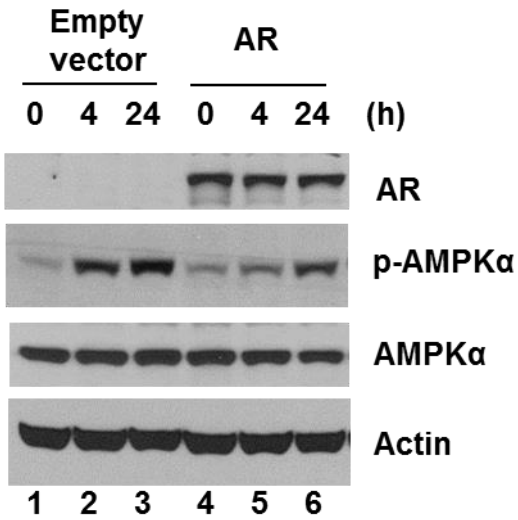

Figure 20. Effect of AR overexpression on metformin-induced AMPK activation in PC3 cells.

PC3 cells were transiently transfected with AR construct (lanes 4-6) or empty vector (lanes 1-3) for 24 hours, and then treated with 30 mM metformin for 0, 4 or 24 hours, followed by Western blot analysis. p-AMPKα, AMPKα phosphorylated at Thr172.

The functional domains in AR required for suppression of AMPK activation. Considering AR is a transcription factor, we asked the question whether AR-mediated suppression of AMPK activation is dependent on its transcriptional activity. For this purpose, we transfected PC3 cells with full length or various mutants of AR cDNAs, followed by metformin treatment. As a control, full length AR transfection again delayed metformin-indued AMPK activation from 4 to 24 h (Figure 21, lanes 4-6 *vs.* 1-3). Interestingly, similar to full length AR, both AR(A/B) construct, which only contains the N-terminal domain, and AR(Δ1-37) construct, which lacks the first 37 amino acids, reserved the ability to delay metformin-induced AMPK activation (Figure 21, lanes 7-9 and 16-18, respectively). In contrast, truncated forms AR(C/D), which contains only the DNA binding domain, and AR(D/E), which contains a part of ligand binding domain, failed to delay metformin-induced AMPK activation (Figure 21, lanes 10-12 and 13-15, respectively). This result suggests that the ability of AR to suppress AMPK activation requires the N-terminal domain of AR and may not require DNA-binding or ligand-binding domains of AR. It is therefore possible that AR inhibits AMPK activation through a direct protein-protein interaction mechanism with either AMPK itself or its upstream kinase(s) or phosphatase(s).

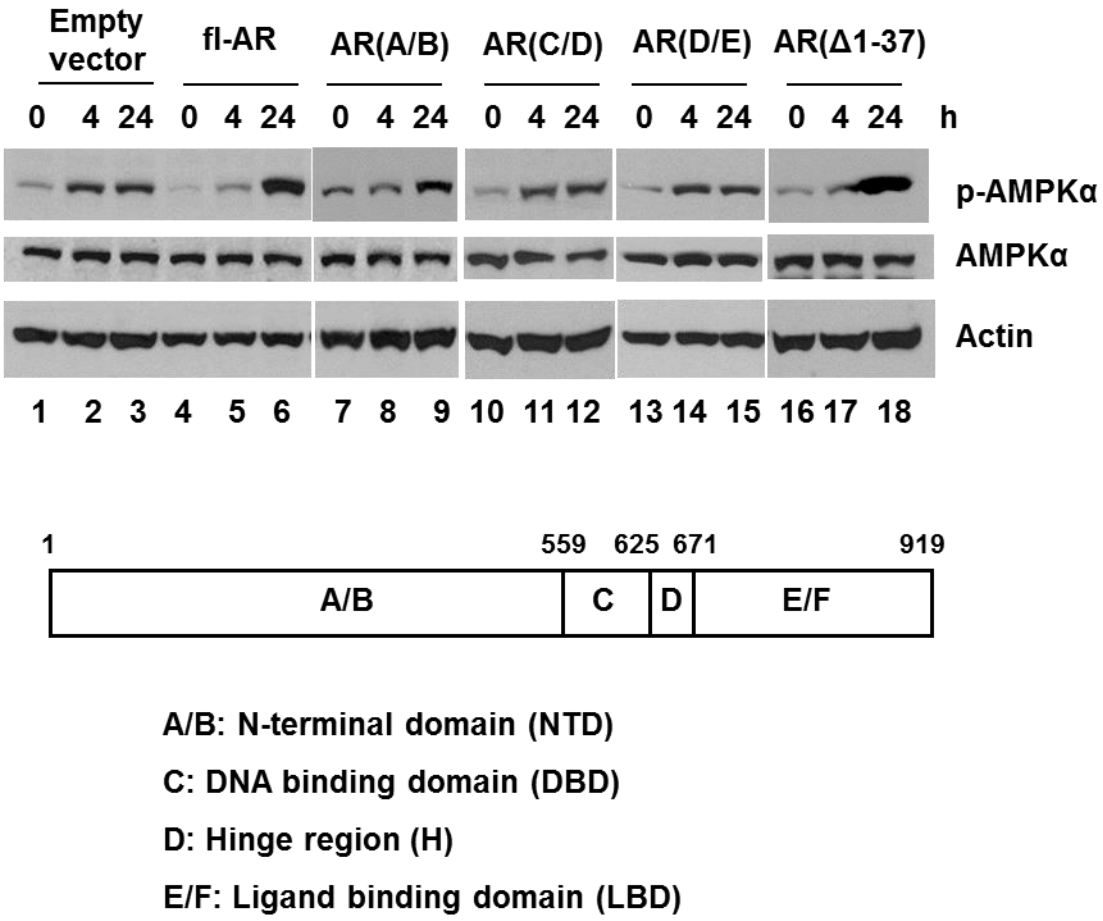

Figure 21. The functional domains in AR required for suppression of AMPK activation.

PC3 cells were transiently transfected with empty vector, full length (fl) AR, or indicated truncated AR constructs for 24 hours. Cells were then treated with 30 mM metformin for 0, 4 or 24 hours, followed by Western blot analysis. p-AMPKα, AMPKα phosphorylated at Thr172.

Inhibition of AMPK signaling prevented metformin-induced AR degradation. Finally, we studied whether metformin-induced AR protein downregulation could be blocked by Compound C, a chemical AMPK inhibitor (Zhou et al., 2001). Although it is a commonly used AMPK inhibitor in cell-based assays, it needs to be noted that Compound C has significantly limited specificity as an AMPK inhibitor with an IC50 value of 0.1-0.2 μM. At this concentration a number of other protein kinases were also inhibited, including ERK8, MNK1, PHK, MELK, DYRK isoforms, HIPK2, Src and Lck (Bain et al., 2007). In the cell culture medium, a concentration of 40 μM is needed to inhibit AMPK completely in cells (Bain et al., 2007).

In the current experiment, exponentially growing LNCaP cells were pretreated with 20 μM of compound C or the solvent DMSO for 12 hours, followed by metformin co-treatment for up to 30 hours. Cells treated with only compound C were also included as control. In untreated control cells, AR antibody recognized several bands with molecular weight lower than full-length AR (110 kDa), which could be the basal level of AR degradation fragments (Figure 22, lanes 1 and 13). These bands increased in cells treated with metformin, suggesting that, in addition to suppressed expression of AR mRNA (Figure 11), metformin treatment also causes AR protein degradation (Figure 22, lanes 2-5 vs. 1). Importantly, compared to the DMSO-pretreated cells, pretreatment with compound C prevented the generation of AR degradation fragments induced by metformin (Figure 22, lane 7-12 *vs*. lane 1-6). As expected, compound C also suppressed AMPK signaling as evident by decreased levels of its downstream substrates, phospho-ACC and phospho-Raptor (Figure 22, lanes 7-12 *vs*. 1-6). No AR degradation fragments were observed in cells treated with only compound C, either (Figure 22, lanes 14-19).

These results verify that activation of AMPK signaling is required for both induced and basal levels of AR protein degradation.

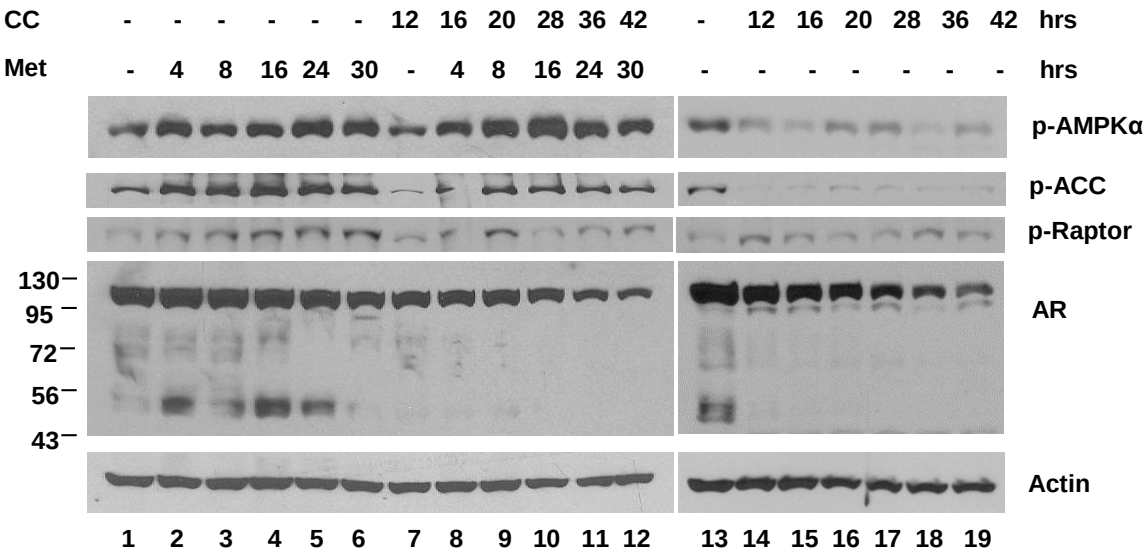

Figure 22. Compound C prevents metformin-induced AMPK activation and AR degradation in LNCaP cells.

LNCaP cells were pretreated with compound C (CC) at 20 μM (lanes 7-12) or equal volume of DMSO (lanes 1-6) for 12 hours, followed by co-treatment with 30 mM metformin (Met) for indicated hours. Cell lysates were prepared and subjected to Western blot analysis. p-AMPKα, AMPKα phosphorylated at Thr172; p-ACC, ACC phosphorylated at Ser79; p-Raptor, Raptor phosphorylated at Ser792.

Discussion

In the current study, we showed that (i) activation of AMPK by metformin caused decrease of AR protein level through suppressed expression of AR mRNA and promoted degradation of AR protein; and (ii) AR inhibited AMPK signaling-mediated growth suppression and apoptosis in prostate cancer cells by suppressing AMPK activation. Our findings reveal a novel AMPK-AR regulatory loop that plays a key role in determining prostate cancer cell growth and death (Figure 23).

AR plays a vital role in prostate cancer development and progression by regulating cell proliferation, differentiation and apoptosis (Richter et al., 2007). Degradation of AR is a critical step in the induction of apoptosis in prostate cancer cells under various cytotoxic stimuli. For example, a study by Li *et al* demonstrated that AR degradation is a direct effect of berberine, rather than a bystander effect of apoptosis (Li et al., 2011). Similarly, a novel curcumin analogue, B-DIM, was found to enhance androgen receptor degradation activity, thereby leading to inhibition of proliferation and induction of apoptosis in prostate cancer cells (Shi et al., 2009a). In the current study, we showed that metformin-induced AMPK activation caused AR protein decrease by suppression of AR mRNA expression and promotion of AR protein degradation (Figures 9, 11, 14 & 22). These data clearly suggest that the decrease of AR protein is a direct effect of AMPK activation rather than a consequence of apoptosis. This finding sheds light on a new pathway that can lead to downregulation of AR protein.

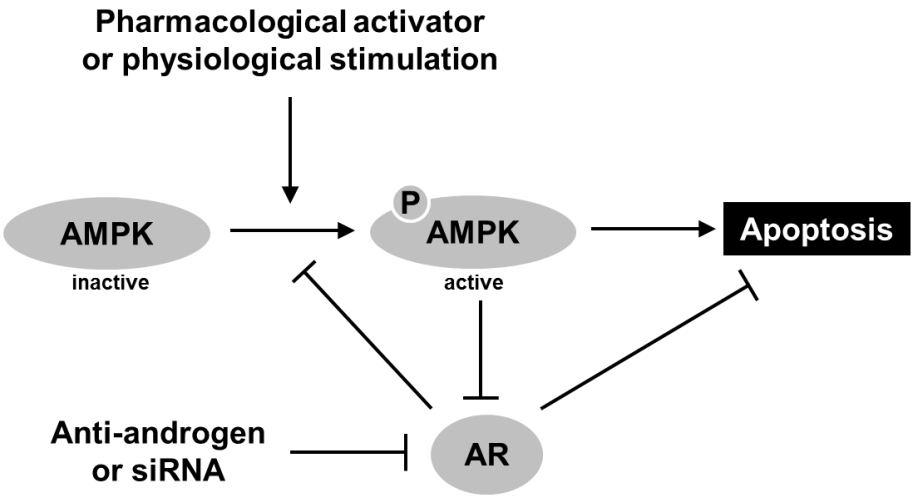

Figure 23. Schematic diagram represents the regulatory loop of AR and AMPK in prostate cancer cells.

The study presented in this chapter suggests that AR and AMPK negatively regulate each other in prostate cancer cells. On one hand, AMPK activation induced AR protein decrease; on the other hand, AR showed an inhibitory effect on AMPK signaling.

In the current study, we also showed that AR negatively regulates AMPK signaling-mediated growth arrest in prostate cancer cells by suppressing AMPK activation (Figures 18 & 20). Besides phosphatases such as protein phosphatase 2C (PP2C) which directly dephosphorylates AMPKα at Thr172 (Moore et al., 1991), a couple of other proteins have been reported to negatively regulate AMPK activity through different mechanisms. For example, Akt has been found to phosphorylate AMPKα at Ser485/491 which reduces phosphorylation of AMPKα at Thr172 that is required for AMPK activity (Horman et al., 2006). Similarly, Djouder *et al* reported that protein kinase A (PKA) directly associates with and phosphorylates AMPKα1 at Ser173 to impede Thr172 phosphorylation by LKB1 (Djouder et al., 2010). More recently, it was reported that the orphan nuclear receptor Nur77 negatively regulates AMPK activation by binding to and sequestering LKB1 in the nucleus (Zhan et al., 2012). In our case, we showed that the ability of AR to suppress AMPK activation requires the N-terminal domain of AR and does not need DNA-binding or ligand-binding domains of AR, suggesting the possible involvement of nonclassical effects of AR (Figure 21). Nowadays, the nonclassical effects of nuclear receptors have drawn more and more attention (Wehling and Losel, 2006). For example, in addition to classical intracellular AR, the membrane-bound form of AR has been identified and found to mediate the fast, nongenomic effects of steroid hormones (Kampa et al., 2002). Furthermore, the identification of numerous transcript variants of AR in various prostate cell lines and clinical samples, most of which lack partial or entire DNA binding domain, also stimulated the study on hormone-independent effects of AR (Gonit et al., 2011; Haile and

Sadar, 2011). Therefore, further investigation on how AR suppresses AMPK activation will definitely contribute to our understanding of the nonclassical effects of AR.

With respect to the concern of the apparent discrepancy between the concentrations of metformin used in cultured cells *vs.* in patients, there are several explanations. Typically the concentration of metformin used to activate AMPK in cultured cells is 1-20 mM. These are 1-2 orders of magnitude higher than the concentrations estimated to occur in human plasma (10-40 μM) following a therapeutic dose of around 30 mg/kg. One explanation is that many cultured cell lines lack the expression of OCT1 transporter that is required to transport biguanide compounds like metformin into the cell (Fogarty and Hardie, 2010). In contrast, OCT1 is highly expressed in liver, and facilitates the selective uptake of metformin into hepatocytes. In mice lacking OCT1, the effect of metformin on AMPK activation and gluconeogenesis is reduced, correlated with reduced hepatic accumulation of metformin (Wang et al., 2002). Another *in vivo* study showed that metformin accumulates in multiple tissues of diabetic mice in concentrations several fold higher than those in blood, with the greatest accumulation occurred in the small intestine (Wilcock and Bailey, 1994). These observations suggest that it may be possible to reach therapeutic levels in tumor tissue when used for cancer treatment. An alternative explanation for the discrepant concentration of metformin used in cultured cells and in patients involves the non-physiological growth conditions used in the cell culture models to assess the *in vitro* growth inhibitory effect of metformin. The majority of cancer cell lines are maintained in non-physiological conditions that are optimized for maximum growth and proliferation with extremely high amounts of growth factors and glucose in culture media. For instance,

tissue culture media usually contains 10-25 mM glucose which is well above the fasting level of glucose observed in non-diabetic patients (< 6 mM). Most tissue culture media is also supplemented with 5-10% fetal bovine serum, which contains high concentrations of growth factors and hormones such as insulin and EGF. Therefore, the excessive concentrations of glucose, insulin and growth factors in tissue culture media may account for the elevated doses of metformin required to elicit cellular responses *in vitro* (Dowling et al., 2012).

Another concern in the field of AMPK research is the use of Compound C as an AMPK inhibitor. Compound C is reported to act as a direct inhibitor of AMPKα in an ATP competitive manner (Zhou et al., 2001). Later on, a crystal structural study revealed that Compound C binding dramatically alters the conformation of the activation loop of AMPKα. This induced fit forms a Compound-C binding pocket which partially overlaps with the putative ATP-binding pocket on AMPKα, therefore competitively preventing ATP binding to AMPKα, which is the source of the phosphate group to be transferred to AMPK substrate by AMPK (Handa et al., 2011). As mentioned earlier, it is important to keep in mind that Compound C is a relatively non-specific AMPK inhibitor with an IC50 value of 0.1-0.2 μM. At this concentration a number of other protein kinases were also inhibited, including ERK8, MNK1, PHK, MELK, DYRK isoforms, HIPK2, Src and Lck (Bain et al., 2007). In the cell culture medium, Compound C at a concentration of 40 μM is needed to inhibit AMPK completely in cells (Bain et al., 2007). Given that no better AMPK inhibitor is available thus far, Compound C is still widely used to inhibit AMPK activity. Therefore, extra cautious needs to be paid to interpret the result involving the use of Compound C. In our current study, we observed the decrease of full-

length AR in groups treated with Compound C along as well as metformin plus Compound C but not in the group treated with metformin alone (Figure 22). Considering the non-specific property of Compound C, we speculate that the decrease of full-length AR in Compound C-treated groups is likely due to the cytotoxicity caused by the off-target effect of Compound C.

Although a large body of studies showed that AMPK activation induces growth arrest and/or cell death in many types of cancer cells, a few studies have conversely reported that AMPK could serve as a tumor promoter in prostate cancer and astrocytoma under certain conditions. For example, CaMKKβ, one of the AMPK upstream kinases, was found to be overexpressed in both hormone-sensitive and castrate-resistant prostate cancer cells and CaMKKβ-mediated activation of AMPK was found to be required for androgen-dependent migration of prostate cancer cells (Frigo et al., 2011; Massie et al., 2011). In the case of astrocytoma, Rios *et al* reported that oncogenic HRas mutation and Pten deletion lead to AMPK activation, and this activation is required to maintain cancer cell proliferation, which may involve AMPK-mediated phosphorylation of Rb protein (Rios et al., 2013). These findings stressed the necessity of proper interpretation of AMPK signaling according to different contexts. In addition, the isoform composition and the subcellular localization of AMPK complex might also affect the consequences of AMPK activation.

In summary, our current study demonstrated that activation of AMPK leads to a decrease in AR protein level, whereas AR, on the other hand, suppresses AMPK signaling-mediated cell growth inhibition in prostate cancer cells. These findings have established a new connection between AMPK and AR signaling pathways, and provided

preclinical evidence that administration of metformin or other APMK activators may benefit the therapeutic outcome of AR-positive prostate cancer.

CHAPTER 3

Overcoming Bortezomib Resistance by Inducing Activation of AMP-activated Protein Kinase in Multiple Myeloma Cells

While bortezomib as the first proteasome inhibitor used for the treatment of multiple myeloma achieved great success in clinical applications, resistance was observed in some of the patients (Moriuchi et al., 2010). Up-regulation of the insulin-like growth factor-1 (IGF-1)/ IGF-1 receptor (IGF-1R) axis was reported to contribute to the development of bortezomib resistance in cultured multiple myeloma cells, with increased autocrine and paracrine secretion of IGF-1, leading to increased activation of the IGF-1R (Kuhn et al., 2012). The mammalian target of rapamycin (mTOR) is one of the major downstream effectors of IGF-1R signaling. On the other hand, AMPK is known to negatively regulate the activity of the mTOR complex. The objective of the current study is to investigate whether inhibiting mTOR, the downstream effector of IGF-1R signaling, by activating AMPK could restore the response of bortezomib-resistant multiple myeloma cells to bortezomib. By using paired bortezomib-sensitive and -resistant multiple myeloma cells, we found that 1) bortezomib-sensitive and -resistant multiple myeloma cells are about equally sensitive to AMPK activators; 2) AMPK signaling is suppressed in bortezomib-resistant multiple myeloma cells; 3) the suppressed AMPK signaling in bortezomib-resistant multiple myeloma cells is intact and inducible by AMPK activators; 4) combination treatment with bortezomib and an AMPK activator is more effective than each drug alone in bortezomib-resistant multiple myeloma cells; 5)

bortezomib-resistant multiple myeloma cells used in the current study are cross-resistance to carfilzomib, and combination of carfilzomib with an AMPK activator also achieved better outcome than each drug alone. The findings from this study support the further investigation of AMPK signaling in multiple myeloma patient samples as well as *in vivo* evaluation of metformin use in multiple myeloma mouse models.

Materials and Methods

Materials. Metformin was purchased from Toronto Research Chemicals (North York, Ontario, Canada). 5-amino-1-β-D-ribofuranosyl-imidazole-4-carboxamide (AICAR) was purchased from Tocris Bioscience (Minneapolis, MN). Bortezomib (Velcade®) was purchased from LC Laboratories (Woburn, MA). Carfilzomib (Kyprolis®) was obtained from Drs. Jeffrey Zonder and Ramzi Mohammad. 3-(4,5-dimethylthiazol-2-yl)-2,5-diphenyltetrazolium bromide (MTT) was obtained from Sigma-Aldrich (St. Louis, MO). Sodium dodecyl sulfate (SDS) was obtained from Bio-Rad (Hercules, CA). Antibodies against poly(ADP-ribose) polymerase (PARP)-1 (F-2) and actin (C-11) were from Santa Cruz Biotechnology (Santa Cruz). Antibodies against AMPKα (23A3), phospho-AMPKα (Thr172) (40H9), phospho-ACC (Ser79), and phospho-Raptor (Ser792) were purchased from Cell Signaling Technology (Danvers, MA). RPMI1640, penicillin and streptomycin were obtained from Invitrogen (Carlsbad, CA). Fetal bovine serum (FBS) was obtained from Aleken Biologicals (Nash, TX). IL-6 was obtained from R&D systems (Minneapolis, MN).

Cell culture. ANBL6, ANBL6-V10R, Kas6, Kas6-V8R, 8226 and 8226 V7R multiple myeloma cell lines were obtained from Drs. Robert Orlowski and Deborah Kuhn (University of Texas M. D. Anderson Cancer Center, Houston, TX). All six cell lines were grown in RPMI1640 medium supplemented with 10% FBS, 100 units/ml of penicillin and 100 μg/ml of streptomycin, and maintained in a humidified incubator at 37^{o}C and 5% CO_2. IL-6 dependent ANBL6, ANBL6-V10R, Kas6 and Kas6-V8R cells were additionally supplied with 1 ng/ml IL-6 in the medium whereas IL-6 independent 8226 and 8226 V7R cells were not. Bortezomib-resistant ANBL6-V10R, Kas6-V8R and

8226 V7R cell lines were generated from corresponding parental cell lines by continuous drug exposure, and routinely maintained in mediums containing 10, 8 and 7 nM of bortezomib, respectively, to keep the bortezomib-resistant phenotype. Cells used for experiments were free of drug for at least three days.

MTT assay. Fifty µl cells were seeded in a 96-well plate (2~6 $\times 10^4$ cells/well), followed by addition of 50 µl drugs at indicated concentrations. After incubation for indicated amount of time, 100 µl MTT (5 mg/ml) was added. After another 2 hour incubation at 37°C, 50 µl of 10% SDS (pH 3.7) was added overnight for complete dissolution of the purple formazon crystals. Colorimetric analysis was then performed at 560 nm by Wallac Victor 3 Multilabel Counter (PerkinElmer, Boston, MA). The relative absorbance values are expressed as percentage of control (100%) and shown as means ± SD of triplicates.

Whole cell extract preparation. Cells were harvested, washed with ice-cold PBS twice, and homogenized in a lysis buffer [50 mM Tris-HCl at pH 8.0, 150 mM NaCl, 0.5% NP40 (v/v)]. After rocking at 4 ℃ for 30 min, the mixtures were centrifuged at 12,000 g for 15 minutes, and the supernatants were collected as whole cell extracts. The protein concentrations in whole cell extracts were determined by Bio-Rad Protein Assay Kit (Bio-Rad Laboratories, Hercules, CA).

Caspase-3 activity assay. Fresh-made whole cell extract (20 µg per sample) was incubated with 20 µM fluorogenic caspase-3 substrate Ac-DEVD-AMC (Calbiochem, La Jolla, CA) in 100 µL of Tris-HCl (20 mM, pH 7.5). After 2 hours incubation at 37°C, the AMC liberated from the fluorogenic substrate was detected spectrofluorometrically (λex = 355 nm and λem = 460 nm) by Wallac Victor 3 Multilabel Counter (PerkinElmer,

Boston, MA). The data are expressed as percentage of control (100%) and shown as means ± SD of triplicates.

Chymotrypsin-like activity assay. Fresh-made whole cell extract (10 μg per sample) was incubated with 20 μM fluorogenic substrate Suc-LLVY-AMC specific for the chymotrypsin-like activity of the 20S proteasome (Calbiochem, La Jolla, CA) in 100 μL of Tris-HCl (20 mM, pH 7.5). After 2 hours incubation at 37^{o}C, the AMC liberated from the fluorogenic substrate was detected spectrofluorometrically (λex = 355 nm and λem = 460 nm) by Wallac Victor 3 Multilabel Counter (PerkinElmer, Boston, MA). The data are expressed as percentage of control (100%) and shown as means ± SD of triplicates.

Western blot analysis. Whole cell extract (40 μg per sample) was denatured by boiling with 2x SDS sample buffer containing 5% β-mercaptoethanol (v/v), separated by 10% or 6% SDS-PAGE (Bio-Rad Laboratories, Hercules, CA), transferred to a nitrocellulose membrane (GE Healthcare, Piscataway, NJ), immunoblotted with indicated antibodies, and detected by HyGLO Chemiluminescent HRP Antibody Detection Reagent (Denville Scientific, Metuchen, NJ).

Statistical analysis. Data are presented as means ± SD of triplicates. Statistical analysis was performed with GraphPad Prism 6 software. To evaluate the differences between single drug- and multi drug-treated groups in three drug combination studies, the unpaired Student's *t*-test was applied with the level of significance set at $P < 0.05$.

Results

Bortezomib-resistant phenotype does not affect the inhibitory effect of AMPK activators on multiple myeloma cell growth. To investigate if bortezomib-resistant phenotype affects multiple myeloma cells in response to AMPK activators, we treated two pairs of bortezomib-sensitive parental multiple myeloma cells and their bortezomib-resistant counterparts (the ANBL6 *vs.* ANBL6-V10R pair which is IL-6 dependent; and the 8226 *vs.* 8226-V7R pair which is IL-6 independent) with metformin for 24 hours. Bortezomib treatment was used to verify the sensitivity of these cell lines to bortezomib (Figure 24). In contrast to the differential sensitivities to bortezomib, in both pairs, the bortezomib-sensitive and bortezomib-resistant cells were about equally sensitive to metformin-induced growth inhibition (Figure 25). Similarly, when treated with another AMPK activator, AICAR, the bortezomib-sensitive and bortezomib-resistant cells again exhibited comparable sensitivity (Figure 26). These results indicate that the bortezomib-resistant phenotype does not affect multiple myeloma cells in response to AMPK activators.

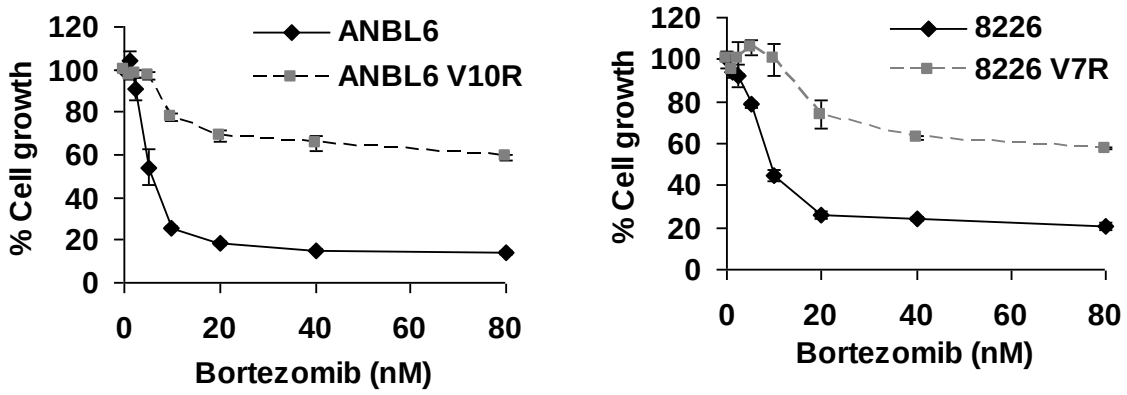

Figure 24. Comparison of bortezomib-induced growth inhibition in paired bortezomib-sensitive and -resistant multiple myeloma cells.

Exponentially growing paired bortezomib-sensitive (solid black line) and -resistant (dashed grey line) multiple myeloma cells were seeded in a 96-well plate (2~6 $\times 10^4$ cells/well), treated with bortezomib at indicated concentrations for 24 hours, followed by MTT assay. The data are expressed as percentage of vehicle-treated control (100%) and shown as means $\pm$ SD of triplicates.

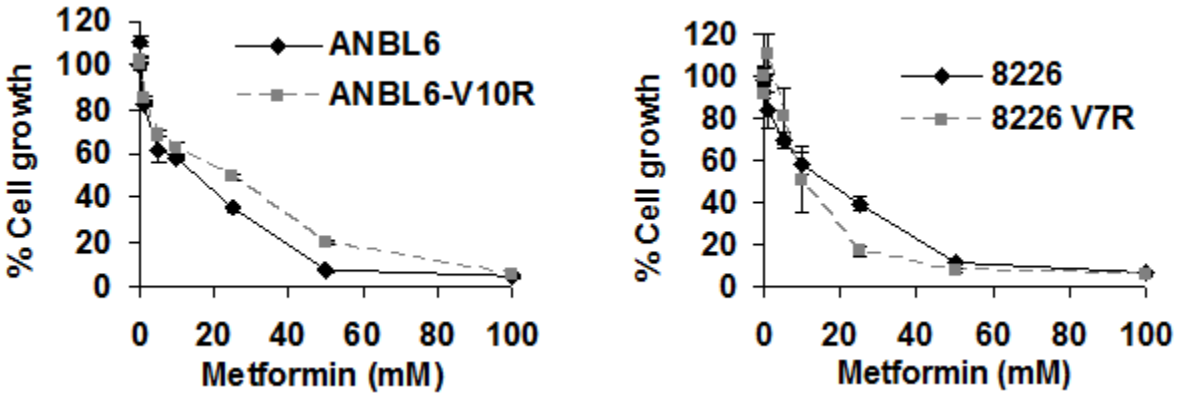

Figure 25. Comparison of metformin-induced growth inhibition in paired bortezomib-sensitive and -resistant multiple myeloma cells.

Exponentially growing paired bortezomib-sensitive (solid black line) and -resistant (dashed grey line) multiple myeloma cells were seeded in a 96-well plate (2~6 $\times 10^4$ cells/well), treated with metformin at indicated concentrations for 24 hours, followed by MTT assay. The data are expressed as percentage of vehicle-treated control (100%) and shown as means ± SD of triplicates.

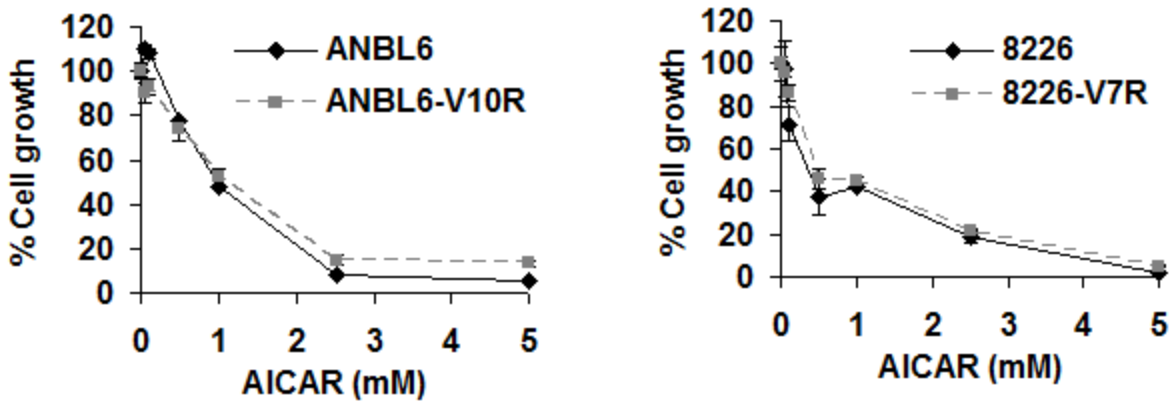

Figure 26. Comparison of AICAR-induced growth inhibition in paired bortezomib-sensitive and -resistant multiple myeloma cells.

Exponentially growing paired bortezomib-sensitive (solid black line) and -resistant (dashed grey line) multiple myeloma cells were seeded in a 96-well plate (2~6 $\times 10^4$ cells/well), treated with AICAR at indicated concentrations for 24 hours, followed by MTT assay. The data are expressed as percentage of vehicle-treated control (100%) and shown as means ± SD of triplicates.

Bortezomib-resistant multiple myeloma cells were cross-resistant to the second-generation proteasome inhibitor carfilzomib. Next, we wondered whether or not these bortezomib-resistant cells are cross-resistant to the next-generation proteasome inhibitor carfilzomib. Carfilzomib is developed for patients who are resistant or intolerant to bortezomib treatment. In contrast to bortezomib which is a reversible proteasome inhibitor, carfilzomib inhibits proteasomal activity in an irreversible way. As a member of the peptide epoxyketone-based proteasome inhibitors, carfilzomib represents one of the most specific and potent proteasome inhibitors discovered thus far. To determine whether our bortezomib-resistant cells are cross-resistant to carfilzomib, we treated two pairs of bortezomib-sensitive and -resistant cells with carfilzomib at various concentrations for 24 hours. As shown in Figure 27, bortezomib-resistant ANBL6-V10R and 8226-V7R cells were also resistant to carfilzomib, suggesting that alternative strategies other than second-generation proteasome inhibitors are needed to overcome bortezomib resistance in multiple myeloma cells.

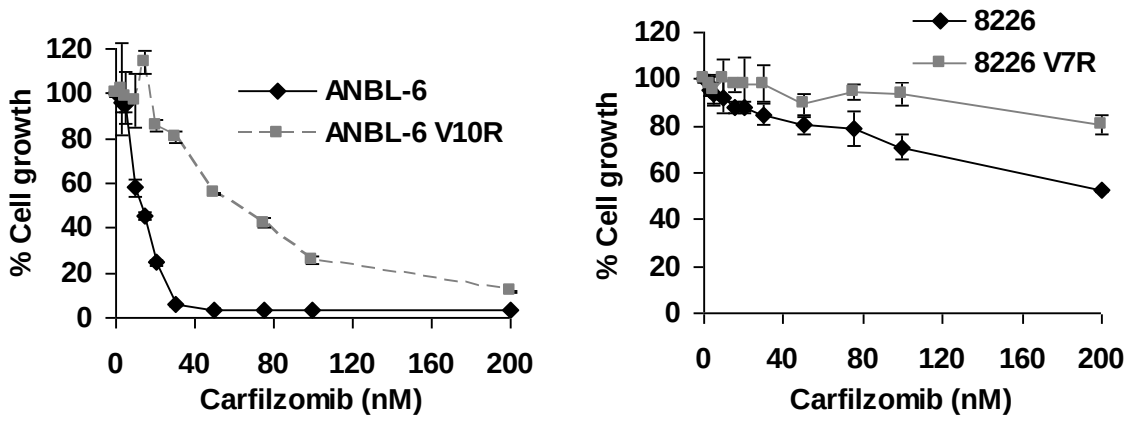

Figure 27. Cross-resistance to carfilzomib in bortezomib-resistant multiple myeloma cells.

Exponentially growing paired bortezomib-sensitive (solid black line) and -resistant (dashed grey line) multiple myeloma cells were seeded in a 96-well plate (2~6 $\times 10^4$ cells/well), treated with carfilzomib at indicated concentrations for 24 hours, followed by MTT assay. The data are expressed as percentage of vehicle-treated control (100%) and shown as means ± SD of triplicates.

The basal level expression and/or phosphorylation status of AMPK/mTOR pathway proteins are low in bortezomib-resistant multiple myeloma cells. We then investigated the basal level expression and phosphorylation status of AMPK pathway proteins in paired bortezomib-sensitive and -resistant multiple myeloma cells. Compared to corresponding bortezomib-sensitive parental cells, all three bortezomib-resistant counterparts express lower levels of phospho-AMPK and, to a less extent, total-AMPK (Figure 28). Consistently, the phosphorylation levels of Raptor and ACC, two well-known AMPK downstream targets, are also low in these bortezomib-resistant counterparts (Figure 28). These results suggest that suppression of AMPK signaling via inhibition of protein expression and activation is associated with gain of bortezomib-resistance phenotype in multiple myeloma cells.

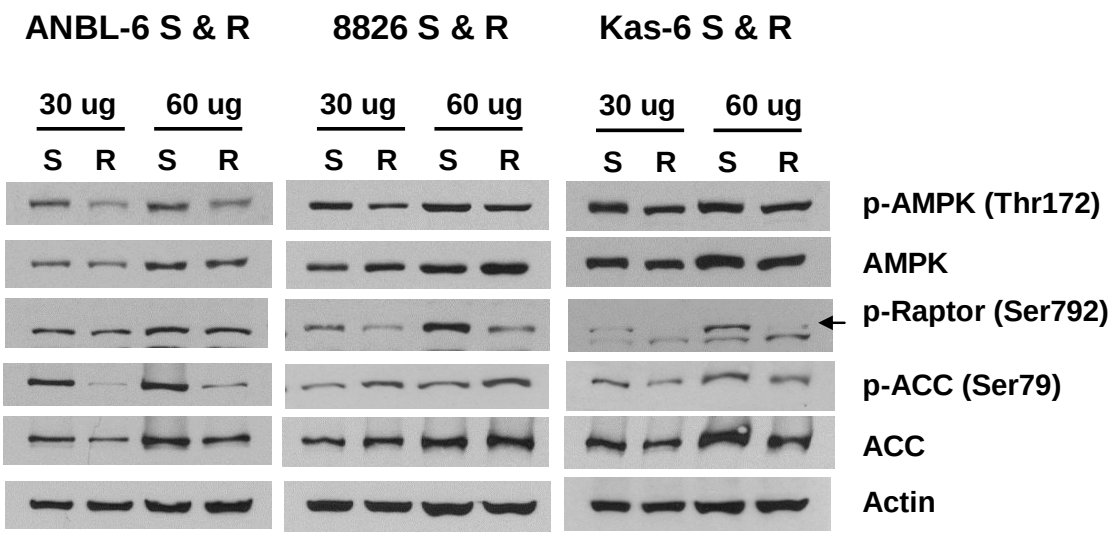

Figure 28. Basal level expression and phosphorylation status of AMPK, Raptor and ACC in paired bortezomib-sensitive and -resistant multiple myeloma cells.

Exponentially growing paired bortezomib-sensitive and -resistant multiple myeloma cells were harvested, lysated and subjected to Western blot analysis.

Induction of AMPK signaling by metformin in bortezomib-resistant multiple myeloma cells. With the knowledge that AMPK signaling is suppressed in bortezomib-resistant multiple myeloma cells, we studied whether the AMPK pathway in the resistant cells is intact and, if yes, whether it is inducible by metformin. ANBL6-V10R cells treated with metformin for 24 hours showed enhanced activation of AMPK signaling pathway, as evident by increased levels of phospho-AMPKα, phospho-Raptor and phospho-ACC (Figure 29). In the following kinetic experiment, ANBL6-V10R cells were treated with 0.5 or 1 mM metformin for 24, 48 or 72 hours. The level of phospho-AMPKα significantly increased 24 hours after treatment, accompanied by increased levels of phospho-Raptor and phospho-ACC, while the total-AMPKα and total-ACC proteins remained the same (Figure 30). These results suggest the integrity and functionality of AMPK signaling in the bortezomib-resistant MM cells which could be re-activated by challenging with an AMPK activator.

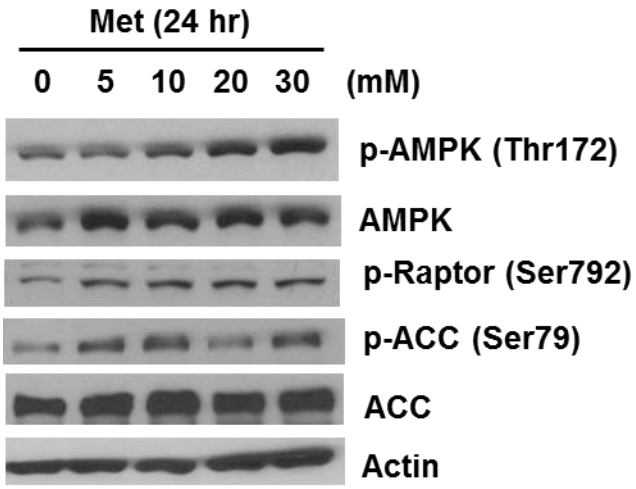

Figure 29. Dose response of metformin treatment in bortezomib-resistant multiple myeloma cells.

Exponentially growing ANBL6-V10R cells were treated with 5, 10, 20 or 30 mM metformin for 24 hours, followed by Western blot analysis.

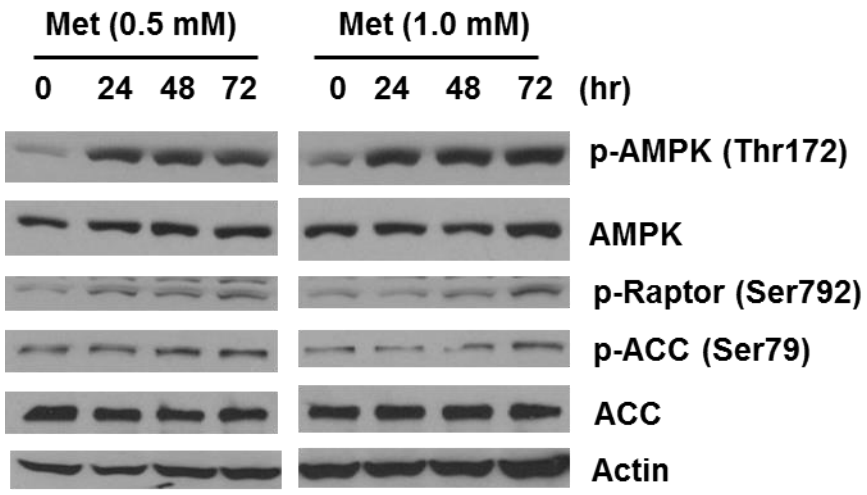

Figure 30. Kinetic effect of metformin in bortezomib-resistant multiple myeloma cells.

Exponentially growing ANBL6-V10R cells were treated with 0.5 or 1.0 mM metformin for 24, 48 or 72 hours, followed by Western blot analysis.

Combination treatment with bortezomib and an AMPK activator is more effective than each drug alone in bortezomib-resistant multiple myeloma cells. The observations that AMPK signaling was suppressed in bortezomib-resistant cells and that the signaling was intact and can be re-activated by an AMPK activator led us to ask the question whether we can achieve a better outcome in bortezomib-resistant multiple myeloma cells by combining bortezomib with an AMPK activator. To test this, we treated ANBL6-V10R cells with bortezomib in the presence or absence of metformin for 48 hours. As shown in Figure 31 (left panel), addition of metformin caused more growth inhibition in ANBL6-V10R cells as compared to each drug alone. Similarly, addition of AICAR also achieved a better growth inhibitory effect (Figure 31, right panel). Taken together, these data suggest that activating AMPK signaling by an AMPK activator is an effective strategy to overcome bortezomib resistance in multiple myeloma cells.

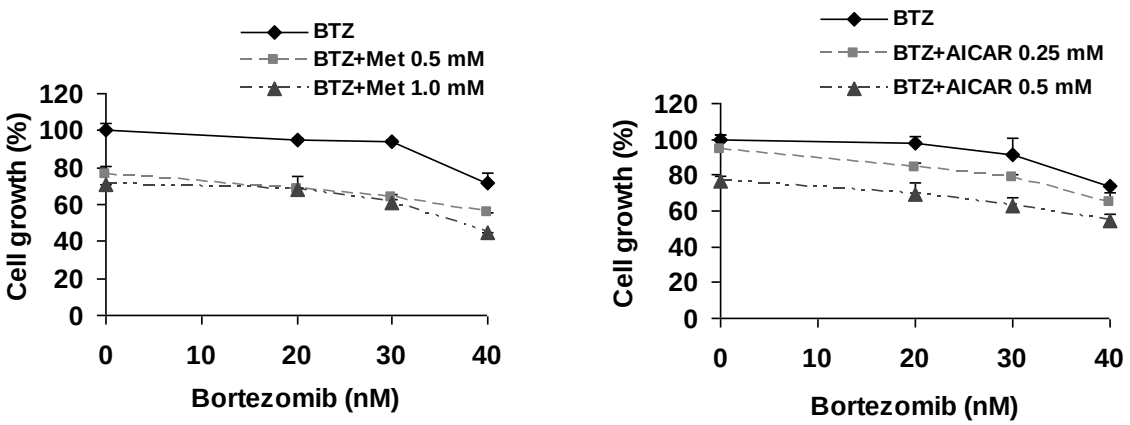

Figure 31. Growth inhibitory effect of bortezomib plus an AMPK activator in bortezomib-resistant multiple myeloma cells.

Exponentially growing ANBL6-V10R cells were seeded in a 96-well plate (2~6 $\times 10^4$ cells/well), treated with bortezomib at indicated concentrations with (dashed grey line) or without (solid black line) metformin (left panel) or AICAR (right panel) for 48 hours, followed by MTT assay. The data are expressed as percentage of vehicle-treated control (100%) and shown as means ± SD of triplicates.

Combination of carfilzomib with an AMPK activator showed more cell growth inhibition than each drug alone in bortezomib-resistant multiple myeloma cells. Finally, we examined if AMPK activators can also help improve the efficacy of carfilzomib in bortezomib-resistant multiple myeloma cells. For this purpose, ANBL6-V10R cells were treated with carfilzomib in the presence or absence of 15 mM metformin for 24 hours. As expected, more growth inhibition was observed in combination treatment (Figure 32, left panel). A similar result was obtained when combining carfilzomib with another AMPK activator AICAR at 2 mM concentration (Figure 32, right panel). Collectively, these data showed that AMPK activators are capable of inducing more growth inhibition in multiple myeloma cells when combined with a proteasome inhibitor, suggesting that AMPK activators may represent an alternative treatment option for proteasome inhibitor-resistant multiple myeloma.

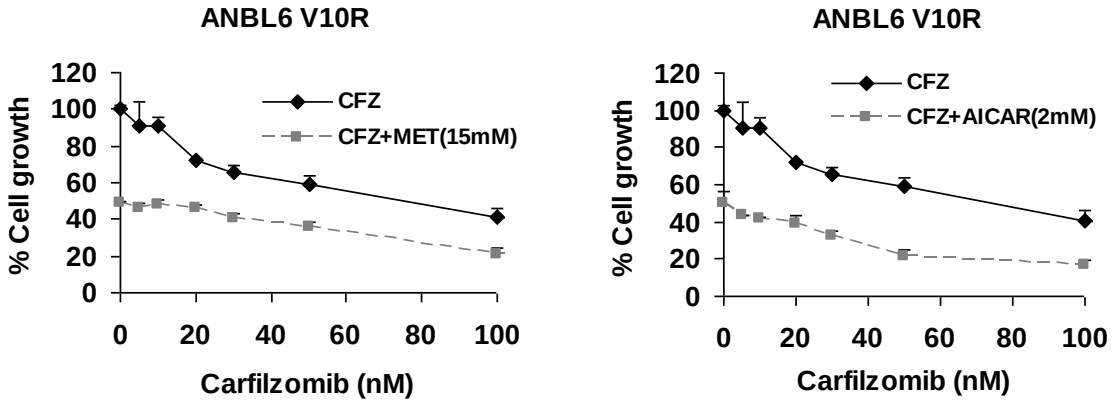

Figure 32. Growth inhibitory effect of carfilzomib plus an AMPK activator in bortezomib-resistant multiple myeloma cells.

Exponentially growing ANBL6-V10R cells were seeded in a 96-well plate (2~6 $\times 10^4$ cells/well), treated with carfilzomib at indicated concentrations with (dashed grey line) or without (solid black line) 15 mM metformin (left panel) or 2 mM AICAR (right panel) for 24 hours, followed by MTT assay. The data are expressed as percentage of vehicle-treated control (100%) and shown as means ± SD of triplicates.

Celastrol helped metformin in boosting and maintaining high level of active AMPK in bortezomib-resistant multiple myeloma cells. In order to achieve the optimum outcome, we introduced a third drug celastrol, which is a triterpene from the root bark of Chinese "Thunder God Vine". We previously reported that celastrol has appreciable proteasome inhibitory and anti-cancer activity (Yang et al., 2006). A recent study from Kim et al indicated that celastrol also caused AMPK activation in breast cancer cells, leading to the activation of p53 and PLK-2 pathway and apoptosis (Kim et al., 2013). We therefore studied the effect of triple-drug cocktail consisting of bortezomib, metformin and celastrol. Addition of metformin and celastrol greatly enhanced the growth inhibitory effect of bortezomib in ANBL6-V10R cells (Figure 33). Results from proteasomal chymotrypsin-like activity assay and Western blot analysis probing ubiquitinated proteins showed that the proteasomal activity in bortezomib-resistant cells was indeed inhibited by single bortezomib treatment (Figures 34 & 36), suggesting that the bortezomib resistance phenotype in these multiple myeloma cells is not due to the development of mutations at drug-binding site, but rather due to the factors that are irrelevant to proteasome. This can also at least partially explain why these resistant cells showed cross-resistance to the second-generation proteasome inhibitor carfilzomib in the current study (Figure 27). Furthermore, metformin and/or celastrol treatment resulted in AMPK activation, as evident by increased level of phospho-AMPK and decreased levels of phospho-mTOR and phospho-p70 S6K (Figure 36). Accompanied with proteasome inhibition and AMPK activation, the triple-drug treatment led to significant increases in apoptotic caspase-3 activation and PARP cleavage (Figures 35 &36). Taken together, our data suggest that inducing AMPK signaling and suppressing mTOR pathway by an

AMPK activator is an effective strategy to overcome bortezomib resistance in multiple myeloma cells.

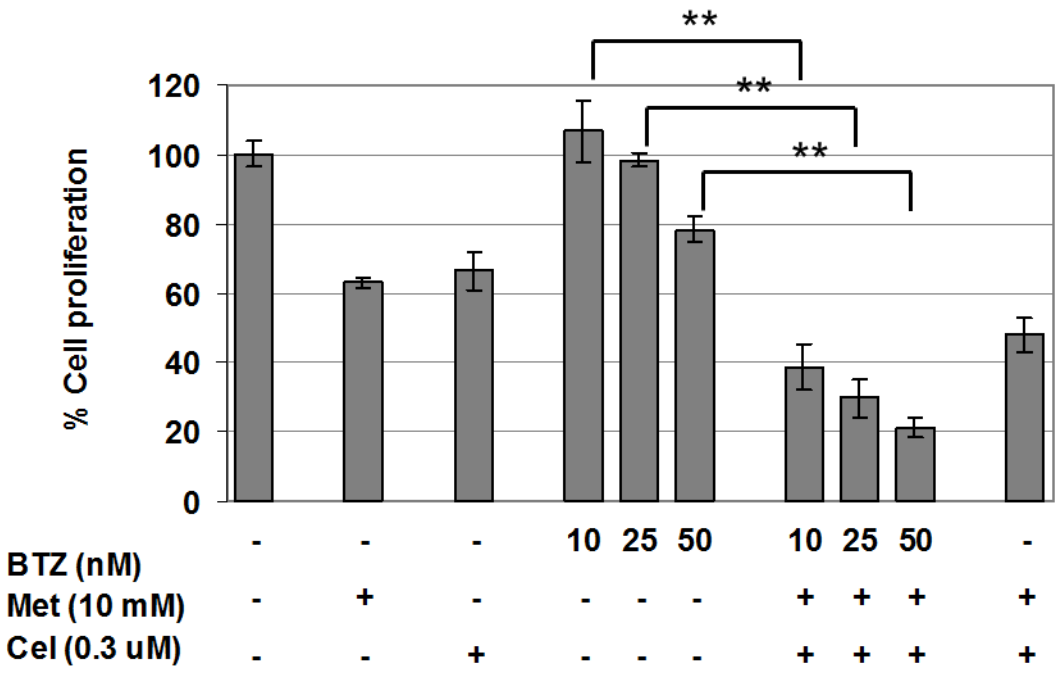

Figure 33. Growth inhibitory effect of bortezomib, metformin and celastrol, each alone or in combination, in ANBL6-V10R cells.

Exponentially growing ANBL6-V10R cells were seeded in a 96-well plate (2~6 $\times 10^4$ cells/well) treated with bortezomib, metformin and celastrol, each alone or in combination, at indicated concentrations for 24 hours, followed by MTT assay. The data are expressed as percentage of vehicle-treated control (100%) and shown as means ± SD of triplicates. **, $p < 0.01$ in Student's *t*-test.

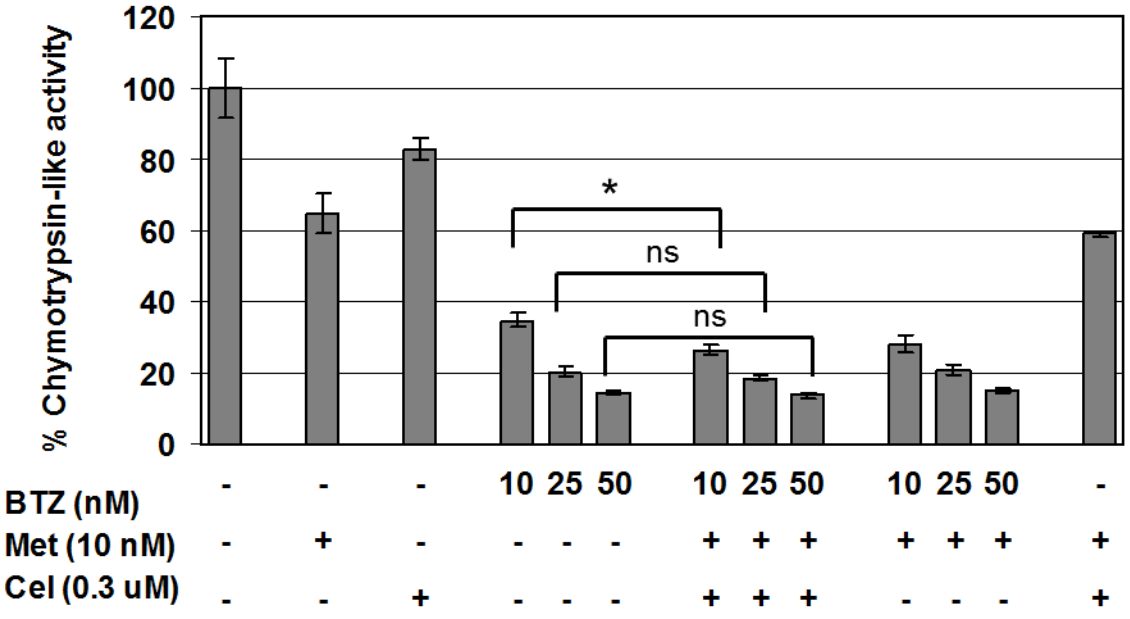

Figure 34. Proteasomal chymotrypsin-like activity in ANBL6-V10R cells treated with bortezomib, metformin and celastrol each alone or in combination.

Exponentially growing ANBL6-V10R cells were treated with bortezomib, metformin and celastrol, each alone or in combination, for 6 hours. Whole cell extracts were prepared and subjected to chymotrypsin-like activity assay using a fluorogenic substrate (Suc-LLVY-AMC) specific for the chymotrypsin-like activity of the 20S proteasome, as described in Materials and Methods. The data are expressed as percentage of vehicle-treated control (100%) and shown as means ± SD of triplicates. *, $p < 0.05$ in Student's *t*-test; ns, not significant in Student's *t*-test.

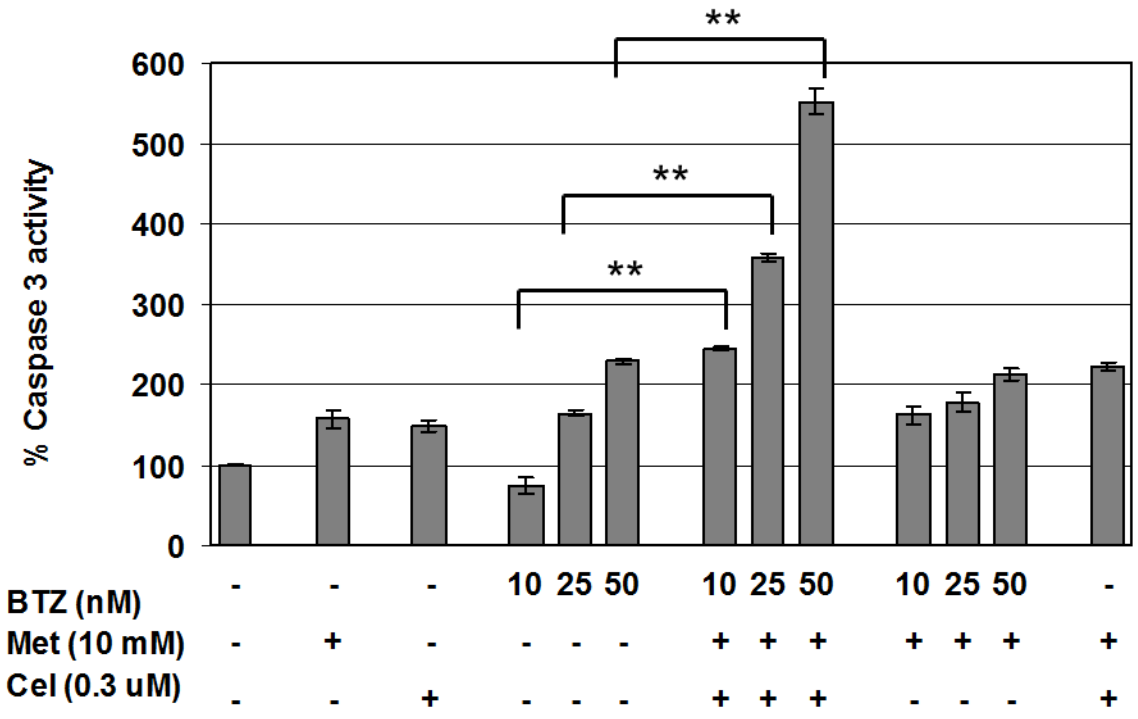

Figure 35. Apoptotic activity in ANBL6-V10R cells treated with bortezomib, metformin and celastrol each alone or in combination.

Exponentially growing ANBL6-V10R cells were treated with bortezomib, metformin and celastrol, each alone or in combination, for 6 hours. Whole cell extracts were prepared and subjected to chymotrypsin-like activity assay using a fluorogenic substrate (Ac-DEVD-AMC) specific for caspase-3/7, as described in Materials and Methods. The data are expressed as percentage of vehicle-treated control (100%) and shown as means ± SD of triplicates.

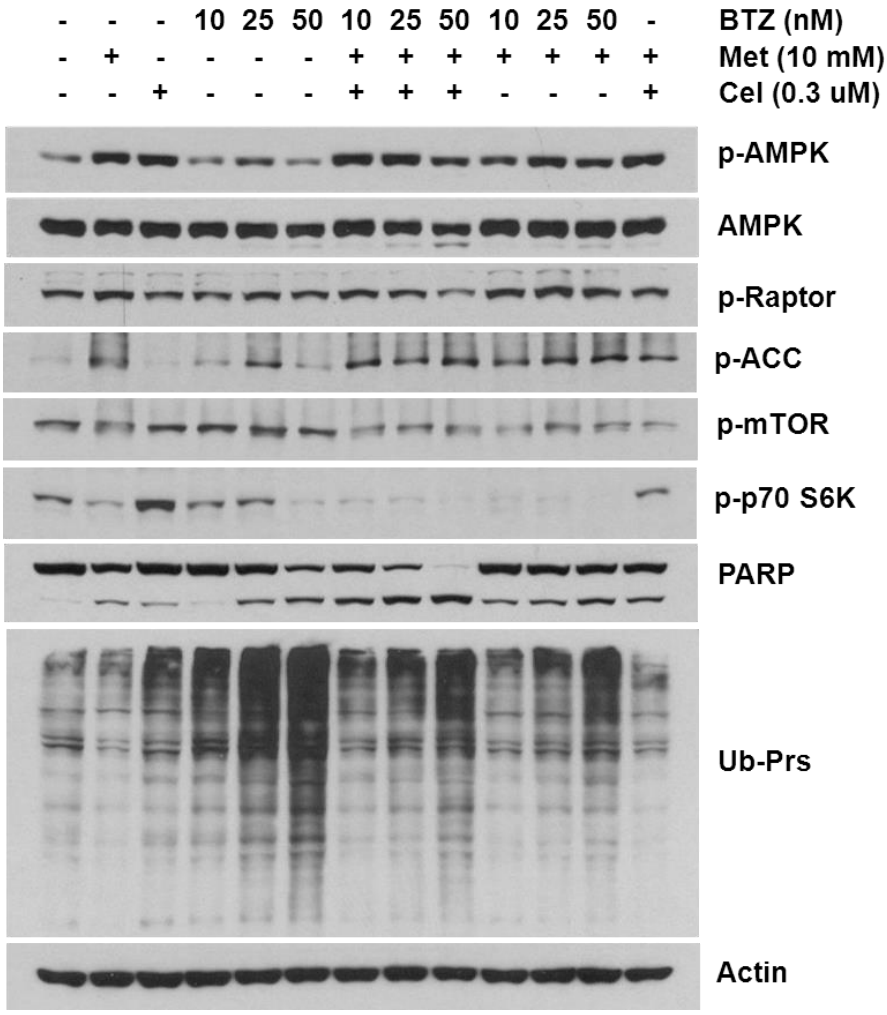

Figure 36. Activation of AMPK/mTOR signaling pathway in ANBL6-V10R cells treated with metformin, celastrol and bortezomib.

Exponentially growing ANBL6-V10R cells were treated with bortezomib, metformin and celastrol, each alone or in combination, for 24 hours, lysated and subjected to Western blot analysis.

Discussion

In the current study, we found that paired bortezomib-sensitive and -resistant multiple myeloma cells were about equally sensitive to AMPK activators metformin and AICAR (Figures 25 & 26). These results suggest that the obtainment of bortezomib-resistant phenotype may not due to the development of multi-drug resistance, at least in the cell lines we used. This provides the opportunity of overcoming bortezomib resistance in multiple myeloma cells by combining bortezomib with other types of drugs, for example AMPK activators here.

Carfilzomib is developed as next-generation proteasome inhibitor to overcome bortezomib resistance; however, the two bortezomib-resistant multiple myeloma cell lines we tested in the current study exhibited cross-resistance to carfilzomib (Figure 27). Stessman et al also reported that the bortezomib-resistant mouse cell lines created from the Bcl-XL/Myc double-transgenic mouse model of multiple myeloma showed cross-resistance to the next-generation proteasome inhibitors, MLN2238 and carfilzomib (Stessman et al., 2013). These observations suggest that some of the bortezomib-resistant phenotype are raised irrelevant to proteasome function, and in those cases, secondary therapies are needed to effectively overcome bortezomib resistance.

We further found that AMPK signaling is suppressed in bortezomib-resistant multiple myeloma cells (Figure 28). As discussed in Chapter 2 pp. 59, several proteins have been reported to negatively regulate AMPK activity by competitively phosphorylating AMPK at a different site which will prevent the phosphorylation of the active site Thr172 (Horman et al., 2006; Djouder et al., 2010). AMPK signaling can alternatively be suppressed through inhibition of its upstream kinases such as LKB1,

CaMKKβ or TAK1. Two independent studies have indicated that LKB1 is inhibited by an active mutant of B-Raf through Ras/Raf/MEK/ERK1/2 signaling (Esteve-Puig et al., 2009; Zheng et al., 2009). Additionally, ERK1/2 is constitutively activated in cancer cells containing Ras mutations, which is found in about 30% of multiple myeloma patients (Kyle and Rajkumar, 2004; Luo et al., 2010). More recently, it was reported that the orphan nuclear receptor Nur77 negatively regulates AMPK activation by binding to and sequestering LKB1 in the nucleus (Zhan et al., 2012). In the current study, we further showed that the suppressed AMPK signaling in bortezomib-resistant multiple myeloma cells can be elevated by challenging with an AMPK activator (Figures 29 & 30). This observation suggests that the suppression of AMPK signaling is mostly likely due to the inhibition of AMPK itself instead of inhibition of its upstream kinase; otherwise the AMPK signaling will remain suppressed even when challenged with an AMPK activator like metformin.

Finally, we showed that AMPK activators were able to overcome not only resistance to bortezomib but also cross-resistance to carfilzomib in bortezomib-resistant multiple myeloma cells (Figures 31 & 32). Although the combinational effect of a proteasome inhibitor plus an AMPK activator was mild to moderate in our *in vitro* MTT assays, we would expect a boosted effect in the *in vivo* evaluation using xenograft mouse models in the future. This is because, like proteasome inhibitors, metformin has the potential of targeting both the multiple myeloma cells and the bone marrow microenvironment. The progression of multiple myeloma is heavily dependent on NF-κB signaling-mediated transcription and paracrine secretion of IL-6 from the bone marrow stem cells. Metformin has been reported to inhibit NF-κB signaling and IL-6 production

in endothelia cells (Huang et al., 2009). It is very likely that metformin could also inhibit IL-6 production from bone marrow stem cells which are critical for multiple myeloma cell growth.

It needs to be noted that there exists an apparent discrepancy between the concentration of metformin used in cultured cells and in patients. This issue was extensively discussed in Chapter 2 pp. 60-61.

In summary, our current study showed that AMPK signaling was suppressed in bortezomib-resistant multiple myeloma cells and it can be re-activated by pharmacological AMPK activators. AMPK activators were about equally effective in bortezomib-sensitive and -resistant multiple myeloma cells. AMPK activators were able to cause more growth inhibition when combined with bortezomib or carfilzomib in bortezomib-resistance multiple myeloma cells with cross-resistance to carfilzomib. These findings support the further investigation of AMPK signaling in multiple myeloma patient samples and *in vivo* evaluation of metformin use in multiple myeloma mouse models.

CHAPTER 4

Overcoming Chemoresistance by Inducing Degradation of Bcr-Abl Oncoprotein

Adapted from published materials in Open Journal of Pharmacology 2011; 1-3 and International Journal of Molecular Medicine 2010; 25:465-70.

The chimeric Bcr-Abl oncoprotein with constitutive tyrosine kinase activity plays a pivotal role in the pathogenesis of chronic myeloid leukemia (CML), therefore being an ideal target for the drug development. Celastrol is a quinone methide triterpene with various biological activities including anticancer activity. The objective of the current study is to examine the effect of celastrol on Bcr-Abl oncoprotein and explore the potential combination therapies for Bcr-Abl-driven leukemia. We found that (i) celastrol induced apoptosis and Bcr-Abl degradation in a time-dependent manner; (ii) celastrol-induced apoptosis was not blocked by newly synthesized Bcr-Abl protein, once the cells were committed; (iii) celastrol-induced Bcr-Abl degradation and apoptosis were not prevented by selected protease inhibitors or their mixture under the selected experimental conditions. These findings shed light on the mechanism how celastrol inhibits Bcr-Abl protein expression/function and provide support for the potential use of celastrol in the CML treatment.

Materials and Methods

Materials. Celastrol was purchased from Cayman Chemicals (Ann Arbor, MI). The antibody against c-Abl was from Cell Signaling (Beverly, MA); antibodies against poly(ADP-ribose) polymerase (PARP), tubulin and actin were from Santa Cruz Biotechnology (Santa Cruz, CA). Cycloheximide solution, CA074-Me, aprotinin, leupeptin, and N-ethylmaleimide (NEM) were from Sigma-Aldrich (St Louis, MO). Pepstatin was ordered from Roche (Mannheim, Germany). All these reagents were prepared according to the manufacturer's instructions.

Cell culture. The human chronic myelogenous leukemia K562 cells were grown in RPMI 1640 medium (Invitrogen, Carlsbad, CA) containing 10% fetal bovine serum (Aleken Biologicals, Nash, TX), 100 Units/mL of penicillin, 100 μg/mL of streptomycin and 0.3 mg/mL L-glutamine (Invitrogen, Carlsbad, CA) at 37 ^{o}C in a humidified atmosphere of 5% CO_2.

Cell number counting. Total cell numbers were counted manually by hemocytometer. The data are expressed as percentage of control at time 0 (100%) and shown as means ± SD of triplicates.

Trypan blue exclusion assay. A hundred μL of the cell suspension was mixed with 100 μL of 0.4% (w/v) of trypan blue solusion in a 96-well plate. Twenty μL of cell mixture was transferred to the hemocytometer. The numbers of viable (unstained) and nonviable (trypan blue stained) cells were counted manually. Percentage of cell death was calculated as number of nonviable cells / total number of viable and nonviable cells * 100. The data are shown as means ± SD of triplicates.

Whole cell extract preparation. Cells were harvested, washed with ice-cold PBS twice, and homogenized in a lysis buffer [50 mM Tris-HCl at pH 8.0, 150 mM NaCl, 0.5% NP40 (v/v)]. After rocking at 4 ℃ for 30 min, the mixtures were centrifuged at 12,000 g for 15 minutes, and the supernatants were collected as whole cell extracts. The protein concentrations in whole cell extracts were determined by Bio-Rad Protein Assay Kit (Bio-Rad Laboratories, Hercules, CA).

Caspase-3 activity assay. Fresh-made whole cell extract (20 μg per sample) was incubated with 20 μM fluorogenic caspase-3 substrate Ac-DEVD-AMC (Calbiochem, La Jolla, CA) in 100 μL of Tris-HCl (20 mM, pH 7.5). After 2 hours incubation at 37^{o}C, the AMC liberated from the fluorogenic substrate was detected spectrofluorometrically (λex = 355 nm and λem = 460 nm) by Wallac Victor 3 Multilabel Counter (PerkinElmer, Boston, MA). The data are expressed as relative fluorescence units per minute and per mg of protein (RFU/min/mg) and shown as means ± SD of triplicates.

Western blot analysis. Whole cell extract (40 μg per sample) was denatured by boiling with 2x SDS sample buffer containing 5% β-mercaptoethanol (v/v), separated by 6% SDS-PAGE (Bio-Rad Laboratories, Hercules, CA), transferred to a nitrocellulose membrane (GE Healthcare, Piscataway, NJ), immunoblotted with indicated antibodies, and detected by HyGLO Chemiluminescent HRP Antibody Detection Reagent (Denville Scientific, Metuchen, NJ). The band intensity was quantified by densitometry using AlphaEase FC software (Alpha Innotech, San Leandro, CA). The data are normalized to loading control and expressed as fold of vehicle-treated control.

RNA extraction and RT-PCR. Total RNA from cells was extracted using the High Pure RNA Isolation Kit (Roche, Mannheim, Germany). RNA concentration was

determined spectrophotometrically. Total RNA (2 μg) was reverse transcribed with random hexamer primers using the SuperScript III First-Strand Synthesis System (Invitrogen, Carlsbad, CA). Four μL of the cDNA product was used as template for PCR amplification with 0.2 μM gene specific primers using Platinum PCR SuperMix (Invitrogen, Carlsbad, CA). The primers for Bcr-Abl were 5'-TTCAGAAGCTTCTCCCTGACAT-3' and 5'-TGTTGACTGGCGTGATGTAGTTGCTTGG-3'. The PCR condition for Bcr-Abl was 10 min at 96 ^{o}C, followed by 35 cycles of 1 min at 96 ^{o}C, 1 min at 64 ^{o}C and 1 min at 72 ^{o}C. The primers for glyceraldehyde 3-phosphate dehydrogenase (GAPDH) were 5'-TTGCAACTGTTTTAGGACTTT-3' and 5'-AGCATTGGGAAATGTTCAAGG-3'. The PCR condition for GAPDH was 10 min at 95^{o}C, followed by 30 cycles of 1 min at 95 ^{o}C, 1 min at 54 ^{o}C and 1 min at 72 ^{o}C. Different PCR cycle numbers were tested for Bcr-Abl and GAPDH to ensure that the assay was in the linear range of amplification. The PCR products were separated by electrophoresis in a 1% agarose gel and visualized by ethidium bromide staining. The band intensity was quantified by densitometry using AlphaEase FC software (Alpha Innotech, San Leandro, CA). The data are normalized to loading control and expressed as fold of vehicle-treated control.

Protease inhibitor experiment. K562 cells were pretreated with either DMSO, CA074-Me (0.5 μM), pepstatin (15 μM), aprotinin (10 μM), leupeptin (400 μM) or NEM (15 μM), or a mixture of the above five inhibitors at the indicated concentrations for 4 hours, followed by treatment with 1 μM celastrol for 12 hours. Cells were then collected for caspase-3 activity assay and Western Blot analysis.

Statistical analysis. Data are presented as means ± SD of triplicates. Statistical analysis was performed with GraphPad Prism 6 software. To evaluate the differences between control and treated groups, the unpaired Student's *t*-test was performed with the level of significance set at $P < 0.05$.

Results

Celastrol induced apoptosis and Bcr-Abl degradation in a time-dependent manner. We previously reported down-regulation of Bcr-Abl protein level by celastrol treatment (Davenport et al., 2010). In order to explore the involved molecular mechanism, we performed a kinetic experiment. K562 cells were treated with 1 μM celastrol for up to 36 hours which is about 1.5-fold of the doubling time of these cells. A dramatic decrease of cell number was observed in the celastrol-treated group compared to the DMSO control group at the ending time point (Figure 37). Specifically, celastrol-treated cells decreased ~55% while control cells increased ~60% in cell number (Figure 37). Caspase-3 activation occurred at as early as 4 hours under the experimental condition, with a peak at 12 hours (Figure 38). The decrease of caspase-3 activity at 24 and 36 hours was most possibly due to the loss of cells or the formation of apoptotic bodies which might not be included in our cell lysate preparation. Consistently, PARP cleavage occurred at 4 hours (Figure 39). A decrease in the amount of full-length PARP was associated with an increase in p85/PARP fragment (Figure 39). Most importantly, Bcr-Abl degradation also occurred at as early as 4 hours as manifested by the decrease of full length Bcr-Abl protein and the appearance of some new bands with lower molecular weight that might be its cleaved fragments (indicated by arrows; Figure 39). Unlike Bcr-Abl oncoprotein, normal Abl protein was only slightly decreased during celastrol treatment (Figure 39), suggesting that Bcr-Abl oncoprotein is much more sensitive to celastrol exposure than Abl kinase.

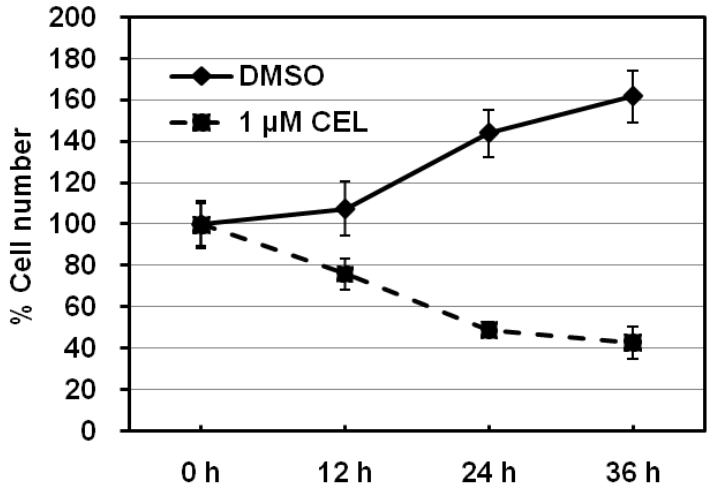

Figure 37. Celastrol induced time-dependent cell death in K562 cells.

K562 cells were exposed to 1 µM celastrol for the indicated times. Total cell numbers were counted manually by hemocytometer. The data are expressed as percentage of control at time 0 (100%) and shown as means ± SD of triplicates.

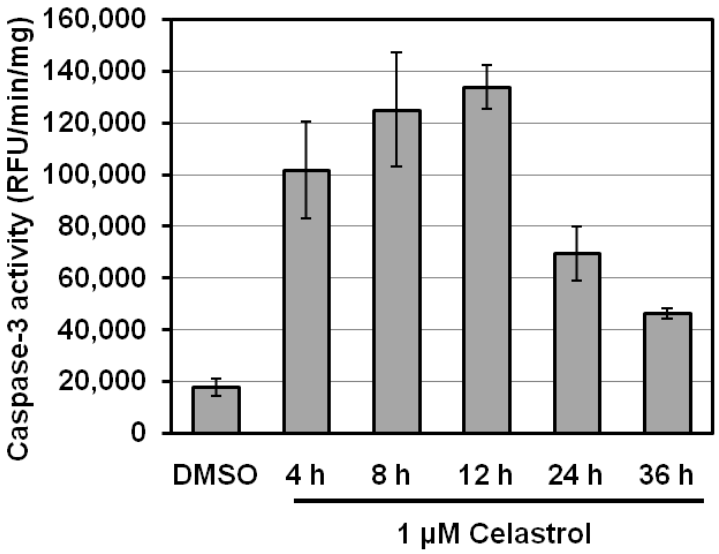

Figure 38. Celastrol induced time-dependent caspase-3 activation in K562 cells.

K562 cells were exposed to 1 µM celastrol for the indicated times. Whole-cell lysates were subjected to caspase-3 activity assay using a fluorogenic substrate (Ac-DEVD-AMC) specific for caspase-3/7, as described in Materials and Methods. The data are expressed as relative fluorescence units per minute and per mg of protein (RFU/min/mg) and shown as means ± SD of triplicates.

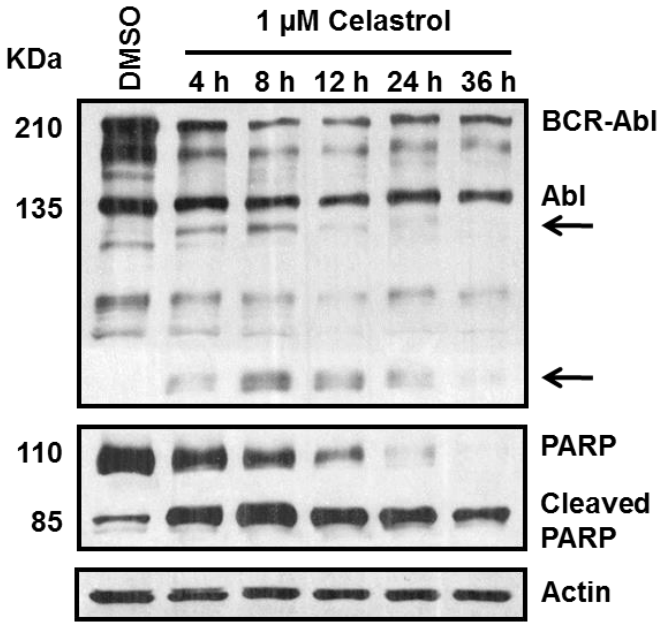

Figure 39. Celastrol induced time-dependent Bcr-Abl protein degradation and PARP cleavage in K562 cells.

K562 cells were exposed to 1 μM celastrol for the indicated times. Cell lysates were separated by SDS-PAGE and analysed by Western Blot. ← indicates Bcr-Abl fragments.

To test the possibility that suppression of Bcr-Abl transcription also contributes to its decrease at protein level, we measured the amount of Bcr-Abl mRNA in the same experiment by RT-PCR analysis. Compared to GAPDH as a control, no significant change in the level of Bcr-Abl mRNA was detected at any time points (Figure 40). Taken together, these results indicate that celastrol induced Bcr-Abl protein degradation, associated with apoptosis induction in K562 cells.

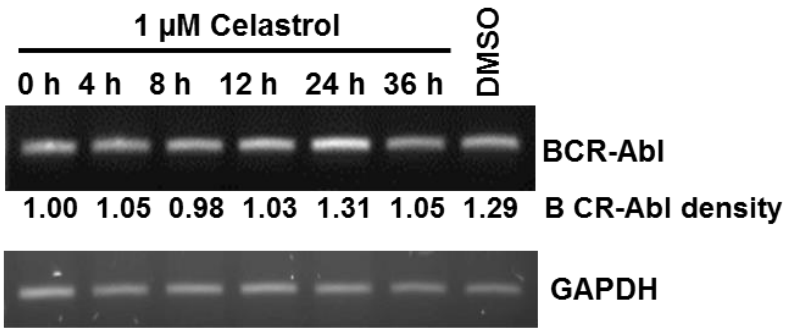

Figure 40. Celastrol didn't affect Bcr-Abl mRNA expression in K562 cells.

K562 cells were exposed to 1 μM celastrol for the indicated times. Bcr-Abl mRNA expression was measured by RT-PCR. The band intensity (BCR-Abl and GAPDH) was quantified by densitometry. The relative density of BCR-Abl was normalized to loading control GAPDH and expressed as fold of control at time 0.

Apoptotic signaling induced by celastrol was not blocked by newly synthesized Bcr-Abl protein. Since Bcr-Abl degradation and apoptosis induction occurred almost simultaneously after the cells were exposed to celastrol, we then asked whether a short time exposure to celastrol is sufficient to trigger apoptosis or a sustained stimulus from celastrol is required to induce apoptosis execution. For this purpose, K562 cells were treated with 1 μM celastrol for 1, 2, 3, 4 or 5 hours. After the treatment, half of the cells was harvested while another half was washed to remove the drug and then put back into fresh media without celastrol for another 12 hour incubation. This extra 12 hours would give cell enough time to continue the apoptotic signal transduction and execution.

In each pair, comparing to the cells harvested immediately after drug exposure, the cells experienced additional 12 hour incubation in fresh media without celastrol gave much higher levels of caspase-3 activity (Figure 41) and PARP cleavage (Figure 42). These results clearly demonstrate that a short time exposure to celastrol was sufficient to trigger apoptotic execution, if further time was given. Surprisingly, opposite to the apoptotic signaling pattern in this experiment, Bcr-Abl protein level was increased in the cells experienced further incubation after removal of celastrol (Figure 42). One interpretation is that new Bcr-Abl protein had been synthesized after drug removal as a cell survival mechanism, but this newly synthesized Bcr-Abl protein failed to stop or reverse the already triggered apoptotic signaling.

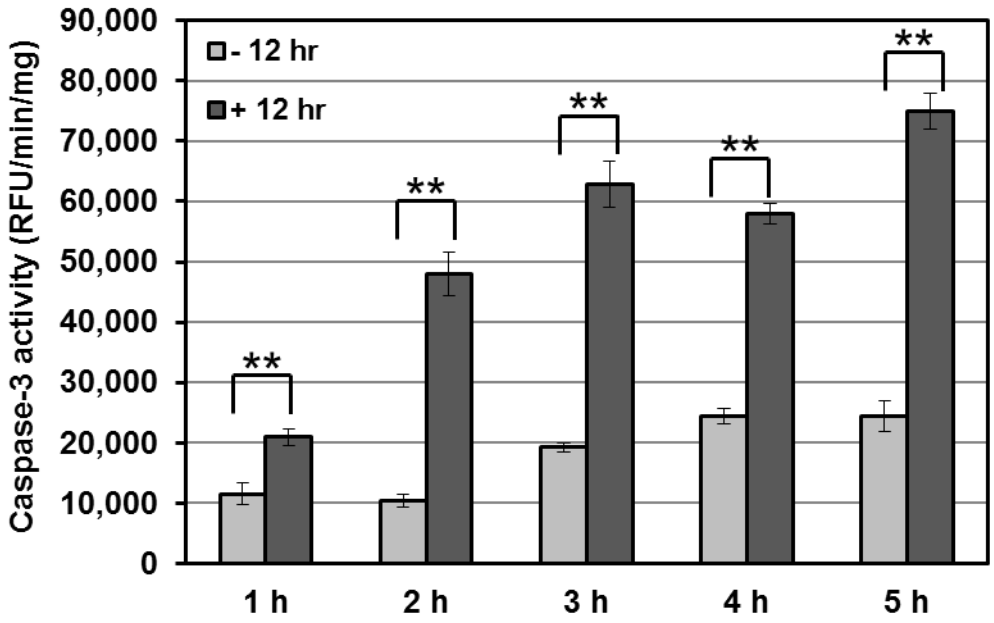

Figure 41. Short-time exposure to celastrol was sufficient to induce committed apoptotic signal.

K562 cells were exposed to 1 μM celastrol for 1 to 5 hours. At each time point, one flask of cells was harvested, while the other was changed to fresh media and cultured for another 12 hours Whole-cell lysates were subjected to caspase-3 activity assay using a fluorogenic substrate (Ac-DEVD-AMC) specific for caspase-3/7, as described in Materials and Methods. The data are expressed as relative fluorescence units per minute and per mg of protein (RFU/min/mg) and shown as means ± SD of triplicates. **, $p < 0.01$ in Student's *t*-test.

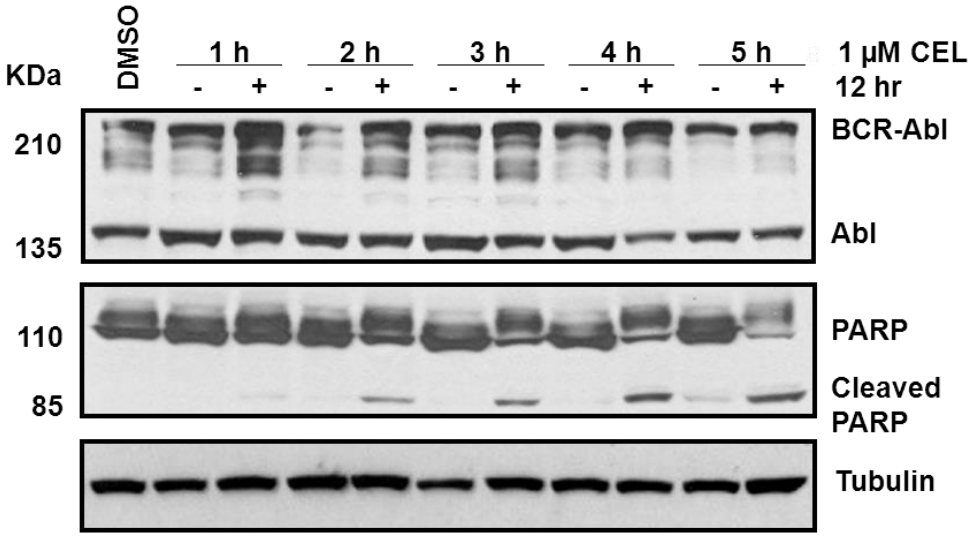

Figure 42. Bcr-Abl protein expression pattern after the removal of celastrol.

K562 cells were exposed to 1 μM celastrol for 1 to 5 hours. At each time point, one flask of cells was harvested, while the other was changed to fresh media and cultured for another 12 hours. Cell lysates were separated by SDS-PAGE and analyzed by Western blot.

To prove the possibility that new Bcr-Abl protein is synthesized after drug removal, we used cycloheximide (CHX) at a relatively non-cytotoxic dose (2 μg/mL) to block protein synthesis. Again, K562 cells were exposed to 1.5 μM celastrol for 2, 3, 4 or 5 hours. After drug removal, cells were incubated in fresh media with or without CHX for another 12 hours. As predicted, the cells incubated with CHX contained lower level of Bcr-Abl protein as compared to the cells incubated without CHX (Figure 43). Consistently, higher levels of caspase-3 activity (Figure 44) and PARP cleavage (Figure 43) were achieved in the cells incubated with CHX. Taken together, these results indicate that K562 cells undergo committed apoptosis after a short time exposure to celastrol and removal of celastrol may cause re-expression of Bcr-Abl protein, which however cannot rescue the cell from the fate of apoptotic death.

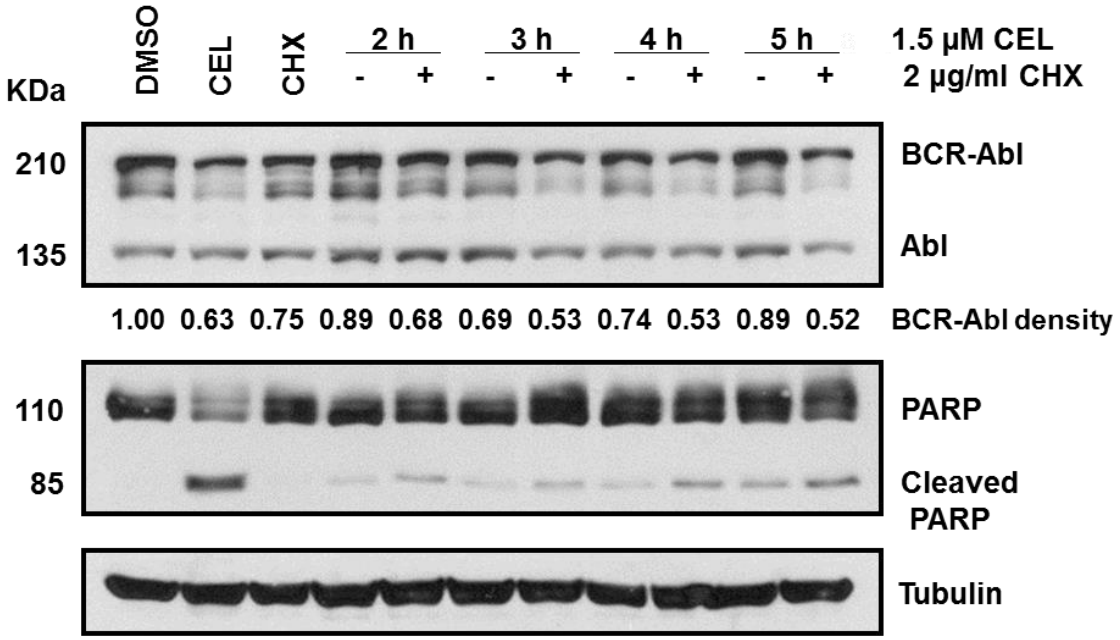

Figure 43. Increased synthesis of Bcr-Abl protein after the removal of celastrol.

K562 cells were exposed to 1.5 µM celastrol for 2 to 5 hours. After that, cells were changed to fresh media with (+) or without (-) CHX (2 µg/mL) and cultured for another 12 hours. Cell lysates were separated by SDS-PAGE and analysed by Western Blot. The band intensity (BCR-Abl and β-Tubulin) was quantified by densitometry. The relative density of BCR-Abl was normalized to loading control β-Tubulin and expressed as fold of vehicle-treated control.

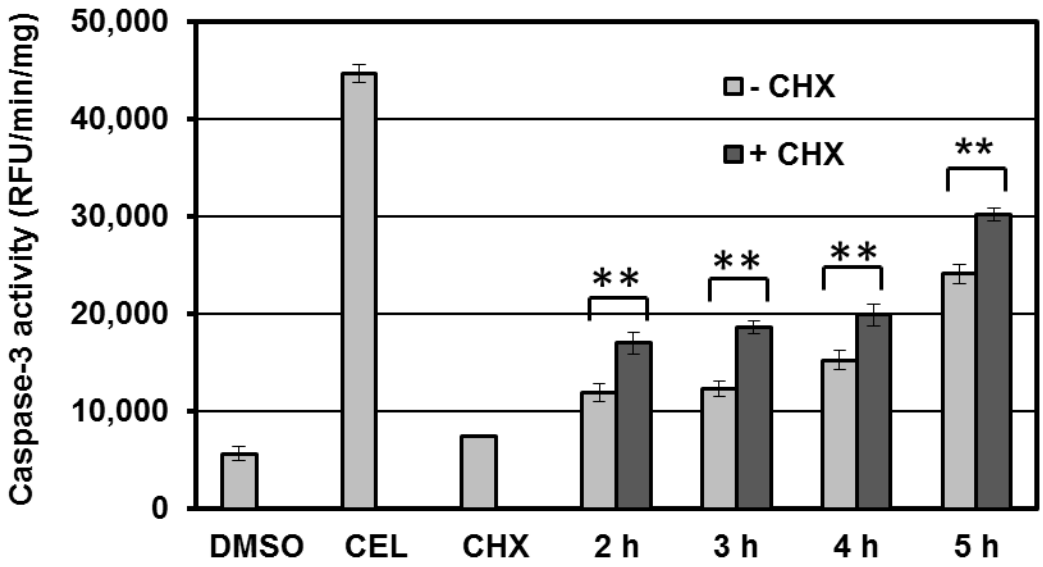

Figure 44. Increased Bcr-Abl protein synthesis cannot abrogate the apoptotic signal triggered by celastrol.

K562 cells were exposed to 1.5 μM celastrol for 2 to 5 hours. After that, cells were changed to fresh media with (+) or without (-) CHX (2 μg/mL) and cultured for another 12 hours. Whole-cell lysates were subjected to caspase-3 activity assay using a fluorogenic substrate (Ac-DEVD-AMC) specific for caspase-3/7, as described in Materials and Methods. The data are expressed as relative fluorescence units per minute and per mg of protein (RFU/min/mg) and shown as means ± SD of triplicates. **, $p < 0.01$ in Student's *t*-test.

A variety of protease inhibitors failed to inhibit celastrol-induced Bcr-Abl degradation and apoptosis. Based on the observation of Bcr-Abl degradation under celastrol exposure, we asked which protease is responsible for this degradation. To do this, we tested whether or not a commonly used protease inhibitor or an inhibitor mixture could block celastrol-induced Bcr-Abl degradation. A panel of protease inhibitors was tested including CA074-Me (0.5 μM, cathepsin B inhibitor), pepstatin (15 μM, aspartyl protease inhibitor), aprotinin (10 μM, serine protease inhibitor), leupeptin (400 μM, prefers to inhibit cysteine proteases but also inhibit serine proteases), and NEM (15 μM, cysteine protease inhibitor). The chosen concentration of each protease inhibitor was effective but relatively non-toxic to cells. We found that none of the single protease inhibitors was able to prevent or suppress Bcr-Abl degradation induced by celastrol (Figure 46). Compared to the cells treated with celastrol alone in the absence of a protease inhibitor, the similar levels of Bcr-Abl degradation, caspase-3 activation and PARP cleavage were observed in the cells co-treated with celastrol and a protease inhibitor (Figures 45 & 46). NEM-treated cells exhibited even severer Bcr-Abl degradaqtion. This is because although the concentration of NEM we used is non-toxic to normally growing cells, depletion of thiols by NEM could possibly exaggerates cellular stress/damage induced by the drug, in this case celastrol. A mixture of the protease inhibitors only slightly suppressed caspase-3 activation and PARP cleavage (Figures 45 & 46). Nevertheless, it failed to suppress Bcr-Abl degradation and rescue the cells from cell death (Figure 45). Therefore, neither a single protease inhibitor nor their mixture tested was able to suppress celastrol-induced Bcr-Abl degradation under the selected experimental conditions.

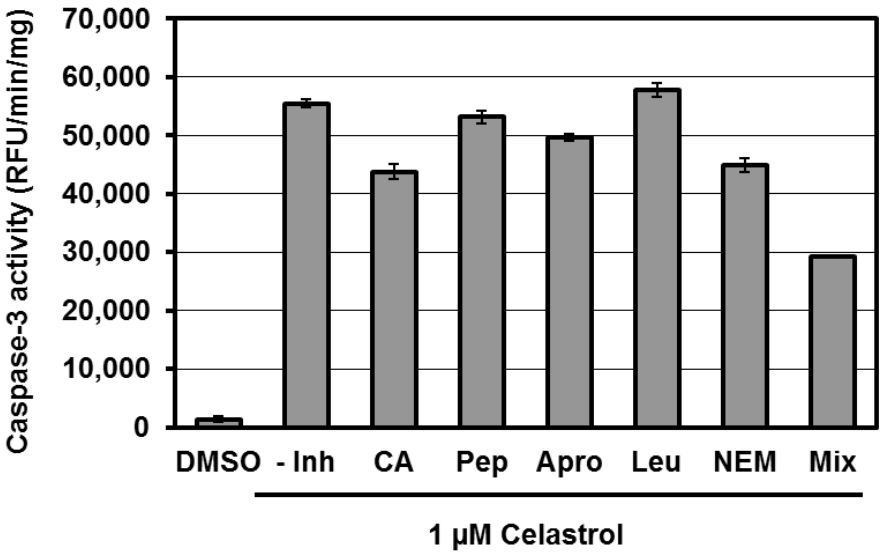

Figure 45. Effect of different protease inhibitors on celastrol-triggered apoptotic signal.

K562 cells were pre-incubated with either DMSO, CA074-Me (0.5 µM), pepstatin (15 µM), aprotinin (10 µM), leupeptin (400 µM) or NEM (15 µM), or a mixture of the above five inhibitors at the indicated concentrations for 4 hours, followed by exposure to 1 µM celastrol for 12 hours. Whole-cell lysates were subjected to caspase-3 activity assay using a fluorogenic substrate (Ac-DEVD-AMC) specific for caspase-3/7, as described in Materials and Methods. The data are expressed as relative fluorescence units per minute and per mg of protein (RFU/min/mg) and shown as means ± SD of triplicates.

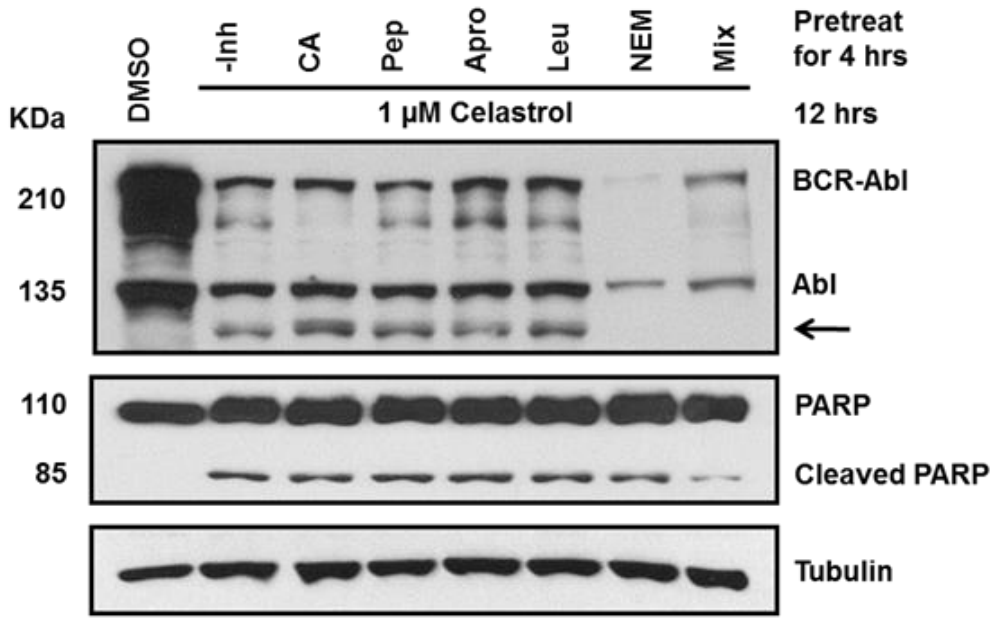

Figure 46. Effect of different protease inhibitors on celastrol-triggered Bcr-Abl protein degradation.

K562 cells were pre-incubated with either DMSO, CA074-Me (0.5 μM), pepstatin (15 μM), aprotinin (10 μM), leupeptin (400 μM) or NEM (15 μM), or a mixture of the above five inhibitors at the indicated concentrations for 4 hours, followed by exposure to 1 μM celastrol for 12 hours. Whole cell lysates were separated by SDS-PAGE and analysed by Western Blot. ← indicates Bcr-Abl fragment.

Celastrol enhanced the efficacy of chemotherapeutic drugs by inducing Bcr-Abl degradation. We then assessed the ability of celastrol to enhance the cytotoxic activity of two conventional chemotherapeutic drugs, daunorubicin (DNR) and cytarabine (also known as arabinofuranosyl cytidine or Ara-C) in K562 cells. As shown in Figure 47, K562 cells were treated with celastrol (250 nM), clinically relevant doses of daunorubicin (100 nM) or cytarabine (200 nM), or combination of celastrol and one cytotoxic drug for 72 h. Cell death rate was determined by trypan blue exclusion assay. Compared with single drug treatment, a combination of celastrol and daunorubicin or cytarabine significantly increased cell death ($p < 0.01$).

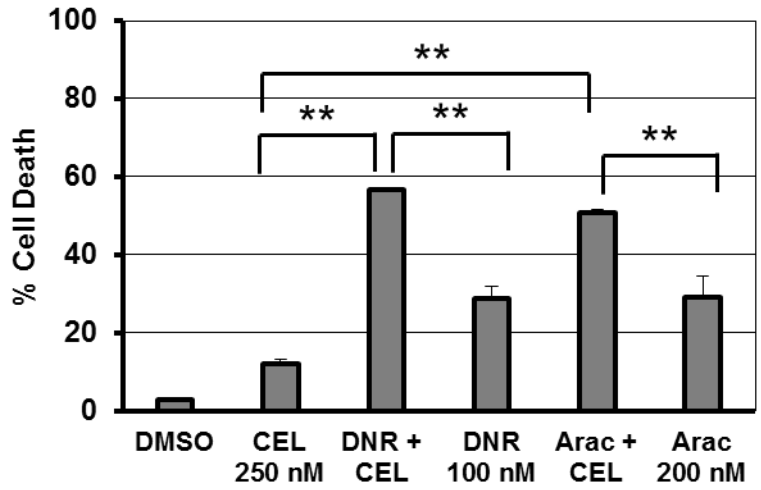

Figure 47. Cytotoxic profile of celastrol as chemosensitizing agent in K562 cells.

K562 cells were treated with celastrol alone or in combination with a chemotherapeutic drug (daunorubicin or cytarabine) for 72 hours, followed by trypan blue exclusion assay, as described in Materials and Methods. Percentage of cell death was calculated as total number of nonviable cells / total number of viable and nonviable cells * 100. The data are shown as means ± SD of triplicates. **, $p < 0.01$ in Student's *t*-test.

We next investigated whether enhanced apoptotic cell death is responsible for chemosensitization by celastrol. K562 cells were incubated with celastrol and daunorubicin, either alone or in combination, for 72 h. Caspase-3 activity in cell lysates was measured as an indicator of apoptosis induction since different upstream pathways leading to apoptosis depend on caspase-3 activation for final apoptotic execution. Compared to single drug treatment which induced low to moderate caspase-3 activity, a combination of celastrol and daunorubicin resulted in a significantly higher level of caspase-3 activity (Figure 48). Consistent with caspase-3 activation, Western blot analysis confirmed that a significant level of PARP cleavage was achieved under combination treatment while little or no PARP cleavage was observed in cells treated with celastrol or daunorubicin alone (Figure 49). Taken together, these results indicate that chemosensitization by celastrol is achieved, at least in part, by enhancing apoptotic cell death.

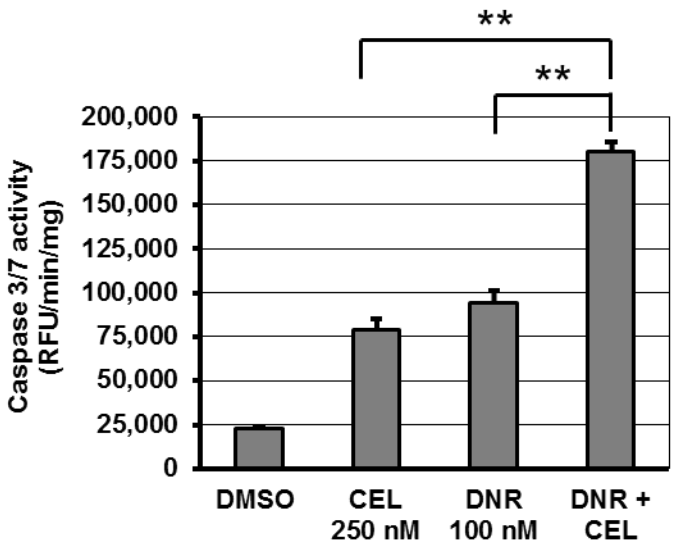

Figure 48. Induction of apoptosis by combination treatment of celastrol and daunorubicin.

K562 cells were treated with celastrol (250 nM), daunorubicin (100 nM) or celastrol plus daunorubicin for 72 hours. Whole-cell extracts were prepared and subjected to caspase-3/7 activity assay using a fluorogenic substrate (Ac-DEVD-AMC) specific for caspase-3/7, as described in Materials and Methods. The data are expressed as relative fluorescence units per minute and per mg of protein (RFU/min/mg) and shown as means ± SD of triplicates. **, $p < 0.01$ in Student's *t*-test.

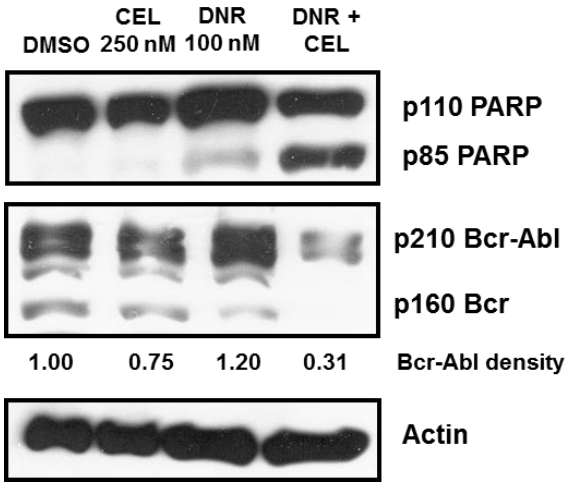

Figure 49. Combination treatment of celastrol and daunorubicin caused dramatic decrease of Bcr-Abl protein and cleavage of PARP.

K562 cells were treated with celastrol (250 nM), daunorubicin (100 nM) or celastrol plus daunorubicin for 72 hours. Whole cell lysates were prepared for Western blot analysis. The band intensity (Bcr-Abl and Actin) was quantified by densitometry. The relative density of Bcr-Abl was normalized to loading control Actin and expressed as fold of vehicle-treated control.

To investigate whether the appreciable cell death inducing effect of celastrol plus daunorubicin is associated with an effect on Bcr-Abl oncoprotein, we measured the expression of Bcr-Abl protein and mRNA. As shown in Figure 49, ~70% decrease of Bcr-Abl at protein level was observed in K562 cells treated with celastrol (250 nM) and daunorubicin (100 nM) in combination. However, no change of Bcr-Abl at mRNA level was detected in the same sample by RT-PCR analysis (Figure 50). Taken together, these results demonstrated that the cell death enhancing effect of celastrol and daunorubicin in K562 cells was associated with decreased level of Bcr-Abl oncoprotein but not mRNA expression, suggesting that increased Bcr-Abl protein degradation is achieved under combination treatment.

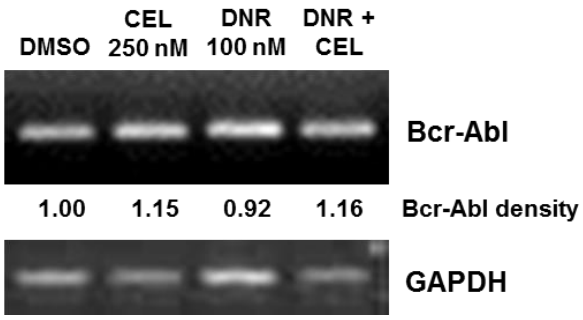

Figure 50. Combination treatment of celastrol and daunorubicin did not affect Bcr-Abl expression at mRNA level.

K562 cells were treated with celastrol (250 nM), daunorubicin (100 nM) or celastrol plus daunorubicin for 72 hours. Total cellular RNA was extracted for RT-PCR analysis. The band intensity (Bcr-Abl and GAPDH) was quantified by densitometry. The relative density of Bcr-Abl was normalized to loading control GAPDH and expressed as fold of vehicle-treated control.

Discussion

In an attempt to effectively treat imatinib-resistant Bcr-Abl-positive leukemia, new strategies such as to decrease the amount of Bcr-Abl protein instead of to inhibit its kinase activity have been investigated. Here, we reported that 1 μM celastrol caused time-dependent reduction of Bcr-Abl protein and induction of apoptosis in K562 cells. This result is consistent with studies from Lu *et al* (Lu et al., 2010b). The reduction of Bcr-Abl protein was due to protein degradation rather than transcriptional suppression (Figures 39 & 40). Interestingly, different from celastrol, other two active compounds isolated from Celastraceae family, triptolide and pristimerin (which is celastrol methyl ether), have been reported to induce the loss of Bcr-Abl at both mRNA and protein levels (Lou and Jin, 2004; Shi et al., 2009b; Lu et al., 2010a). Investigation on detailed molecular mechanisms of celastrol versus triptolide or pristimerin should be conducted in the future.

In an ensuing study on the celastrol-induced apoptotic signaling, we found that apoptotic signal triggered by celastrol within several hours was sufficient to cause apoptosis execution and cell death (Figure 41). This finding has great clinical significance because unlike in cultured cells, in the body drugs will be metabolized and eliminated after a certain period; a quick action ensures the drug exert its effect before elimination. After removal of celastrol, the amount of Bcr-Abl protein increased slightly but steadily due to active Bcr-Abl synthesis (Figures 42 & 43). Bcr-Abl is under the transcriptional control of Bcr promoter. In a recent study, the presence of an "*in trans*" deregulated transcription of both Bcr and Bcr-Abl promoter has been reported, which is associated with CML progression from chronic phase to blast crisis (Marega et al., 2010). In such a scenario, it would not be surprised to see enhanced Bcr-Abl synthesis under

intracellular stress as a cell survival mechanism. Whether the enhanced Bcr-Abl synthesis is due to increased RNA transcription and/or increased protein translation remains to be addressed. Nevertheless, this survival response as an upstream event failed to rescue K562 cells from the fate of apoptotic cell death (Figure 44). These results implied an effective and efficient action of celastrol.

Both caspase-mediated and cathepsin-mediated Bcr-Abl cleavage has been reported under different stimuli (Di Bacco and Cotter, 2002; Puissant et al., 2010). In our experimental conditions, neither a single protease inhibitor to cysteine, serine or aspartyl proteases nor a mixture of these protease inhibitors was able to prevent or suppress celastrol-induced Bcr-Abl degradation (Figure 46). Another possibility is that Bcr-Abl is degraded by a pro-apoptotic protease such as a caspase family member. However, it has been reported that pristimerin-induced decrease of Bcr-Abl protein was not rescued by the presence of caspase inhibitor (Lu et al., 2010a). It is therefore possible that the Bcr-Abl cleavage enzyme mobilized by celastrol is novel which cannot be fully inhibited by any of the protease inhibitors we tested. The cleavage sites of Bcr-Abl and the function of Bcr-Abl cleaved fragments need further investigation.

Despite the progress made in the treatment of leukemia, accumulation of non-specific toxicity and development of drug resistance that preclude desired clinical outcomes persist. Therefore, novel treatment strategies that could decrease the dosage of cytotoxic drugs and/or overcome drug resistance are needed. Here we demonstrate that celastrol is capable of sensitizing human leukemia cells to conventional cytotoxic drugs daunorubicin and cytarabine with enhanced apoptosis induction (Figures 47 & 48). Combination of celastrol and daunorubicin caused increased degradation of the

oncoprotein Bcr-Abl in K562 cells (Figure 49). The dramatic augmentation of sensitivity to cytotoxic drugs by celastrol observed in this study present a compelling rationale for employing celastrol as a sensitizer in leukemia chemotherapy.

SUMMARY

Although considerable progress has been achieved in the field of cancer therapeutics, primary or acquired drug resistance remains a fundamental cause of therapeutic failure in cancer therapy. In my dissertation study, I explored two strategies to overcome tumor drug resistance. The first strategy is to activate AMPK signaling, which regulates cellular energy balance. In AR-positive prostate cancer cells, I found that AMPK and AR negatively regulate each other, forming a regulatory loop: on one hand, AMPK activation induces AR downregulation through suppression of AR mRNA expression and promotion of AR protein degradation; on the other hand, AR is an endogenous inhibitor of AMPK signaling as inhibition of AR function by an anti-androgen or its siRNA enhanced metformin-induced AMPK activation and cell growth inhibition whereas overexpression of AR delayed AMPK activation and increased prostate cancer cellular resistance to metformin treatment. Combination of an anti-androgen and an AMPK activator elicited better anti-proliferative effect in AR-positive cells than each treatment alone. In bortezomib-resistant multiple myeloma cells, I found that AMPK signaling is suppressed in these cells as compared to their drug-naïve counterparts, which may actually contribute to their bortezomib-resistant phenotype. The suppressed AMPK signaling in resistant cells remains functionally intact and can be elevated by pharmacological activators. Combining bortezomib with an AMPK activator is able to induce more cell growth inhibition in bortezomib-resistant cells as compared to each drug alone. These results imply that, for patients whose AMPK activity is

suppressed in tumor tissue, metformin or other AMPK activators may work collaboratively with current treatments to achieve better clinical outcome.

The second strategy that I explored to overcome tumor drug resistance is to destabilize tumor-driven oncoproteins. In AR-positive prostate cancer cells, we observed AR destabilization upon AMPK activation by metformin. In BCR-ABL-driven CML cells, we observed BCR-ABL destabilization with celastrol treatment. The implication from this part of the study is that in certain types of cancer, destabilizing oncoproteins via pharmacological intervention is feasible and effective in cell death induction. Therefore, if the pharmacological intervention is applicable in the clinic, it will very possibly lead to a favorable long-term outcome.

Taken together, the studies presented in this dissertation will definitely help elucidating the role of AMPK signaling in cancer cells and promote the seeking of novel strategies that can cause destabilization of certain key oncoproteins.

REFERENCES

Ablain J, Nasr R, Bazarbachi A and de The H (2011) The drug-induced degradation of oncoproteins: an unexpected Achilles' heel of cancer cells? *Cancer discovery* **1**:117-127.

Adams J (2004) The development of proteasome inhibitors as anticancer drugs. *Cancer Cell* **5**:417-421.

An X, Tiwari AK, Sun Y, Ding PR, Ashby CR, Jr. and Chen ZS (2010) BCR-ABL tyrosine kinase inhibitors in the treatment of Philadelphia chromosome positive chronic myeloid leukemia: a review. *Leukemia research* **34**:1255-1268.

Bain J, Plater L, Elliott M, Shpiro N, Hastie CJ, McLauchlan H, Klevernic I, Arthur JS, Alessi DR and Cohen P (2007) The selectivity of protein kinase inhibitors: a further update. *The Biochemical journal* **408**:297-315.

Benanti JA (2012) Coordination of cell growth and division by the ubiquitin-proteasome system. *Seminars in cell & developmental biology* **23**:492-498.

Butler EB, Zhao Y, Munoz-Pinedo C, Lu J and Tan M (2013) Stalling the engine of resistance: targeting cancer metabolism to overcome therapeutic resistance. *Cancer research* **73**:2709-2717.

Chauhan D, Hideshima T, Mitsiades C, Richardson P and Anderson KC (2005) Proteasome inhibitor therapy in multiple myeloma. *Mol Cancer Ther* **4**:686-692.

Chen CD, Welsbie DS, Tran C, Baek SH, Chen R, Vessella R, Rosenfeld MG and Sawyers CL (2004) Molecular determinants of resistance to antiandrogen therapy. *Nat Med* **10**:33-39.

Chen D, Banerjee S, Cui QC, Kong D, Sarkar FH and Dou QP (2012a) Activation of AMP-activated protein kinase by 3,3'-Diindolylmethane (DIM) is associated with human prostate cancer cell death in vitro and in vivo. *PloS one* **7**:e47186.

Chen D, Pamu S, Cui Q, Chan TH and Dou QP (2012b) Novel epigallocatechin gallate (EGCG) analogs activate AMP-activated protein kinase pathway and target cancer stem cells. *Bioorg Med Chem* **20**:3031-3037.

Chen M, Rose AE, Doudican N, Osman I and Orlow SJ (2009) Celastrol synergistically enhances temozolomide cytotoxicity in melanoma cells. *Molecular cancer research : MCR* **7**:1946-1953.

Cheung PC, Salt IP, Davies SP, Hardie DG and Carling D (2000) Characterization of AMP-activated protein kinase gamma-subunit isoforms and their role in AMP binding. *Biochem J* **346 Pt 3**:659-669.

Cool B, Zinker B, Chiou W, Kifle L, Cao N, Perham M, Dickinson R, Adler A, Gagne G, Iyengar R, Zhao G, Marsh K, Kym P, Jung P, Camp HS and Frevert E (2006) Identification and characterization of a small molecule AMPK activator that treats key components of type 2 diabetes and the metabolic syndrome. *Cell metabolism* **3**:403-416.

Corton JM, Gillespie JG, Hawley SA and Hardie DG (1995) 5-aminoimidazole-4-carboxamide ribonucleoside. A specific method for activating AMP-activated protein kinase in intact cells? *Eur J Biochem* **229**:558-565.

Dai Y, DeSano JT, Meng Y, Ji Q, Ljungman M, Lawrence TS and Xu L (2009) Celastrol potentiates radiotherapy by impairment of DNA damage processing in human

prostate cancer. *International journal of radiation oncology, biology, physics* **74**:1217-1225.

Davenport A, Frezza M, Shen M, Ge Y, Huo C, Chan TH and Dou QP (2010) Celastrol and an EGCG pro-drug exhibit potent chemosensitizing activity in human leukemia cells. *International journal of molecular medicine* **25**:465-470.

Davies SP, Sim AT and Hardie DG (1990) Location and function of three sites phosphorylated on rat acetyl-CoA carboxylase by the AMP-activated protein kinase. *Eur J Biochem* **187**:183-190.

Devlin HL and Mudryj M (2009) Progression of prostate cancer: multiple pathways to androgen independence. *Cancer letters* **274**:177-186.

Di Bacco AM and Cotter TG (2002) p53 expression in K562 cells is associated with caspase-mediated cleavage of c-ABL and BCR-ABL protein kinases. *British journal of haematology* **117**:588-597.

Dispenzieri A, Jacobus S, Vesole DH, Callandar N, Fonseca R and Greipp PR (2010) Primary therapy with single agent bortezomib as induction, maintenance and re-induction in patients with high-risk myeloma: results of the ECOG E2A02 trial. *Leukemia* **24**:1406-1411.

Djouder N, Tuerk RD, Suter M, Salvioni P, Thali RF, Scholz R, Vaahtomeri K, Auchli Y, Rechsteiner H, Brunisholz RA, Viollet B, Makela TP, Wallimann T, Neumann D and Krek W (2010) PKA phosphorylates and inactivates AMPKalpha to promote efficient lipolysis. *EMBO J* **29**:469-481.

Dou QP, McGuire TF, Peng Y and An B (1999) Proteasome inhibition leads to significant reduction of Bcr-Abl expression and subsequent induction of apoptosis

in K562 human chronic myelogenous leukemia cells. *The Journal of pharmacology and experimental therapeutics* **289**:781-790.

Dowling RJ, Niraula S, Stambolic V and Goodwin PJ (2012) Metformin in cancer: translational challenges. *J Mol Endocrinol* **48**:R31-43.

Esteve-Puig R, Canals F, Colome N, Merlino G and Recio JA (2009) Uncoupling of the LKB1-AMPKalpha energy sensor pathway by growth factors and oncogenic BRAF. *PloS one* **4**:e4771.

Evans JM, Donnelly LA, Emslie-Smith AM, Alessi DR and Morris AD (2005) Metformin and reduced risk of cancer in diabetic patients. *Bmj* **330**:1304-1305.

Feldman BJ and Feldman D (2001) The development of androgen-independent prostate cancer. *Nat Rev Cancer* **1**:34-45.

Fogarty S and Hardie DG (2010) Development of protein kinase activators: AMPK as a target in metabolic disorders and cancer. *Biochim Biophys Acta* **1804**:581-591.

Franke NE, Niewerth D, Assaraf YG, van Meerloo J, Vojtekova K, van Zantwijk CH, Zweegman S, Chan ET, Kirk CJ, Geerke DP, Schimmer AD, Kaspers GJ, Jansen G and Cloos J (2011) Impaired bortezomib binding to mutant beta5 subunit of the proteasome is the underlying basis for bortezomib resistance in leukemia cells. *Leukemia : official journal of the Leukemia Society of America, Leukemia Research Fund, UK*.

Frigo DE, Howe MK, Wittmann BM, Brunner AM, Cushman I, Wang Q, Brown M, Means AR and McDonnell DP (2011) CaM kinase kinase beta-mediated activation of the growth regulatory kinase AMPK is required for androgen-dependent migration of prostate cancer cells. *Cancer Res* **71**:528-537.

Glickman MH and Ciechanover A (2002) The ubiquitin-proteasome proteolytic pathway: destruction for the sake of construction. *Physiological reviews* **82**:373-428.

Gonit M, Zhang J, Salazar M, Cui H, Shatnawi A, Trumbly R and Ratnam M (2011) Hormone depletion-insensitivity of prostate cancer cells is supported by the AR without binding to classical response elements. *Mol Endocrinol* **25**:621-634.

Gottesman MM (2002) Mechanisms of cancer drug resistance. *Annual review of medicine* **53**:615-627.

Gutman D, Morales AA and Boise LH (2009) Acquisition of a multidrug-resistant phenotype with a proteasome inhibitor in multiple myeloma. *Leukemia* **23**:2181-2183.

Gwinn DM, Shackelford DB, Egan DF, Mihaylova MM, Mery A, Vasquez DS, Turk BE and Shaw RJ (2008) AMPK phosphorylation of raptor mediates a metabolic checkpoint. *Mol Cell* **30**:214-226.

Haile S and Sadar MD (2011) Androgen receptor and its splice variants in prostate cancer. *Cell Mol Life Sci* **68**:3971-3981.

Hanahan D and Weinberg RA (2011) Hallmarks of cancer: the next generation. *Cell* **144**:646-674.

Handa N, Takagi T, Saijo S, Kishishita S, Takaya D, Toyama M, Terada T, Shirouzu M, Suzuki A, Lee S, Yamauchi T, Okada-Iwabu M, Iwabu M, Kadowaki T, Minokoshi Y and Yokoyama S (2011) Structural basis for compound C inhibition of the human AMP-activated protein kinase alpha2 subunit kinase domain. *Acta crystallographica Section D, Biological crystallography* **67**:480-487.

Hassane DC, Guzman ML, Corbett C, Li X, Abboud R, Young F, Liesveld JL, Carroll M and Jordan CT (2008) Discovery of agents that eradicate leukemia stem cells using an in silico screen of public gene expression data. *Blood* **111**:5654-5662.

Hawley SA, Boudeau J, Reid JL, Mustard KJ, Udd L, Makela TP, Alessi DR and Hardie DG (2003) Complexes between the LKB1 tumor suppressor, STRAD alpha/beta and MO25 alpha/beta are upstream kinases in the AMP-activated protein kinase cascade. *J Biol* **2**:28.

Hawley SA, Davison M, Woods A, Davies SP, Beri RK, Carling D and Hardie DG (1996) Characterization of the AMP-activated protein kinase kinase from rat liver and identification of threonine 172 as the major site at which it phosphorylates AMP-activated protein kinase. *J Biol Chem* **271**:27879-27887.

Hawley SA, Fullerton MD, Ross FA, Schertzer JD, Chevtzoff C, Walker KJ, Peggie MW, Zibrova D, Green KA, Mustard KJ, Kemp BE, Sakamoto K, Steinberg GR and Hardie DG (2012) The ancient drug salicylate directly activates AMP-activated protein kinase. *Science* **336**:918-922.

Hawley SA, Pan DA, Mustard KJ, Ross L, Bain J, Edelman AM, Frenguelli BG and Hardie DG (2005) Calmodulin-dependent protein kinase kinase-beta is an alternative upstream kinase for AMP-activated protein kinase. *Cell metabolism* **2**:9-19.

Hieronymus H, Lamb J, Ross KN, Peng XP, Clement C, Rodina A, Nieto M, Du J, Stegmaier K, Raj SM, Maloney KN, Clardy J, Hahn WC, Chiosis G and Golub TR (2006) Gene expression signature-based chemical genomic prediction identifies a novel class of HSP90 pathway modulators. *Cancer Cell* **10**:321-330.

Horman S, Vertommen D, Heath R, Neumann D, Mouton V, Woods A, Schlattner U, Wallimann T, Carling D, Hue L and Rider MH (2006) Insulin antagonizes ischemia-induced Thr172 phosphorylation of AMP-activated protein kinase alpha-subunits in heart via hierarchical phosphorylation of Ser485/491. *J Biol Chem* **281**:5335-5340.

Huang NL, Chiang SH, Hsueh CH, Liang YJ, Chen YJ and Lai LP (2009) Metformin inhibits TNF-alpha-induced IkappaB kinase phosphorylation, IkappaB-alpha degradation and IL-6 production in endothelial cells through PI3K-dependent AMPK phosphorylation. *International journal of cardiology* **134**:169-175.

Hwang JT, Kwak DW, Lin SK, Kim HM, Kim YM and Park OJ (2007) Resveratrol induces apoptosis in chemoresistant cancer cells via modulation of AMPK signaling pathway. *Ann N Y Acad Sci* **1095**:441-448.

Inoki K, Zhu T and Guan KL (2003) TSC2 mediates cellular energy response to control cell growth and survival. *Cell* **115**:577-590.

Jaworski T (2006) Degradation and beyond: control of androgen receptor activity by the proteasome system. *Cellular & molecular biology letters* **11**:109-131.

Kampa M, Papakonstanti EA, Hatzoglou A, Stathopoulos EN, Stournaras C and Castanas E (2002) The human prostate cancer cell line LNCaP bears functional membrane testosterone receptors that increase PSA secretion and modify actin cytoskeleton. *FASEB J* **16**:1429-1431.

Kern J, Untergasser G, Zenzmaier C, Sarg B, Gastl G, Gunsilius E and Steurer M (2009) GRP-78 secreted by tumor cells blocks the antiangiogenic activity of bortezomib. *Blood* **114**:3960-3967.

Kim JH, Lee JO, Lee SK, Kim N, You GY, Moon JW, Sha J, Kim SJ, Park SH and Kim HS (2013) Celastrol suppresses breast cancer MCF-7 cell viability via the AMP-activated protein kinase (AMPK)-induced p53-polo like kinase 2 (PLK-2) pathway. *Cellular signalling* **25**:805-813.

Kolvenbag GJ, Blackledge GR and Gotting-Smith K (1998) Bicalutamide (Casodex) in the treatment of prostate cancer: history of clinical development. *The Prostate* **34**:61-72.

Kuhn DJ, Berkova Z, Jones RJ, Woessner R, Bjorklund CC, Ma W, Davis RE, Lin P, Wang H, Madden TL, Wei C, Baladandayuthapani V, Wang M, Thomas SK, Shah JJ, Weber DM and Orlowski RZ (2012) Targeting the insulin-like growth factor-1 receptor to overcome bortezomib resistance in preclinical models of multiple myeloma. *Blood* **120**:3260-3270.

Kurzrock R, Kantarjian HM, Druker BJ and Talpaz M (2003) Philadelphia chromosome-positive leukemias: from basic mechanisms to molecular therapeutics. *Annals of internal medicine* **138**:819-830.

Kyle RA and Rajkumar SV (2004) Multiple myeloma. *The New England journal of medicine* **351**:1860-1873.

Lee DH and Goldberg AL (1998) Proteasome inhibitors: valuable new tools for cell biologists. *Trends in cell biology* **8**:397-403.

Lee DK and Chang C (2003) Endocrine mechanisms of disease: Expression and degradation of androgen receptor: mechanism and clinical implication. *The Journal of clinical endocrinology and metabolism* **88**:4043-4054.

Lee JH, Koo TH, Yoon H, Jung HS, Jin HZ, Lee K, Hong YS and Lee JJ (2006) Inhibition of NF-kappa B activation through targeting I kappa B kinase by celastrol, a quinone methide triterpenoid. *Biochemical pharmacology* **72**:1311-1321.

Li J, Cao B, Liu X, Fu X, Xiong Z, Chen L, Sartor O, Dong Y and Zhang H (2011) Berberine suppresses androgen receptor signaling in prostate cancer. *Mol Cancer Ther* **10**:1346-1356.

Lonergan PE and Tindall DJ (2011) Androgen receptor signaling in prostate cancer development and progression. *Journal of carcinogenesis* **10**:20.

Longley DB and Johnston PG (2005) Molecular mechanisms of drug resistance. *J Pathol* **205**:275-292.

Lou YJ and Jin J (2004) Triptolide down-regulates bcr-abl expression and induces apoptosis in chronic myelogenous leukemia cells. *Leukemia & lymphoma* **45**:373-376.

Lu S, Chen Z, Yang J, Chen L, Gong S, Zhou H, Guo L and Wang J (2008) Overexpression of the PSMB5 gene contributes to bortezomib resistance in T-lymphoblastic lymphoma/leukemia cells derived from Jurkat line. *Experimental hematology* **36**:1278-1284.

Lu Z, Jin Y, Chen C, Li J, Cao Q and Pan J (2010a) Pristimerin induces apoptosis in imatinib-resistant chronic myelogenous leukemia cells harboring T315I mutation by blocking NF-kappaB signaling and depleting Bcr-Abl. *Molecular cancer* **9**:112.

Lu Z, Jin Y, Qiu L, Lai Y and Pan J (2010b) Celastrol, a novel HSP90 inhibitor, depletes Bcr-Abl and induces apoptosis in imatinib-resistant chronic myelogenous leukemia cells harboring T315I mutation. *Cancer letters* **290**:182-191.

Luo Z, Zang M and Guo W (2010) AMPK as a metabolic tumor suppressor: control of metabolism and cell growth. *Future oncology* **6**:457-470.

Mahindra A, Hideshima T and Anderson KC (2010) Multiple myeloma: biology of the disease. *Blood reviews* **24 Suppl 1**:S5-11.

Mahindra A, Laubach J, Raje N, Munshi N, Richardson PG and Anderson K (2012) Latest advances and current challenges in the treatment of multiple myeloma. *Nature reviews Clinical oncology* **9**:135-143.

Marega M, Piazza RG, Pirola A, Redaelli S, Mogavero A, Iacobucci I, Meneghetti I, Parma M, Pogliani EM and Gambacorti-Passerini C (2010) BCR and BCR-ABL regulation during myeloid differentiation in healthy donors and in chronic phase/blast crisis CML patients. *Leukemia : official journal of the Leukemia Society of America, Leukemia Research Fund, UK* **24**:1445-1449.

Markovina S, Callander NS, O'Connor SL, Kim J, Werndli JE, Raschko M, Leith CP, Kahl BS, Kim K and Miyamoto S (2008) Bortezomib-resistant nuclear factor-kappaB activity in multiple myeloma cells. *Molecular cancer research : MCR* **6**:1356-1364.

Massie CE, Lynch A, Ramos-Montoya A, Boren J, Stark R, Fazli L, Warren A, Scott H, Madhu B, Sharma N, Bon H, Zecchini V, Smith DM, Denicola GM, Mathews N, Osborne M, Hadfield J, Macarthur S, Adryan B, Lyons SK, Brindle KM, Griffiths J, Gleave ME, Rennie PS, Neal DE and Mills IG (2011) The androgen receptor

fuels prostate cancer by regulating central metabolism and biosynthesis. *EMBO J* **30**:2719-2733.

Masui K, Gini B, Wykosky J, Zanca C, Mischel PS, Furnari FB and Cavenee WK (2013) A tale of two approaches: complementary mechanisms of cytotoxic and targeted therapy resistance may inform next-generation cancer treatments. *Carcinogenesis* **34**:725-738.

Momcilovic M, Hong SP and Carlson M (2006) Mammalian TAK1 activates Snf1 protein kinase in yeast and phosphorylates AMP-activated protein kinase in vitro. *J Biol Chem* **281**:25336-25343.

Moore F, Weekes J and Hardie DG (1991) Evidence that AMP triggers phosphorylation as well as direct allosteric activation of rat liver AMP-activated protein kinase. A sensitive mechanism to protect the cell against ATP depletion. *Eur J Biochem* **199**:691-697.

Moriuchi M, Ohmachi K, Kojima M, Tsuboi K, Ogawa Y, Nakamura N and Ando K (2010) Three cases of bortezomib-resistant multiple myeloma with extramedullary masses. *The Tokai journal of experimental and clinical medicine* **35**:17-20.

Motoshima H, Goldstein BJ, Igata M and Araki E (2006) AMPK and cell proliferation--AMPK as a therapeutic target for atherosclerosis and cancer. *J Physiol* **574**:63-71.

Oerlemans R, Franke NE, Assaraf YG, Cloos J, van Zantwijk I, Berkers CR, Scheffer GL, Debipersad K, Vojtekova K, Lemos C, van der Heijden JW, Ylstra B, Peters GJ, Kaspers GL, Dijkmans BA, Scheper RJ and Jansen G (2008) Molecular basis of

bortezomib resistance: proteasome subunit beta5 (PSMB5) gene mutation and overexpression of PSMB5 protein. *Blood* **112**:2489-2499.

Pang T, Zhang ZS, Gu M, Qiu BY, Yu LF, Cao PR, Shao W, Su MB, Li JY, Nan FJ and Li J (2008) Small molecule antagonizes autoinhibition and activates AMP-activated protein kinase in cells. *J Biol Chem* **283**:16051-16060.

Pelley RP, Chinnakannu K, Murthy S, Strickland FM, Menon M, Dou QP, Barrack ER and Reddy GP (2006) Calmodulin-androgen receptor (AR) interaction: calcium-dependent, calpain-mediated breakdown of AR in LNCaP prostate cancer cells. *Cancer Res* **66**:11754-11762.

Puissant A, Colosetti P, Robert G, Cassuto JP, Raynaud S and Auberger P (2010) Cathepsin B release after imatinib-mediated lysosomal membrane permeabilization triggers BCR-ABL cleavage and elimination of chronic myelogenous leukemia cells. *Leukemia : official journal of the Leukemia Society of America, Leukemia Research Fund, UK* **24**:115-124.

Ren R (2005) Mechanisms of BCR-ABL in the pathogenesis of chronic myelogenous leukaemia. *Nature Reviews Cancer* **5**:172-183.

Richardson PG, Barlogie B, Berenson J, Singhal S, Jagannath S, Irwin D, Rajkumar SV, Srkalovic G, Alsina M, Alexanian R, Siegel D, Orlowski RZ, Kuter D, Limentani SA, Lee S, Hideshima T, Esseltine DL, Kauffman M, Adams J, Schenkein DP and Anderson KC (2003) A phase 2 study of bortezomib in relapsed, refractory myeloma. *N Engl J Med* **348**:2609-2617.

Richter E, Srivastava S and Dobi A (2007) Androgen receptor and prostate cancer. *Prostate Cancer Prostatic Dis* **10**:114-118.

Rios M, Foretz M, Viollet B, Prieto A, Fraga M, Costoya JA and Senaris R (2013) AMPK activation by oncogenesis is required to maintain cancer cell proliferation in astrocytic tumors. *Cancer research*.

Ruschak AM, Slassi M, Kay LE and Schimmer AD (2011) Novel proteasome inhibitors to overcome bortezomib resistance. *Journal of the National Cancer Institute* **103**:1007-1017.

Salminen A, Lehtonen M, Paimela T and Kaarniranta K (2010) Celastrol: Molecular targets of Thunder God Vine. *Biochemical and biophysical research communications* **394**:439-442.

Shen M, Schmitt S, Buac D and Dou QP (2013) Targeting the ubiquitin-proteasome system for cancer therapy. *Expert opinion on therapeutic targets*.

Shi Q, Shih CC and Lee KH (2009a) Novel anti-prostate cancer curcumin analogues that enhance androgen receptor degradation activity. *Anticancer Agents Med Chem* **9**:904-912.

Shi X, Jin Y, Cheng C, Zhang H, Zou W, Zheng Q, Lu Z, Chen Q, Lai Y and Pan J (2009b) Triptolide inhibits Bcr-Abl transcription and induces apoptosis in STI571-resistant chronic myelogenous leukemia cells harboring T315I mutation. *Clinical cancer research : an official journal of the American Association for Cancer Research* **15**:1686-1697.

Shuqing L, Jianmin Y, Chongmei H, Hui C and Wang J (2011) Upregulated expression of the PSMB5 gene may contribute to drug resistance in patient with multiple myeloma when treated with bortezomib-based regimen. *Experimental hematology* **39**:1117-1118.

Siegel R, Naishadham D and Jemal A (2013) Cancer statistics, 2013. *CA: a cancer journal for clinicians* **63**:11-30.

Sorokin AV, Kim ER and Ovchinnikov LP (2009) Proteasome system of protein degradation and processing. *Biochemistry (Mosc)* **74**:1411-1442.

Stein SC, Woods A, Jones NA, Davison MD and Carling D (2000) The regulation of AMP-activated protein kinase by phosphorylation. *Biochem J* **345 Pt 3**:437-443.

Stessman HA, Baughn LB, Sarver A, Xia T, Deshpande R, Mansoor A, Walsh SA, Sunderland JJ, Dolloff NG, Linden MA, Zhan F, Janz S, Myers CL and Van Ness BG (2013) Profiling bortezomib resistance identifies secondary therapies in a mouse myeloma model. *Molecular cancer therapeutics* **12**:1140-1150.

Turner N, Li JY, Gosby A, To SW, Cheng Z, Miyoshi H, Taketo MM, Cooney GJ, Kraegen EW, James DE, Hu LH, Li J and Ye JM (2008) Berberine and its more biologically available derivative, dihydroberberine, inhibit mitochondrial respiratory complex I: a mechanism for the action of berberine to activate AMP-activated protein kinase and improve insulin action. *Diabetes* **57**:1414-1418.

Wang DS, Jonker JW, Kato Y, Kusuhara H, Schinkel AH and Sugiyama Y (2002) Involvement of organic cation transporter 1 in hepatic and intestinal distribution of metformin. *The Journal of pharmacology and experimental therapeutics* **302**:510-515.

Wehling M and Losel R (2006) Non-genomic steroid hormone effects: membrane or intracellular receptors? *J Steroid Biochem Mol Biol* **102**:180-183.

Wilcock C and Bailey CJ (1994) Accumulation of metformin by tissues of the normal and diabetic mouse. *Xenobiotica; the fate of foreign compounds in biological systems* **24**:49-57.

Wilda M, Fuchs U, Wossmann W and Borkhardt A (2002) Killing of leukemic cells with a BCR/ABL fusion gene by RNA interference (RNAi). *Oncogene* **21**:5716-5724.

Withey JM, Marley SB, Kaeda J, Harvey AJ, Crompton MR and Gordon MY (2005) Targeting primary human leukaemia cells with RNA interference: Bcr-Abl targeting inhibits myeloid progenitor self-renewal in chronic myeloid leukaemia cells. *British journal of haematology* **129**:377-380.

Woods A, Cheung PC, Smith FC, Davison MD, Scott J, Beri RK and Carling D (1996) Characterization of AMP-activated protein kinase beta and gamma subunits. Assembly of the heterotrimeric complex in vitro. *J Biol Chem* **271**:10282-10290.

Yang H, Chen D, Cui QC, Yuan X and Dou QP (2006) Celastrol, a triterpene extracted from the Chinese "Thunder of God Vine," is a potent proteasome inhibitor and suppresses human prostate cancer growth in nude mice. *Cancer research* **66**:4758-4765.

Yang H and Dou QP (2010) Targeting apoptosis pathway with natural terpenoids: implications for treatment of breast and prostate cancer. *Current drug targets* **11**:733-744.

Yang H, Murthy S, Sarkar FH, Sheng S, Reddy GP and Dou QP (2008) Calpain-mediated androgen receptor breakdown in apoptotic prostate cancer cells. *J Cell Physiol* **217**:569-576.

Zhan YY, Chen Y, Zhang Q, Zhuang JJ, Tian M, Chen HZ, Zhang LR, Zhang HK, He JP, Wang WJ, Wu R, Wang Y, Shi C, Yang K, Li AZ, Xin YZ, Li TY, Yang JY, Zheng ZH, Yu CD, Lin SC, Chang C, Huang PQ, Lin T and Wu Q (2012) The orphan nuclear receptor Nur77 regulates LKB1 localization and activates AMPK. *Nat Chem Biol* **8**:897-904.

Zheng B, Jeong JH, Asara JM, Yuan YY, Granter SR, Chin L and Cantley LC (2009) Oncogenic B-RAF negatively regulates the tumor suppressor LKB1 to promote melanoma cell proliferation. *Molecular cell* **33**:237-247.

Zhou G, Myers R, Li Y, Chen Y, Shen X, Fenyk-Melody J, Wu M, Ventre J, Doebber T, Fujii N, Musi N, Hirshman MF, Goodyear LJ and Moller DE (2001) Role of AMP-activated protein kinase in mechanism of metformin action. *J Clin Invest* **108**:1167-1174.

ABSTRACT

OVERCOMING TUMOR DRUG RESISTANCE BY ACTIVATING AMP-ACTIVATED PROTEIN KINASE AND DESTABILIZING ONCOPROTEINS

by

MIN SHEN

August 2013

Advisor: Dr. Q. Ping Dou

Major: Pharmacology

Degree: Doctor of Philosophy

Although considerable progress has been achieved in the field of cancer therapeutics, primary or acquired drug resistance remains a fundamental cause of therapeutic failure in cancer therapy. Among different mechanisms characterized that are responsible for tumor drug resistance, there is increasing evidence suggesting that dysregulation of gene expression, especially oncogene or tumor suppressor gene expression, at either gene transcription or protein synthesis level, can contribute to the drug-resistant phenotype. AMP-activated protein kinase (AMPK) is a well-known major cellular energy sensor, which negatively regulates metabolic pathways such as protein synthesis, fatty acid oxidation and glucose consumption. Activation of AMPK may suppress metabolic activities that are in favor of assisting tumor cell growth and resistance to various anti-tumor drugs. Along this line, I hypothesized that activation of AMPK signaling could help overcoming tumor drug resistance. The data presented in this dissertation strongly support this hypothesis.

The hypothesis was investigated in two different types of cancers with resistance to two different types of drugs. The first model system I used to test my hypothesis is

prostate cancer cell models. By using androgen-dependent, androgen receptor (AR)-positive LNCaP cell line and its androgen-independent, AR-positive derivative C4-2B cell line, I found that both cell lines responded to pharmacological AMPK activator metformin, regardless of their androgen dependency. Activation of AMPK by metformin caused AR protein level decrease through suppression of AR mRNA expression and promotion of AR protein degradation. On the other hand, I found that AR is an inhibitor of AMPK signaling-mediated growth suppression and cell death in prostate cancer cells. These findings suggest that combination of AR inhibition therapy with metformin or other AMPK activators may benefit the therapeutic outcome of AR-positive prostate cancer.

The hypothesis has also been studied in multiple myeloma cell models in which paired parental bortezomib-sensitive multiple myeloma cells and their bortezomib-resistant counterparts generated by chronic drug exposure were used. In this study, I found that paired bortezomib-sensitive and -resistant multiple myeloma cells were about equally sensitive to AMPK activators metformin and AICAR. Although carfilzomib is developed as next-generation proteasome inhibitor to overcome bortezomib resistance; the two bortezomib-resistant multiple myeloma cell lines tested in this study exhibited cross-resistance to carfilzomib. I also found that AMPK signaling is suppressed in bortezomib-resistant multiple myeloma cells and that the suppressed AMPK signaling can be elevated by challenging with an AMPK activator. Finally, I found that AMPK activators were able to overcome not only resistance to bortezomib but also cross-resistance to carfilzomib in bortezomib-resistant multiple myeloma cells. These findings

support the further investigation of AMPK signaling in multiple myeloma patient samples and *in vivo* evaluation of metformin use in multiple myeloma mouse models.

Originating from the observation that decrease of AR protein level is a critical step for apoptosis induction in prostate cancer cells, I studied the strategy of destabilizing Bcr-Abl oncoprotein in the scenario of chronic myeloid leukemia (CML). Bcr-Abl is crucial for the pathogenesis of CML by acting as a proliferation activator and apoptosis suppressor. Our laboratory has previously shown that some proteasome inhibitors can efficiently reduce Bcr-Abl protein level. In my study, I examined the effect of celastrol, a natural product with potent proteasome inhibitory activity, on destabilizing Bcr-Abl protein, and explored the potential combination therapies for Bcr-Abl-driven leukemia. I found that (i) celastrol induced apoptosis and Bcr-Abl degradation in a time-dependent manner; (ii) celastrol-induced apoptosis was not blocked by newly synthesized Bcr-Abl protein once the cells were committed; and (iii) celastrol-induced Bcr-Abl degradation and apoptosis were not prevented by selected protease inhibitors or their mixture under the selected experimental conditions. These findings shed light on the mechanism how celastrol inhibits Bcr-Abl protein expression/function and provide support for the potential application of celastrol in the CML treatment.

Taken together, the studies presented in this dissertation will definitely help elucidating the role of AMPK signaling in cancer cells and promote the development of alternative strategies against drug resistance.

AUTOBIOGRAPHICAL STATEMENT

Min Shen

Min received a Bachelor of Science degree in Pharmaceutical Sciences from Zhejiang University, Hangzhou, China in 2005 and a Master of Science degree in Pharmacology from Zhejiang Academy of Medical Sciences, Hangzhou, China in 2008. She commenced her studies in the Pharmacology Ph.D. Program at the Wayne State University School of Medicine in Fall, 2008. Under the guidance of Dr. Q. Ping Dou for her doctoral training, Min published one research article, three review articles and one book chapter as first author. She has contributed to nine publications in total. A major focus of Min's research has been placed on elucidating the role of AMPK signaling in cancer cells and exploring alternative strategies for overcoming tumor drug resistance.